ISSN 1816-8957

No. 22, May 2017

Scientific Drilling

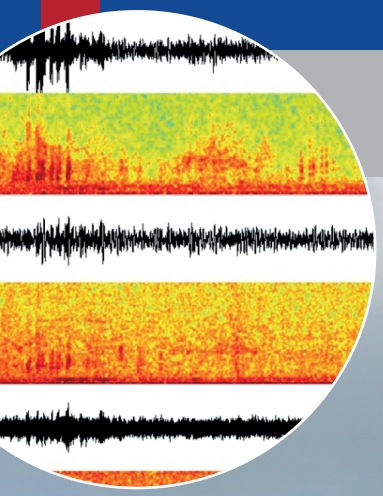

Reports on Deep Earth Sampling and Monitoring

The open-access ICDP and IODP journal • www.scientific-drilling.net

Editorial preface

Dear reader,

Where Great advances have been made in recent years in the understanding of Earth's composition evolution and processes at depth by research drilling. However, innovative research frontiers in Earth sciences remain to be addressed by scientific drilling. This issue of *Scientific Drilling* takes a deeper look at what has been achieved in the past 15 years of the Chinese Continental Scientific Drilling Program, CCSD. The CCSD's story of success began with a 5158 m deep borehole into the Sulu ultrahigh-pressure metamorphic terrain, focusing later on the rapid-response active fault zone drilling in southern China and currently continuing in the Songliao Basin in northeast China, where the deepest hole ever drilled with support of the ICDP is currently underway (see pages 1 to 18).

With this issue of *Scientific Drilling* we also wish to highlight exciting new technology and infrastructure developments. A test bed facility for ice drilling has been constructed for trials of drilling and fluid processing functions under environmental conditions as close as possible to those expected in Antarctica (pages 29 to 33). State-of-the-art non-destructive X-ray and neutron tomographic scanning techniques were applied on drill cores from the Deep Fault Drilling Project in New Zealand (pages 35 to 42) to assess their potential for future research drilling. The "Geophysical Observatory at the North Anatolian Fault", comprising seven 300 m deep boreholes equipped with vertical seismic profiling stations and four collocated 100 m deep borehole strain meters, was recently implemented (pages 19 to 28) to monitor the eastern portion of the North Anatolian Fault, which is currently late in the seismic cycle and estimated to break in a M>7 earthquake.

In preparation for the planned IODP cruises in the South Atlantic, 45 scientists from eight countries attended an IODP workshop to develop a new proposal for drilling the Argentina Passive Volcanic Continental Margin in order to gain new insights on basin evolution, the deep biosphere, gas hydrates, sediment dynamics and ocean evolution (pages 49 to 61). An international group of 25 biologists, paleoecologists and geologists came together to discuss how a scientific drilling campaign at Lake Tanganyika in Africa, the largest, deepest and oldest of the African Rift Valley lakes, might further advance our understanding of the lake's and its watershed's endemic biotic history (pages 43 to 48).

Your editors,
Ulrich Harms, Thomas Wiersberg, Jan Behrmann, Will Sager, and Tomoaki Morishita

Aims & scope

Scientific Drilling (SD) is a multidisciplinary journal focused on bringing the latest science and news from the scientific drilling and related programmes to the geosciences community. Scientific Drilling delivers peer-reviewed science reports from recently completed and ongoing international scientific drilling projects. The journal also includes reports on engineering developments, technical developments, workshops, progress reports, and news and updates from the community.

Editorial board

Additional information

ISSN 1816-8957 | eISSN 1816-3459

Copernicus Publications
The Innovative Open Access Publisher

Copernicus Publications
Bahnhofsallee 1e
37081 Göttingen
Germany
Phone: +49 551 90 03 39 0
Fax: +49 551 90 03 39 70

editorial@copernicus.org
production@copernicus.org

http://publications.copernicus.org

View the online library or learn more about Scientific Drilling on:
www.scientific-drilling.net

Cover figures:
Drilling site WSFD-4 of the Wenchuan Seismic Fault Scientific Drilling along the Longmen Shan thrust belt (China), photo courtesy of Haibing Li
Insert 1: Seismograms and spectograms recorded at the Tesvikiye borehole station of the GONAF network (Turkey)
Insert 2: Circulation of surface and deep-water in the Argentine Basin (Argentina)

Contents

Science Reports

Progress Reports

Technical Developments

Workshop Reports

News & Views

Sci. Dril., 22, 1–18, 2017
www.sci-dril.net/22/1/2017/
doi:10.5194/sd-22-1-2017

Scientific Drilling
Open Access

Fifteen years of the Chinese Continental Scientific Drilling Program

Zhiqin Xu[1,2], Jingsui Yang[2], Chengshan Wang[3], Zhisheng An[4], Haibing Li[2], Qin Wang[1], and Dechen Su[2]

[1]State Key Laboratory for Mineral Deposits Research, School of Earth Sciences and Engineering, Nanjing University, Nanjing 210023, China
[2]Laboratory for Continental Tectonics and Dynamics, Institute of Geology, Chinese Academy of Geological Sciences, Beijing 100037, China
[3]School of Earth Sciences and Resources, China University of Geosciences, Beijing 100083, China
[4]State Key Laboratory of Loess and Quaternary Geology, Institute of Earth Environment, Chinese Academy of Sciences, Xi'an 710061, China

Correspondence to: Qin Wang (qwang@nju.edu.cn) and Dechen Su (sudechen@163.com)

Received: 24 October 2016 – Revised: 10 March 2017 – Accepted: 13 March 2017 – Published: 31 May 2017

Abstract. Continental scientific drilling can be regarded as "a telescope into the Earth's interior" because it provides process insight and uncompromised samples of rocks, fluids, and even sampled from the deep biosphere from the Earth's surface to great depths. As one of the three founding members of the International Continental Scientific Drilling Program (ICDP), ICDP China has made great achievements in many scientific drilling-related research fields. Based on the ICDP participation it attracted global attention of scientists and set up not only the Chinese Continental Scientific Drilling (CCSD) Program in 2001 but also a growing number of ambitious drilling projects in the country.

The 5158 m deep borehole of the CCSD project at Donghai County in the Sulu ultrahigh-pressure metamorphic terrain demonstrates that large amounts of crustal rocks of the South China Block have been subducted to at least 120 km, followed by rapid uplift. After successful completion of drilling at Donghai, several continental scientific drilling projects were conducted with funding of the Chinese government and partially with support of ICDP, resulting in a total drilling depth of more than 35 000 m. These projects encompass the Continental Environmental Scientific Drilling Program of China, the Scientific Drilling Project of Wenchuan Earthquake Fault Zone, the Continental Scientific Drilling Project of Cretaceous Songliao Basin, and the Program of Selected Continental Scientific Drilling and Experiments. On the occasion of the 20th anniversary of the ICDP and the 15th anniversary of the CCSD Program, this paper reviews the history and major progress of the CCSD Program.

1 Introduction

Flying into the outer space, going into the Earth's interior, and investigating the deep ocean floor have been dreams of mankind for the exploration of the nature. Numerous exploration projects to the space and the ocean floor have been carried out since 1950s. Twenty years have passed since the foundation of the International Continental Scientific Drilling Program (ICDP) in 1996. Symbolized as "a telescope into the Earth's interior", the ICDP aims to provide fresh samples from great depths to reveal the complex composition and structure of the continental crust, the Earth's fluid system, microbiological distribution, geothermal energy, and earthquake mechanisms. Chinese scientists were involved in many ICDP projects and contributed to the success of the ICDP in many research fields.

The ICDP only supports projects that address fundamental scientific issues of global significance. One of the most exciting discoveries in the last 3 decades is the global distribution of coesite- and diamond-bearing ultrahigh-pressure (UHP) metamorphic terranes, demonstrating that low-density continental material could be rapidly subducted to depths greater

than 100 km and then exhumed to the surface (Zheng, 2012; Hermann and Rubatto, 2014; Liou et al., 2014). Hence, continental subduction played a critical role in plate tectonics and material recycling between the crust and the upper mantle. Since the discovery of coesite and microdiamond from eclogites and their country rocks in the Dabie Mountains (Okay et al., 1989; Wang et al., 1989; Xu et al., 1992), extensive studies have shown that the Dabie–Sulu orogenic belt is one of the largest ($\sim 30\,000\,km^2$) and best exposed UHP metamorphic terranes in the world (Liou et al., 2014). As the first ICDP project in China, the Chinese Continental Scientific Drilling (CCSD) project began to drill the 5158 m deep borehole in Donghai County (Jiangsu Province) on 4 August 2001, which marked the starting point of the CCSD Program (Xu et al., 2009a).

Uplift of the Tibetan Plateau in the Cenozoic has had profound influence on the global climate change and inland aridification. In order to study the evolution of Asian monsoon and its relationship with regional tectonics and global climate change, the Lake Qinghai Drilling Project was conducted in 2005 to obtain high-quality geological and biological core records (An et al., 2006, 2012). On 12 May 2008, the M_w 7.9 Wenchuan earthquake happened along the Longmenshan thrust belt in the eastern margin of the Tibetan Plateau. In order to better understand the intracontinental earthquake mechanisms, Chinese scientists started the Wenchuan earthquake Fault Scientific Drilling (WFSD) project just 178 days after the earthquake (Li et al., 2013, 2014). The ongoing Continental Scientific Drilling Project of Cretaceous Songliao Basin started in April 2014 and will recover continuous high-resolution terrestrial achieves and Cretaceous climate change (Wang et al., 2008, 2013a, b). Besides these ICDP projects, from 2008 to 2012 the Chinese government also supported the Program of Selected Continental Scientific Drilling and Experiments, which consists of seven drilling projects on some key problems in continental dynamics. These projects provided scientific and technical preparation for the future superdeep borehole (over 10 000 m) in China.

On the occasion of the 20th anniversary of the ICDP and the 15th anniversary of the CCSD Program, we present a brief review of history and achievements of the CCSD Program.

2 The Chinese Continental Scientific Drilling project

2.1 History of the CCSD project

Preparation for the CCSD project can be traced back to 1988. Encouraged by the drilling projects of the Kola superdeep borehole and the Kontinentales Tiefbohrprogramm der Bundesrepublik Deutschland (KTB), Chinese scientists proposed a continental scientific drilling plan in mainland China in 1988. The Ministry of Geology and Mineral Resources of China, which was combined in the Ministry of Land Resources of China in 1998, started to investigate potential scientific drilling sites in 1991. After years of investigation and discussion, China founded the ICDP with Germany and the United States in February 1996. In July 1996, Chinese scientists hosted the ICDP workshop in Qingdao, eastern China, and proposed three UHP localities in the Dabie–Sulu orogenic belt from Jiangsu, Anhui, and Shandong provinces. Based on outcrops of UHP metamorphic rocks, seismic profiles, shallow boreholes, and technical feasibility, the Science Advisory Group of the ICDP agreed to select Maobei village in Donghai County (Jiangsu Province) as the drilling site of the CCSD project.

In June 1997, the CCSD project was listed as one of major scientific projects in the Ninth Five-Year Plan of China. This was an important step to get financial support from Chinese government. The first pre-pilot borehole CCSD-PP1 in the Zhimafang ultramafic massif in Donghai County was accomplished at a depth of 432 m in November 1997. Then in April 1998, the ICDP passed the drilling proposal of the CCSD project and funded USD 1.5 million in the form of drilling facilities. Drilling of the second pre-pilot borehole CCSD-PP2 at Maobei village in Donghai County started in December 1998, and reached a depth of 1028.68 m in June 1999. The CCSD-PP2 was the first scientific borehole with complete sampling and logging in China, and succeeded in core recovery of 92.8 %. Chinese engineers and technicians also used the CCSD-PP2 to test different drilling techniques and materials, as well as on-site measurements. In September 1999, Chinese government agreed the budget of the CCSD project. As the largest and most expensive geoscientific research project ever undertaken in China before 2005, the total cost of the CCSD project was CNY 176 million (about USD 21.3 million).

The CCSD project was the first scientific drilling project in an UHP terrane. The ICDP provided important help by inviting Chinese scientists and engineers to visit the KTB and attend training courses. Test of all drilling facilities and on-site measurements for the CCSD main borehole (CCSD-MH) began on 25 June 2001. Experts from the ICDP came to the drilling site at Maobei village to provide technical support. Chinese engineers developed new drilling and core recovery tools. With funding from the Ministry of Science and Technology, the Ministry of Land and Resources, the National Natural Science Foundation of China and the ICDP, the CCSD-MH was drilled to a depth of 5158 m from 4 August 2001 to 8 March 2005 (Fig. 1). The average core recovery of the CCSD-MH reaches 85.7 %. Meanwhile, the third pre-pilot borehole CCSD-PP3 penetrated 705 m into the Gangshang ultramafic massif in Ganyu County, with about 90 % core recovery.

The principal investigator (PI) of the CCSD project was Chinese Academician Zhiqin Xu, and the drilling project leader was Da Wang, a professor and senior engineer from the Geological Survey of China. More than 2000 people were involved in the CCSD project, including about 120 Chinese

Figure 1. Drilling site of the CCSD-MH at Maobei village in Donghai County, Jiangsu Province, eastern China.

scientists and technicians and 30 scientists from the United States, Germany, France, and Japan.

2.2 Geological background and scientific objectives of the CCSD project

The Dabie–Sulu orogenic belt was formed by northward subduction of the South China Block beneath the North China Block in the Triassic, and was then separated by the left-lateral strike-slip Tan-Lu fault into the Dabie Mountains in the west and the Sulu Terrane in the east (Fig. 2) (e.g., Cong, 1996; Xu et al., 2009a). The wide occurrence of coesite, microdiamond, UHP hydrous phases, and exsolution textures in eclogites, garnet peridotites, and their supracrustal country rocks indicates that the South China Block has been subducted to depths > 120 km at extremely low geotherms (for review see Liou et al., 2009). Most UHP metamorphic rocks in the Dabie–Sulu orogenic belt yield the Neoproterozoic protolith ages of 780–740 Ma and extremely low $\delta^{18}O$ values, which suggests their tectonic affinity to the South China Block (Zheng, 2008, and references therein). It is generally believed that the UHP metamorphism in the Dabie–Sulu orogenic belt occurred in the Triassic, but different methods result in large variations: ∼ 245 Ma from zircon U–Pb ages (Hacker et al., 1998) or 226 ± 2 Ma from a mineral Sm–Nd isochron dating (Li et al., 2000). Sensitive high-resolution ion microprobe (SHRIMP) U–Pb dating on coesite-bearing domains of metamorphic zircon bracketed the UHP metamorphism between 240 and 225 Ma, and the amphibolite facies retrogression between 215 and 205 Ma (e.g., Liu et al., 2004a, b, 2006; Wu et al., 2006). This suggests that the subducted crustal rocks experienced a rapid syn-collisional exhumation at mantle depths.

Both the Dabie Mountains and the Sulu Terrane consist of a series of high-pressure (HP) and UHP metamorphic slices bounded by ductile shear zones (Fig. 2a). The

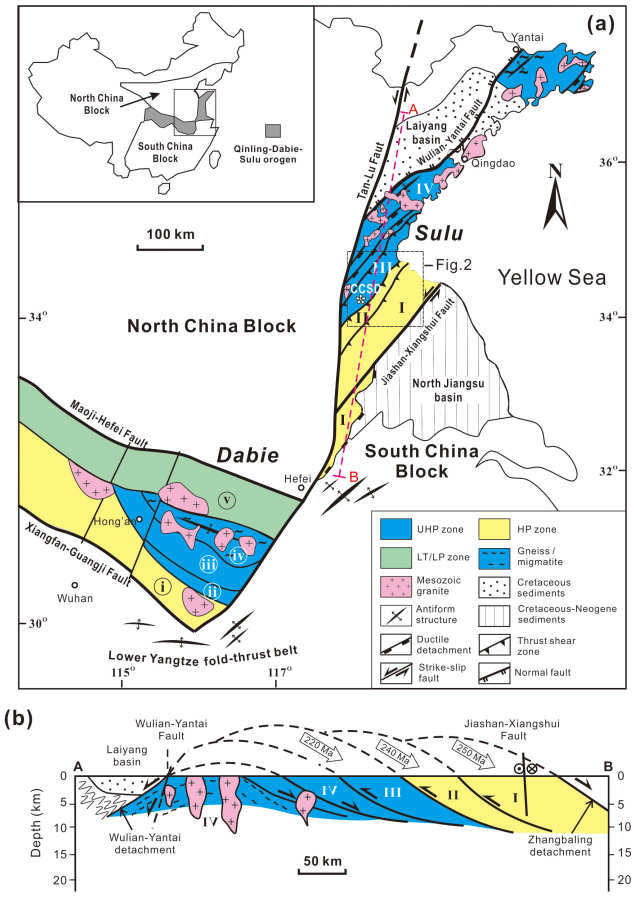

Figure 2. **(a)** Simplified geological map of the Dabie–Sulu orogenic belt and **(b)** cross section of the Sulu Terrane (modified after Xu et al., 2009b). The Sulu Terrane consists of four imbricate tectonic slices with different temperature (T) and pressure (P) conditions: I, southern low-T/high pressure (HP) glaucophane zone; II, central mid-T/HP kyanite zone; III, northern mid-T/ultrahigh-pressure (UHP) supracrustal zone; IV, northern high-T/UHP granitic zone. The Dabie Mountains consists of five zones from south to north: i, Susong low-T/HP blueschist facies zone; ii, south Dabie low-T/UHP zone; iii, central Dabie mid-T/UHP zone; iv, north Dabie high-T/UHP zone; v, Beihuaiyang low-T/low-P greenschist facies zone. Star denotes the drilling site of the CCSD-MH. Open arrows indicate top-to-the-northwest shearing related to exhumation of the Sulu Terrane, with the starting age of exhumation for different zones.

drilling site of the CCSD-MH is located in the northern UHP supracrustal zone in the Sulu Terrane, where eclogites and garnet peridotites appear as lenses, pods, or layers within coesite-bearing gneisses, quartzite, mica schists, and amphibolites. The northern UHP granitic zone is dominated by granitic gneisses and has been strongly modified by Cretaceous granitic plutons. Exhumation of the HP and UHP slices in the Triassic produced top-to-the-northwest (NW) ductile shear zones in the Sulu Terrane (Fig. 2b). Despite the post-collisional crustal extension and granitic intrusion,

Figure 3. Simplified lithological profile of the CCSD-MH in Donghai County (Liu et al., 2007).

the structural relationship between the HP and UHP slices is well preserved in the Sulu Terrane. Therefore, the CCSD-MH provides us a natural laboratory to investigate physical and chemical properties and geodynamic processes in a continental collision zone.

The objectives of the CCSD project were as follows: (1) to obtain multi-parameter profiles of a 5158 m deep borehole in the Sulu Terrane, (2) to reconstruct the composition and structure of a deep continental orogenic root, (3) to reveal subduction and exhumation processes of UHP metamorphic terranes, (4) to search deep life in the borehole and constrain fluid–rock interaction, and (5) to establish a long-term observation station using the CCSD-MH.

2.3 Outstanding progress of the CCSD project

The CCSD project has produced enormous amounts of data as well as technical innovation in drilling and core recovery. Combined with downhole logging, geophysical experiments, field survey, and laboratory measurements, fresh core samples from the CCSD project provide a valuable resource to study the structure, composition, deformation, physical properties, and material cycling in a continental subduction zone. These results made the Sulu Terrane a classic example to other continental collision zones such as the Himalayas and the Caledonides. In addition, a long-term observation station was set up in the CCSD-MH with continuous downhole monitoring on seismicity, fluid activity, stress, and temperature.

The main progress of the CCSD project is summarized below.

1. *Multi-parameter profiles of the 5158 m deep CCSD-MH*. A full range of physical and chemical measurements of core samples, as well as downhole logging, cuttings, and fluid measurements were carried out for the 5158 m deep CCSD-MH. About 60 precise and oriented profiles of the CCSD-MH were established, including petrology (Fig. 3), structure (Fig. 4), geochemistry, petrophysics, wellbore breakout, mineralization, fluids, geochronology, oxygen isotopes, heat production elements, downhole logging, and geophysical experiments. These multi-parameter profiles provide a new window into the deep root of a continental collision belt and set up the correlations between chemical and physical properties of UHP rocks.

2. *Evidence of deep subduction of huge amount of supracrustal materials*. Coesite inclusions in zircon are widely found in eclogites, paragneiss, orthogneiss, schists, kyanite quartzite, and marbles from the surface to 5158 m depth in the CCSD-MH (Fig. 3) (Liu et al., 2007). Combined with the spatial distribution of UHP rocks in the Dabie–Sulu orogenic belt, huge amounts of supracrustal materials of the South China Block have been subducted to depths of > 100 km and experienced in situ UHP metamorphism.

3. *Timing of subduction, exhumation, and uplift of the Sulu Terrane*. The timing of subduction, exhumation, and uplift, as well as the protolith ages of the core samples from the CCSD-MH and pre-pilot boreholes,

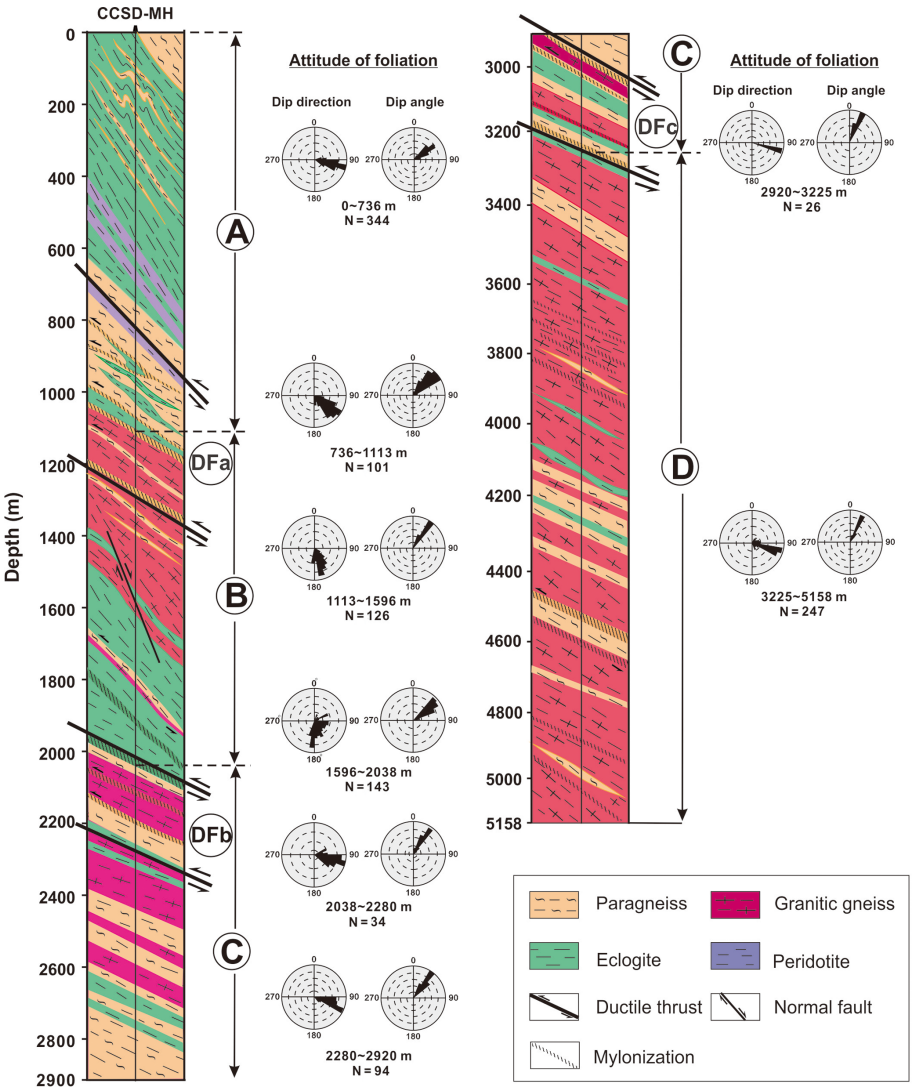

Figure 4. Simplified structural profile of the CCSD-MH in Donghai County (Xu et al., 2009b). The three southeast (SE)-dipping ductile shear zones DFa, DFb, and DFc can be traced to the surface according to seismic reflection profiles.

were determined by integrated studies of petrology and geochronology. Zircon U–Pb dating by the SHRIMP and laser ablation inductively coupled plasma mass spectrometry (LA-ICP-MS) indicate an inherited magmatic core of 790–680 Ma, eclogite facies prograde metamorphism at 246–244 Ma, UHP metamorphism at 235–225 Ma, HP eclogite facies recrystallization at 225–215 Ma, and amphibolite facies retrogression at 215–205 Ma (Liu et al., 2001, 2004a, b, 2007; Liu and Liou, 2011; Zhang et al., 2009). In addition, ^{40}Ar / ^{39}Ar cooling ages of biotite from ductile shear zones in the CCSD-MH vary from 218 to 202 Ma, suggesting the activation of shear zones during exhumation of UHP metamorphic rocks (Xu et al., 2009b). Apatite fission track analysis indicates an average uplift rate of $\sim 35\ m\ Ma^{-1}$ during 89–30 Ma (Liu et al., 2009).

4. *Origin of seismic reflections and crustal structure of the Sulu Terrane*. The origin of seismic reflections in the Sulu Terrane was constrained by comparing the lithological/structural profiles (Figs. 3–4), seismic properties of UHP rocks (Kern et al., 2002; Wang et al., 2005a) with the velocity profile of the CCSD-MH, and the seismic reflection profile across the drilling site (Yang, 2009) (Fig. 5) (Xu et al., 2009a). Strong reflections occur at the lithological interfaces between eclogites and country rocks (i.e., paragneiss, granitic gneiss, amphibolite), as well as between eclogite and retrograde eclogite, between eclogite and serpentinized peridotite. Ductile shear zones are extremely reflective. The HP and UHP slices in the Sulu Terrane occur as an eroded rootless dome structure and have been thrust along a se-

ries of shear zone over a UHP-free middle-lower crust (Figs. 2b and 6) (Wang et al., 2005b; Xu et al., 2009b).

5. *New tectonic model of the Sulu Terrane*. Crustal structure and pressure–temperature–time–deformation paths of the core samples and outcrop rocks indicate a dome-shaped nappe structure and syn-collisional exhumation of the HP and UHP slices in the Sulu Terrane (Fig. 6) (Xu et al., 2009b). The upper crust of the South China Block was subducted northward to a depth of ∼ 30 km before 253 Ma, and then uplifted to the shallow depth at 250–210 Ma (southern low-T/HP glaucophane zone). The supracrustal rocks continued subduction to ∼ 60 km and began exhumation at ∼ 240 Ma (central mid-T/HP kyanite zone). At 240–225 Ma, the supracrustal rocks have been subducted to at least 100 km and experienced UHP metamorphism, and exhumed to ∼ 30 km at 215–205 Ma. Hence, the UHP rocks experienced fast exhumation ($\sim 5\,km\,Ma^{-1}$) at 225–205 Ma at mantle depths, slow uplift ($0.96\,km\,Ma^{-1}$) due to Cretaceous granite intrusion and tectonic extension, and unroofing ($\sim 35\,m\,Ma^{-1}$) at 89–30 Ma.

6. *Significant ^{18}O depletion and limited fluid activity in the Sulu Terrane*. An O isotope profile of the CCSD-MH reveals ^{18}O depletion as deep as 3300 m and O isotope heterogeneity between the different and same lithologies on scales of 20 to 50 cm, which are consistent with observations of outcrop rocks and demonstrate limited fluid activity during continental subduction and UHP metamorphism (Zheng et al., 2009). Retrograde fluids came from decomposition of hydrous minerals and the exsolution of structural hydroxyl in nominally anhydrous minerals such as omphacite and garnet. The lithological contacts between eclogites and gneisses are the most favorable place for fluid activity.

7. *Bacteria and archaea discovered in the CCSD-MH*. About 20 species of bacteria and 4–5 species of archaea were identified from eclogites, amphibolites, and gneisses of the CCSD-MH by DNA analysis. Microbes show a great diversity including metal reducers, methanogens, and methanotrophs, but the diversity decreases with depth. The deepest bacteria occur at 4406.49 m, which gives the bottom boundary for life under extreme conditions in a deep borehole (Fig. 7) (Wang et al., 2006).

3 The Continental Environmental Scientific Drilling Program of China

In the late 1990s, Zhisheng An and his group at the Institute of Earth Environment, the Chinese Academy of Sciences proposed to carry out environmental scientific drilling

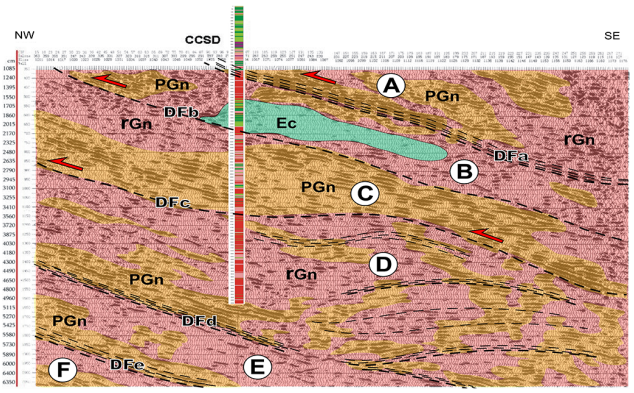

Figure 5. Interpretation of seismic reflection profile across the CCSD-MH (Xu et al., 2009a). A, B, C, D, E and F represent slices of UHP rocks. Ductile shear zones (DFa, DFb, DFc, DFd, and DFe) are recognized according to lithological/ structural profiles and reflectivity. Ec: eclogite; PGn: paragneiss; rGn: granitic gneiss.

in China. The Continental Environmental Scientific Drilling (CESD) Program of China started in 2001 under joint support from the Ministry of Science and Technology, Chinese Academy of Sciences, National Natural Science Foundation of China. This program aims to obtain high-quality geological and biological core records in different environments in China. The core samples will allow scientists to investigate the evolution of Asian monsoon and inland aridification and its relations with regional tectonics and global climate change, and to predict the climate trend in the future. Zhisheng An is the PI of the CESD Program.

The first borehole of the CESD Program was drilled in 2001 in the Heqing Basin in Yunnan Province, to obtain lacustrine deposits for glacial–interglacial Indian summer monsoon dynamics. In 2003 and 2004, ∼ 2000 m core samples in total (including two deep boreholes: 751.98 m deep Ls1 and 1050.60 m deep Ls2) were retrieved from Lop Nor, a former salt lake in the Tarim Basin. In 2005, Lake Qinghai Drilling Project was co-funded by the ICDP, Chinese Academy of Sciences and the Ministry of Science and Technology, to investigate the correlation between Asian monsoon and inland aridification during uplift of the Tibetan Plateau.

In addition, late Cenozoic eolian loess–red clay sequences on the Chinese Loess Plateau contain abundant paleoclimatic and paleoenvironmental information, which have been regarded as indicators of paleomonsoon changes and inland Asia desertification. In 2006, two boreholes (555.7 m deep ZL1 and 308.5 m deep ZL2) were obtained at Zhuanglang County in the western Chinese Loess Plateau and mainly consist of red clay sediments. Since then, a series of drilling projects on loess and lacustrine deposits have been carried out in the Chinese Loess Plateau (e.g., Luochuan, Jingbian) and Xinjiang (e.g., Ili Basin, Junggar Basin). So far the CESD Program has obtained over 10 000 m core samples

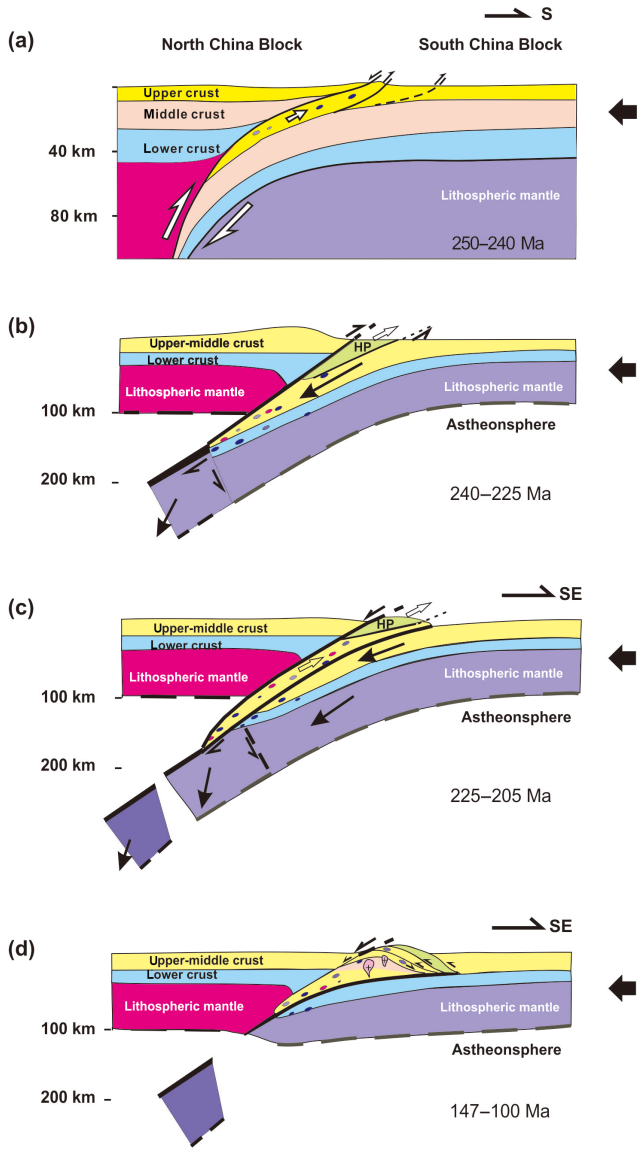

Figure 6. Subduction and exhumation history of the Sulu Terrane (modified after Xu et al., 2009b).

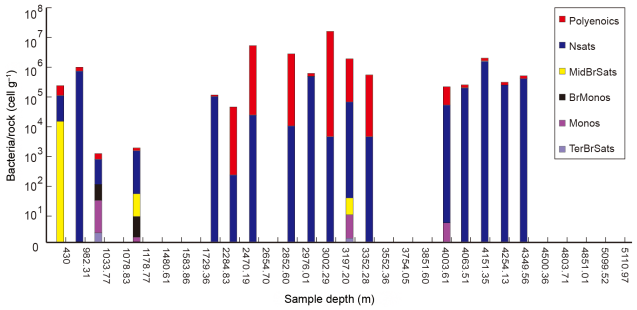

Figure 7. Bacteria and Archaea species from core samples of the CCSD-MH.

from the Tarim Basin and the Ili Basin in the western arid area, Lake Qinghai and the Loess Plateau in semiarid area, the Heqing Basin in the Indian monsoon area, and the Jianghan Plain in the eastern monsoon area. Great advances have been made in recent years. Here we briefly summarize the results of the Heqing Basin and Lake Qinghai drilling projects.

3.1 Heqing Basin Drilling Project: glacial–interglacial Indian summer monsoon dynamics

The modern Indian summer monsoon (ISM) is characterized by exceptionally strong interhemispheric transport, indicating the importance of both Northern and Southern hemispheres processes driving monsoon variability. The first borehole of the CESD penetrated 666 m sedimentary sequence in the Heqing paleolake in the southeastern margin of the Tibetan Plateau in 2002. It is so far the longest high-resolution continental record for the ISM evolution.

High-resolution continental record from the Heqing Basin demonstrates the importance of interhemispheric forcing in driving ISM variability at the glacial–interglacial timescale. Interglacial ISM maxima are dominated by an enhanced Indian low associated with global ice volume minima. In contrast, the glacial ISM reaches a minimum, and actually begins to increase, before global ice volume reaches its maximum (Fig. 8). An et al. (2011) indicated that the changing ISM was driven by the relative dominance of the northern low-pressure and southern high-pressure systems during the Pleistocene; both are indispensable for understanding monsoon dynamics. They attribute this early strengthening to an increased cross-equatorial pressure gradient derived from Southern Hemisphere high-latitude cooling. This mechanism explains much of the non-orbital scale variance in the Pleistocene ISM record. The new insight into the ISM on the geological timescale is important for our understanding of global climate evolution in the past. It also provides background information for present and future monsoon changes under global warming (An et al., 2006).

3.2 Lake Qinghai Drilling Project: interplay between the Westerlies and Asian monsoon

As the second ICDP project in China, Lake Qinghai Drilling Project was conducted in 2005. A total of 323.23 m cores were acquired with GLAD800 drilling system by US Lake Drilling Company (DOSECC) at different sub-basins in Lake Qinghai. In addition, two onshore sites were drilled successfully at Erlangjian (1108.9 m with core recovery > 90 %) and Yilangjian (628.5 m) on the southeastern shore of the lake using Chinese equipment (An et al., 2006).

Lake Qinghai is located in the northeastern margin of the Tibetan Plateau. It is extremely sensitive to climate changes because it lies in a critical transitional zone between the humid climate region controlled by the East Asian monsoon and the dry inland region affected by westerly winds. High-

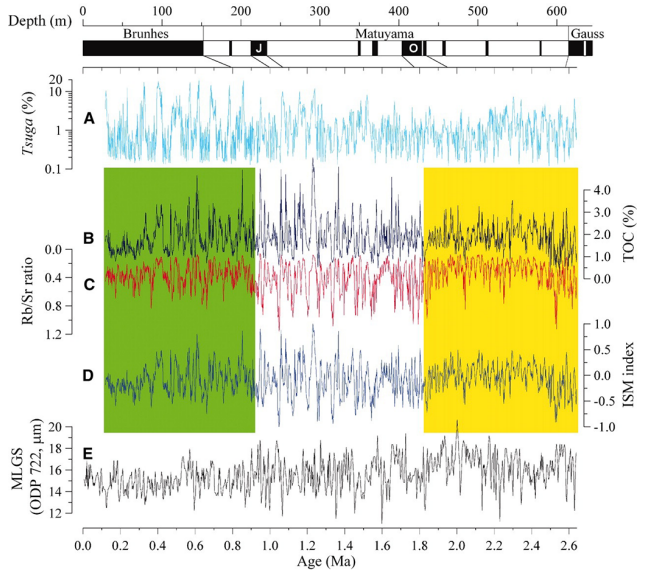

Figure 8. Proxy ISM records since 2.60 Ma from the Heqing Basin, southwestern China (An et al., 2011).

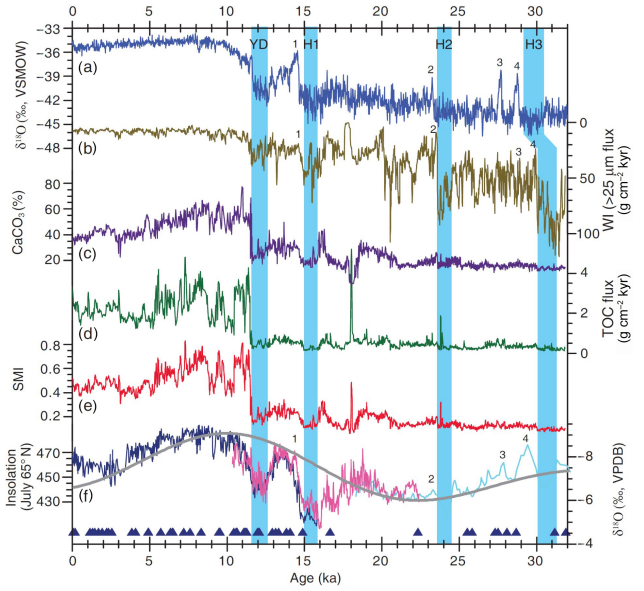

Figure 9. Comparison of Lake Qinghai records with other records during the last 32 kyr (An et al., 2012). **(a)** NGRIP $\delta^{18}O$[26]; **(b)** North Atlantic ice-rafted hematite stained grains; **(c)** Lake Qinghai Westerlies climate index (WI, flux of >25 μm fraction); **(d)** Lake Qinghai Asian summer monsoon index (SMI); **(e)** $\delta^{18}O$ record of ostracods from Lake Qinghai; **(f)** Dongge cave speleothem $\delta^{18}O$[21]; **(g)** atmosphere $\Delta^{14}C$[38].

resolution magnetostratigraphy of Yilangjian core samples provides a chronological record back to ~5.1 Ma (Fig. 9). Analysis of lithofacies and depositional environments reveal that the change from eolian to lacustrine facies occurred ~4.63 Ma, corresponding to a shift from an arid/semi-arid to a more humid climate, which resulted in the origin of Lake Qinghai (Fu et al., 2013). Changes in sediment lithology and mean grain size indicate that the lake level fluctuated considerably, superimposed on a long-term trend from higher to lower levels in response to East Asian Monsoon variations. This archive provides important information on regional and global environmental change, because so far records from northern China are mainly based on analysis of loess.

The longest core in the Lake Qinghai was obtained in the depositional center of the southwestern sub-basin. The results, constrained by high-resolution AMS ^{14}C dating (An et al., 2012), show the variability of both the Westerlies and the Asian summer monsoon (ASM) since 32 ka. These records document the anti-phase relationship of the Westerlies and the ASM on both glacial–interglacial and glacial millennial timescales (Fig. 9). During the last glaciation, the influence of the Westerlies dominated. Prominent dust-rich intervals, correlated with Heinrich events, reflect intensified Westerlies linked to northern high-latitude climate. During the Holocene, the dominant ASM circulation, punctuated by weak events, indicates linkages of the ASM to orbital forcing, North Atlantic abrupt events, and perhaps solar activity changes (An et al., 2012).

4 Wenchuan earthquake Fault Scientific Drilling project

4.1 Geological background and scientific objectives of the WFSD project

On 12 May 2008, the M_w 7.9 Wenchuan earthquake happened along the northeast (NE)-striking Longmen Shan thrust belt in the eastern margin of the Tibetan Plateau and caused death of over 69 227 people and enormous economic loss. In contrast to extremely low GPS shortening rate in the Longmen Shan thrust belt before the earthquake (Zhang et al., 2004), the Wenchuan earthquake is characterized by >4 m coseismic slip with comparable magnitude of reverse and right-slip components. It produced 270 km long surface rupture along the NE-striking Yingxiu–Beichuan fault, and 80 km long surface rupture along the Anxian–Guanxian fault simultaneously (Li et al., 2008; Liu-Zeng et al., 2009) (Fig. 10).

In order to better understand the fault mechanism and the physical and chemical characteristics of the eastern margin of the Tibetan Plateau, Chinese scientists carried out the WFSD project just 178 days after the earthquake, as an extremely rapid response to the devastating Wenchuan earthquake. The PI of the WFSD project was Zhqin Xu from Chinese Academy of Geological Sciences. The WFSD project eventually drilled six boreholes along the two main earthquake faults (Fig. 11). The first hole (WFSD-1) started on 6

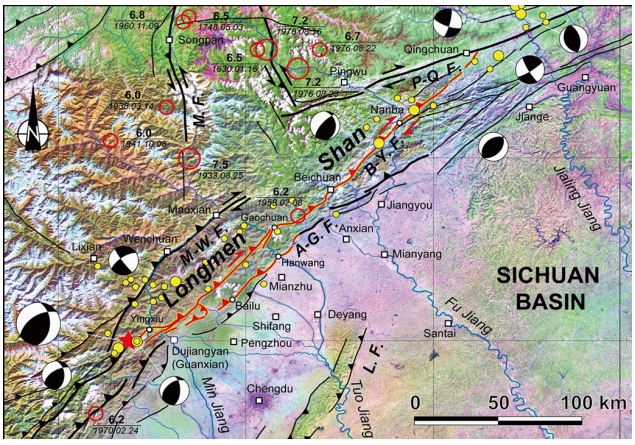

Figure 10. Recent large earthquakes along the eastern margin of the Tibetan Plateau. Red lines show two surface rupture zones caused by the M_W 7.9 Wenchuan earthquake.

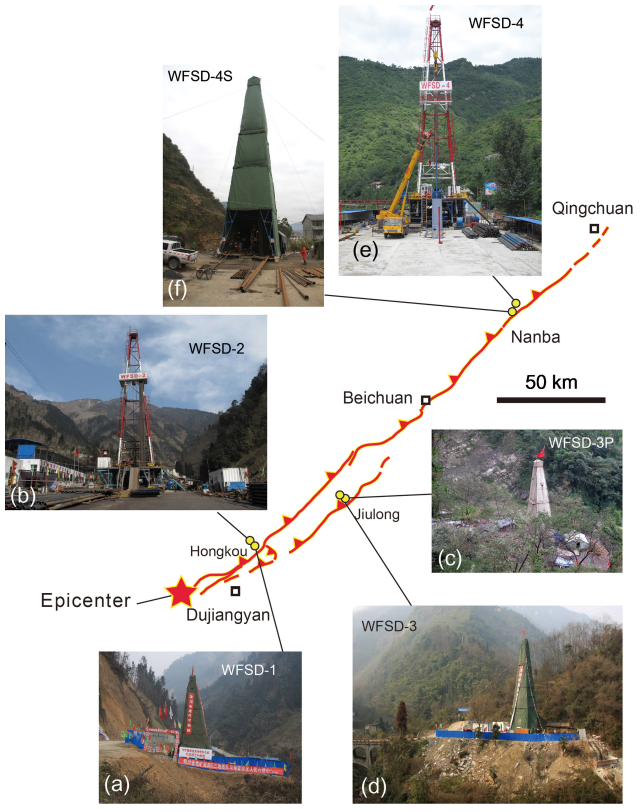

Figure 11. Drilling sites of the Wenchuan Seismic Fault Scientific Drilling along the Longmen Shan thrust belt.

November 2008 and was completed on 12 July 2009, with a total depth of 1201.15 m.

The scientific objectives of the WFSD project are as follows: (1) to determine the composition, texture, and structure of the fault zones; (2) to reconstruct the physical and chemical properties of the fault zones during the earthquake (frictional coefficient, pore pressure, stress, permeability, seismic velocities, mineral, and chemical compositions), energy budget, and rupture processes; (3) to improve our understanding of the transpressional behavior of this fault zone; (4) to provide key information for the early warning system of future large earthquakes; and (5) to establish a long-term earthquake monitoring station by putting instruments the boreholes.

4.2 Main progress of the WFSD project

So far the main results from the WFSD project are as follows:

1. Based on petrological and structural analysis of the core samples from the WFSD project, fault-related rocks (fault gouge, cataclasite, and fault breccia) in the Yingxiu–Beichuan fault and the principle slip zone (PSZ) of the Wenchuan earthquake were determined. Twelve of the 12 fault zones were identified in the entire core profile. At least 10 fault zones, including the Yingxiu–Beichuan fault zone, show a minimum thickness of $\sim$ 100 m. All major fault zones are characterized by high magnetic susceptibility, low density, and high porosity, with mostly low resistivity, high natural gamma ray, and sound wave velocity (Fig. 12). The high magnetic susceptibility values most likely result from the transformation of magnetic minerals by frictional heating due to the earthquake (Li et al., 2013).

2. The PSZ of the Wenchuan earthquake was found at a depth of 590 m with 1 cm wide fresh fault gouge, as determined by logging data, such as temperature, natural gamma ray, P-wave velocity, and resistivity, combined with the fresh appearance, magnetic susceptibility, and microstructure of the gouge (Fig. 12). The high gamma radiation, porosity, and P-wave velocity, as well as low resistivity, temperature anomalies, and clay mineral anomalies indicate that the Wenchuan earthquake fault zone is located at depth of 585.75–594.5 m, with an average inclination and dip angle of 305° N and 71°, respectively (Li et al., 2014; Si et al., 2014). The Wenchuan earthquake slip plane has a dip angle of 71–65° in the WFSD-1, showing the high-angle thrust feature.

3. The dominant fractures in the core samples of the WFSD-1 above 600 m are dipping south with a dip angle of 60°, and change to the NE dipping with a dip angle of 61–83° below 780 m, which represent the fracture characteristics in the Pengguan Complex and the Xujiahe Formation, respectively. Hence, the hanging wall and footwall of the Yingxiu–Beichuan fault have different stress fields, implying that the Pengguan Complex is allochthon (Li et al., 2014).

4. Deformation experiments and microstructural observations of core samples from the fault slip zone of the

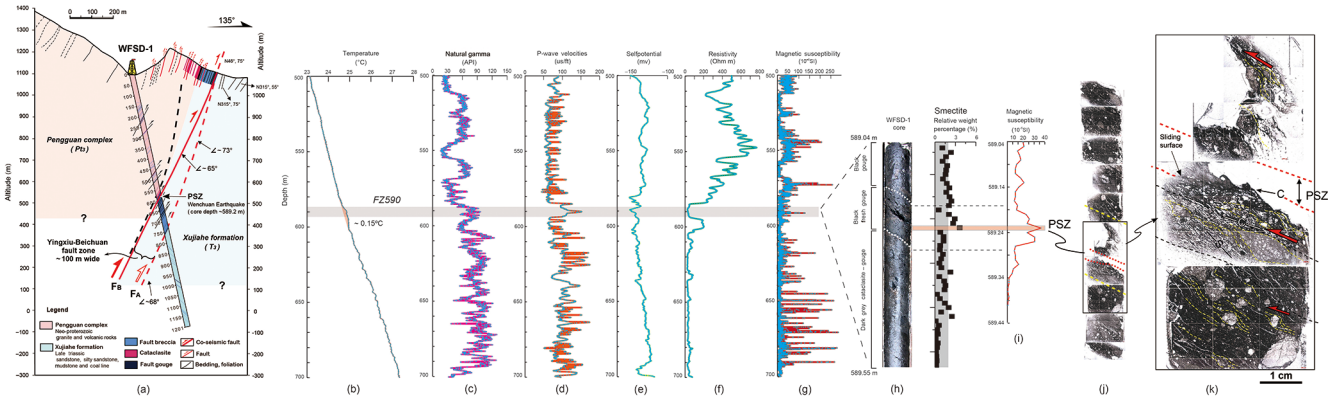

Figure 12. Cross section, logging, and core data of the WFSD-1. The physical anomalies in logging data **(b–g)** correspond to the fault gauge **(h–k)** related to the principle slip zone (PSZ) of the Wenchuan earthquake (Li et al., 2013).

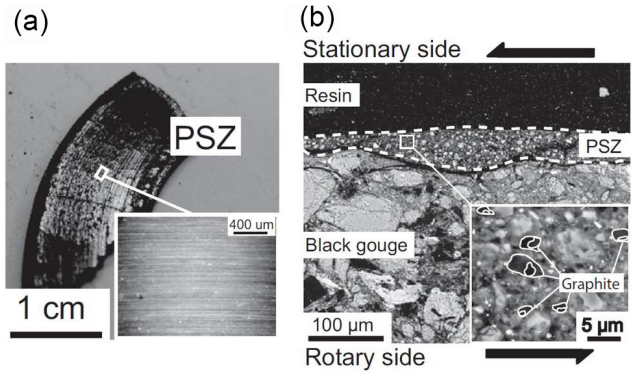

Figure 13. Microstructural characteristics of experimentally deformed black gouges at 15 MPa (Kuo et al., 2014). **(a)** Photograph of highly reflective surface of the principle slip zone (PSZ) lined by slicken lines and grooves that track the rotary motion of the gouge holder. **(b)** Backscattered scanning electron microscope (SEM) image of a thin section. The fine-grained PSZ developed adjacent to the stationary side of the gouge holder. Inset backscattered SEM image shows occurrence of small graphite particles by heating of carbonaceous materials (mainly anthracite) during experiments.

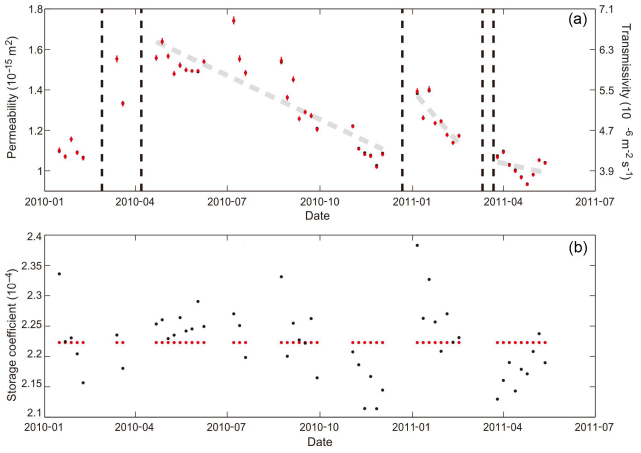

Figure 14. Hydrogeologic properties of the well–aquifer system over time for the WFSD-1 (Xue et al., 2013). **(a)** Permeability and transmissivity; **(b)** storage coefficient. Values were inverted from the phase and amplitude of each 29.6-day segment based on the analytical model. Segments that overlap the remote earthquakes (vertical dashed lines) were not inverted. The black dots denote an unconstrained inversion; the red dots are the results of inversion with the storage coefficient fixed to a single value. The best-fit linear trends between each set of permeability data are shown as light gray dashed lines.

WFSD-1 indicate gouge graphitization and dynamic fault weakening (Fig. 13). This suggests that the Longmen Shan fault was extremely weak at borehole depths during the M_w 7.9 Wenchuan earthquake, and that enrichment of graphite along localized slip zones could be used as an indicator of transient frictional heating during seismic slip in the upper crust (Kuo et al., 2014).

5. Permeability controls fluid flow in fault zones and is a proxy for rock damage after an earthquake. The tidal response of water level in the WFSD-1 was used to track permeability variations for 18 months in the damage zone of the M_w 7.9 Wenchuan earthquake (Fig. 14). The unusually high hydraulic diffusivity of 2.4×10^{-2} m^2 s^{-1} implies a major role for water circulation in the fault zone. For most of the observation period, permeability of the rocks decreased rapidly as the fault healed. The trend was interrupted by abrupt permeability increase due to shaking from remote earthquakes. The continuous permeability measurements reveal a process of punctuated recovery as healing and damage interact in the aftermath of a large earthquake (Xue et al., 2013).

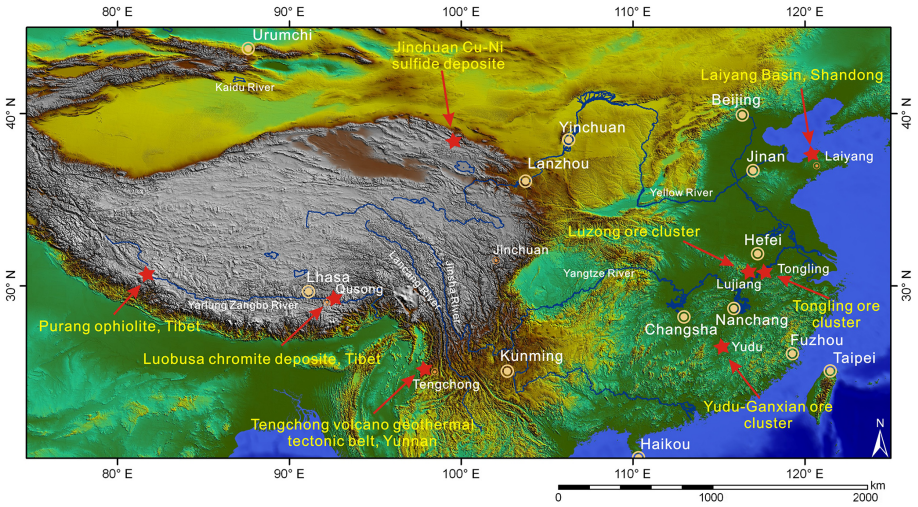

Figure 15. Location of boreholes of Program of Selected Continental Scientific Drilling and Experiments.

5 Program of Selected Continental Scientific Drilling and Experiments

5.1 Scientific objectives

The SinoProbe Program is the Chinese government-funded Earth science program with the overall aim of exploring the composition, structure, and evolution of the continental lithosphere beneath China and the processes causing geohazards and natural resources (Dong et al., 2013). As one part of the SinoProbe Program, the Program of Selected Continental Scientific Drilling and Experiments (SCSDE) consisted of seven drilling projects in critical tectonic and mineral resource regions from 2008 to 2012. It includes the Jinchuan Cu–Ni sulfide deposits in Gansu Province, the Luobusa chromitite deposits in Tibet, the Tengchong volcanothermal tectonic zone in Yunnan Province, the boundary of the North China and South China blocks in the Laiyang Basin of Shandong Province, the Yudu–Ganxian polymetallic deposits in South China, the Tongling polymetallic deposit, and the Luzhong volcanic basin and mineral deposit district in Anhui Province (Fig. 15). The PI of the SCSDE Program is Jingsui Yang from Institute of Geology, Chinese Academy of Geological Sciences.

5.2 Progress of the Luobusa Scientific Drilling Project

Ophiolites along the 2000 km long Yarlung Zangbo suture zone in the Tibetan Plateau mark the collision boundary between the Indian and Eurasian plates. These ophiolites mainly consist of harzburgites and dunites, with minor gabbro dikes and basalts. The Luobusha ophiolite massif contains significant podiform chromitites, which appear as lenticular boudins of high-chrome chromite within dunites (Zhou et al., 1996). This ophiolite massif is believed to have formed initially at an oceanic spreading center at 176 Ma and then been modified by melt–rock reaction in a suprasubduction zone at 126 Ma. However, discovery of diamond and some UHP minerals in the Luobusha ophiolite challenges the traditional formation theory of ophiolites (Yang et al., 2007).

The Luobusa Scientific Drilling Project aims to reveal the formation conditions of the deep mantle minerals, the metallogenic mechanism and prospecting criteria of ophiolite-type chromite deposit. The first borehole LBSD-ZK1 ended at a depth of 1478.8 m with the average core recovery of 94 %. The second borehole LBSD-ZK2 has reached a depth of 1600 m with the average core recovery of > 90 %, and the target depth is 2000 m.

The lithological profile of the LBSD-ZK1 indicates that the upper 70 m is composed of Triassic sandstones, marbles, and chlorite schists, which are in a fault contact with the underlying ultramafic massif. Beneath the fault, there are 1400 m thick ultramafic rocks. The rest over 100 m cores are cumulates of dunites and pyroxenites, suggesting that the Luobusha massif is a tectonic slice with a reversed strata sequence (Fig. 16).

Recent studies found abundant diamonds from peridotites and chromitites in ophiolites along the Yarlung Zangbo suture zone, the early Paleozoic Ray–Iz ophiolite in polar Urals (Russia), and in Myanmar (Fig. 17). Chromitites from ophiolites contain crustal minerals such as zircon, and some highly reducing minerals such as carbides, nitrides, and metal alloys (Yang et al., 2014). Some of the minerals are very high-pressure phases, implying their origin depth near the top of the mantle transition zone. These new results suggest that crustal materials may be subducted to mantle transition zone and subsequently exhumed during the initiation of new subduction zones.

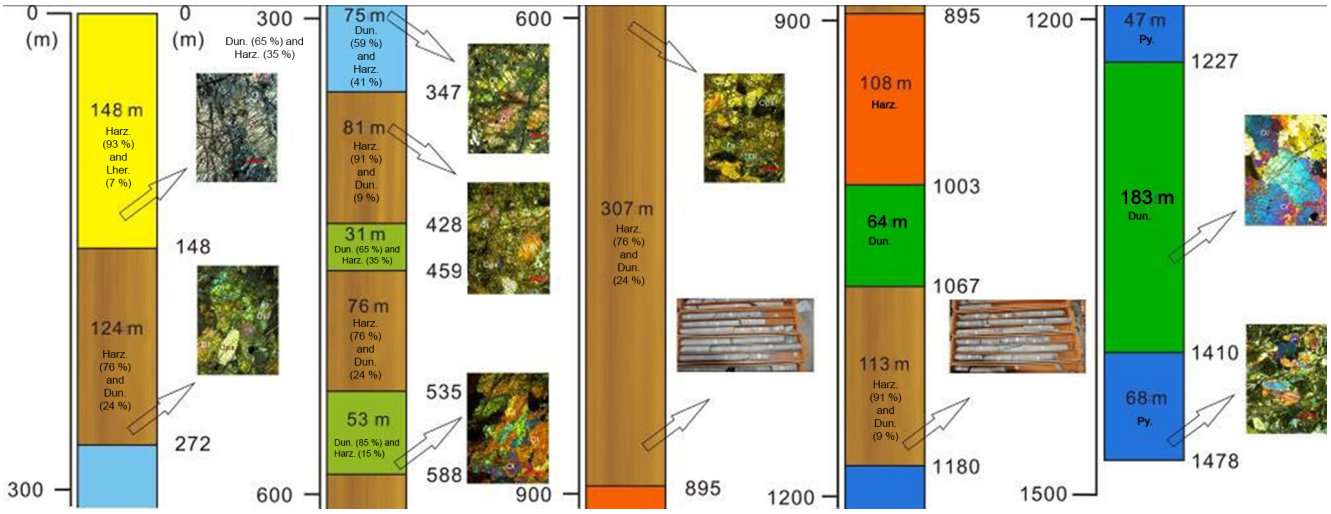

Figure 16. Lithological profiles of the LBSD-ZK1 at the Luobusha ophiolite massif in Tibet.

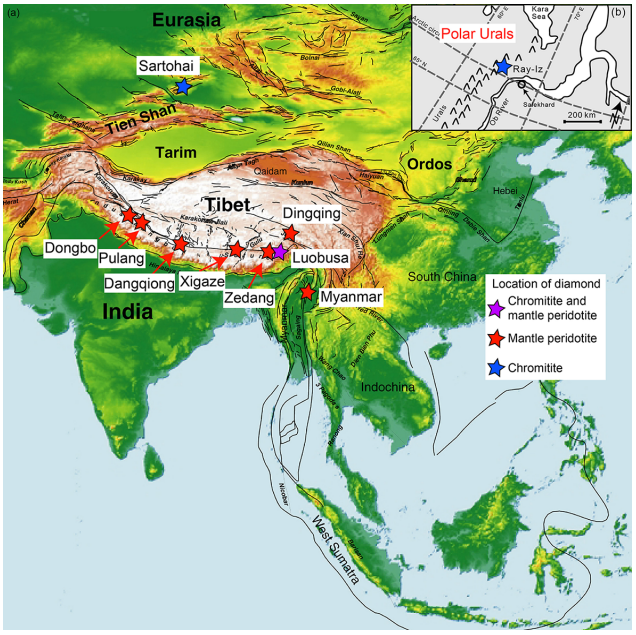

Figure 17. Locations of ophiolite-type diamonds discovered so far. Six locations, including Dongbo, Purang, Dangqiong, Xigaze, Zedang, and Luobusa, and are situated along the Yarlung Zangbo suture zone. One location is at Dingqing in the Bangong–Nujjiang suture, Tibet, one in Myanmar, one in Sartohai in Xinjiang Province (China), and one (see inset map) in the polar Urals, Russia.

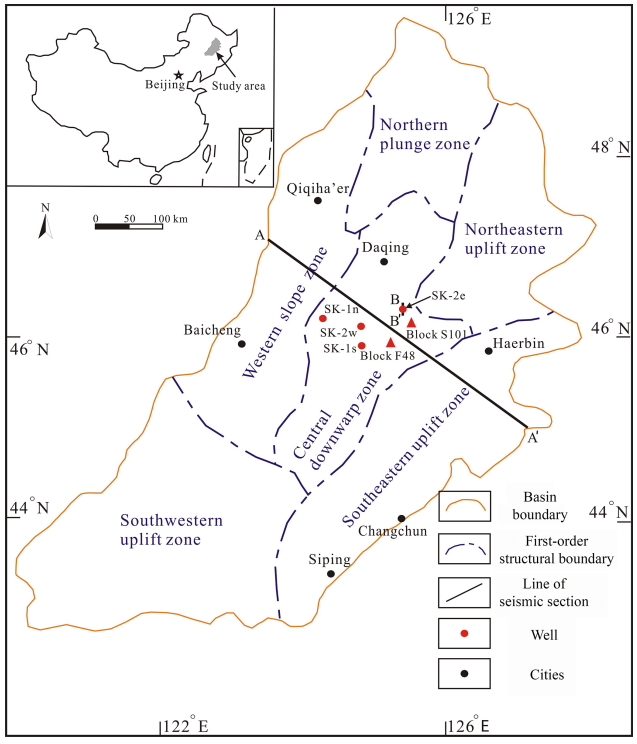

Figure 18. Tectonic scheme of the Songliao Basin with the location of SK-1 and SK-2 boreholes. The tectonic scheme is according to Zhou and Littke (1999). SK-1s and SK-1n are the north and south hole sites of SK-1, respectively, while SK-2e and SK-2w are the east and west hole sites of SK-2, respectively. A–A′: the SE–NW cross-seismic profile.

6 Continental Scientific Drilling Project of Cretaceous Songliao Basin

6.1 Geological background and scientific objectives

The Songliao Basin in northeastern China is one of the largest oil- and gas-bearing basins in China. Above a pre-Mesozoic basement, the Songliao Basin was filled predominantly with volcanoclastic, alluvial fan, fluvial, and lacustrine sediments of Late Jurassic, Cretaceous, and Paleogene ages. It can be divided into the six tectonic units: western

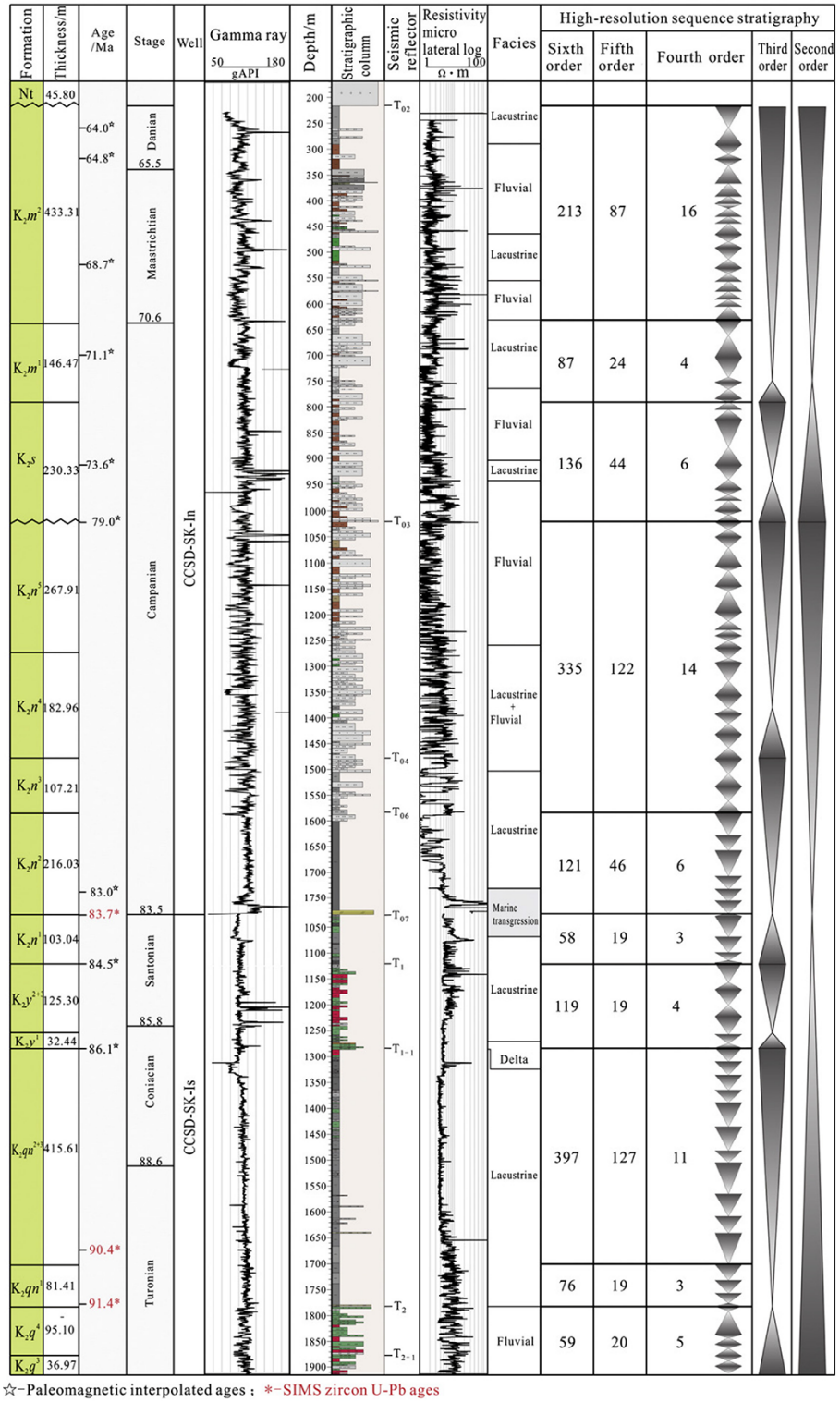

Figure 19. High-resolution sequence stratigraphy of Upper Cretaceous in the Songliao Basin. The figure on the right side of each segment is the number of cycles in each member or formation. Modified from Gao et al. (2009) (Wang et al., 2013b).

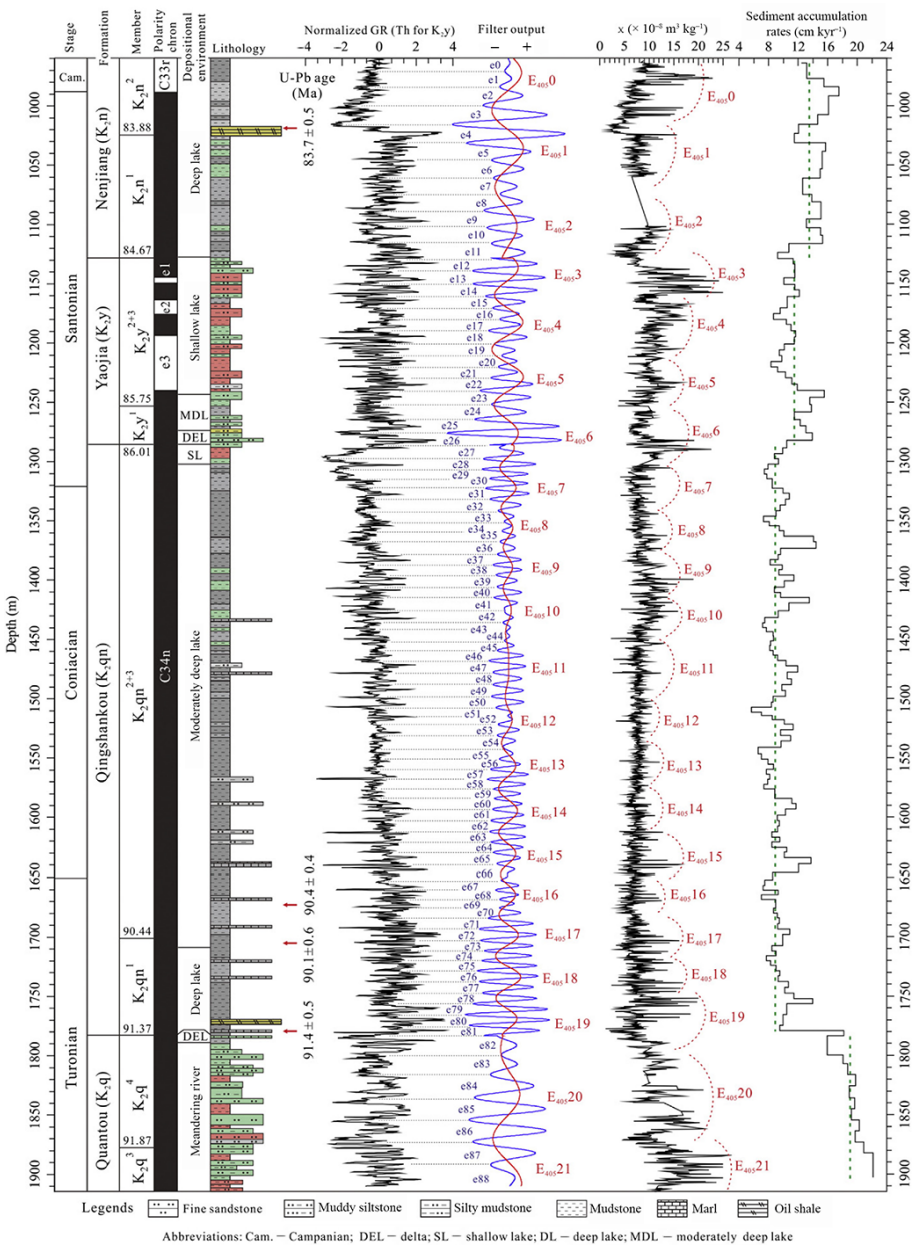

Figure 20. Cyclostratigraphic interpretation and sedimentary accumulation rates of the SK-1 south core in the Songliao Basin (Wang et al., 2013b). The numbers at the member column are the astronomical timescale ages in "Ma" for the strata boundaries. The "e" (blue) and "E" (red) represent 100 kyr short and 405 kyr long eccentricity cycles, respectively.

ramp region, northern plunge region, central depression region, northeastern uplift region, southeastern uplift region, and southwestern uplift region (Fig. 18) (Wang et al., 2013a).

There is an increasing likelihood that our world is moving toward a greenhouse state due to increases in anthropogenic carbon dioxide in the atmosphere (Hay, 2011). This change provides a powerful motivation for understanding the dynamics of Earth's past "greenhouse" climate. Cretaceous is characterized by long-term climate stability with warm equable climates due to a higher atmospheric greenhouse gas content, and punctuated by rapid climate events related to global carbon and hydrological cycle (Bornemann et al., 2008). The Continental Scientific Drilling Project of the Cretaceous Songliao Basin, composed of SK-1 and SK-2 boreholes, was proposed to recover almost full Cretaceous strata in the Songliao Basin in eastern China (Feng et al., 2013). The PI of this project is Chengshan Wang from China University of Geosciences (Beijing).

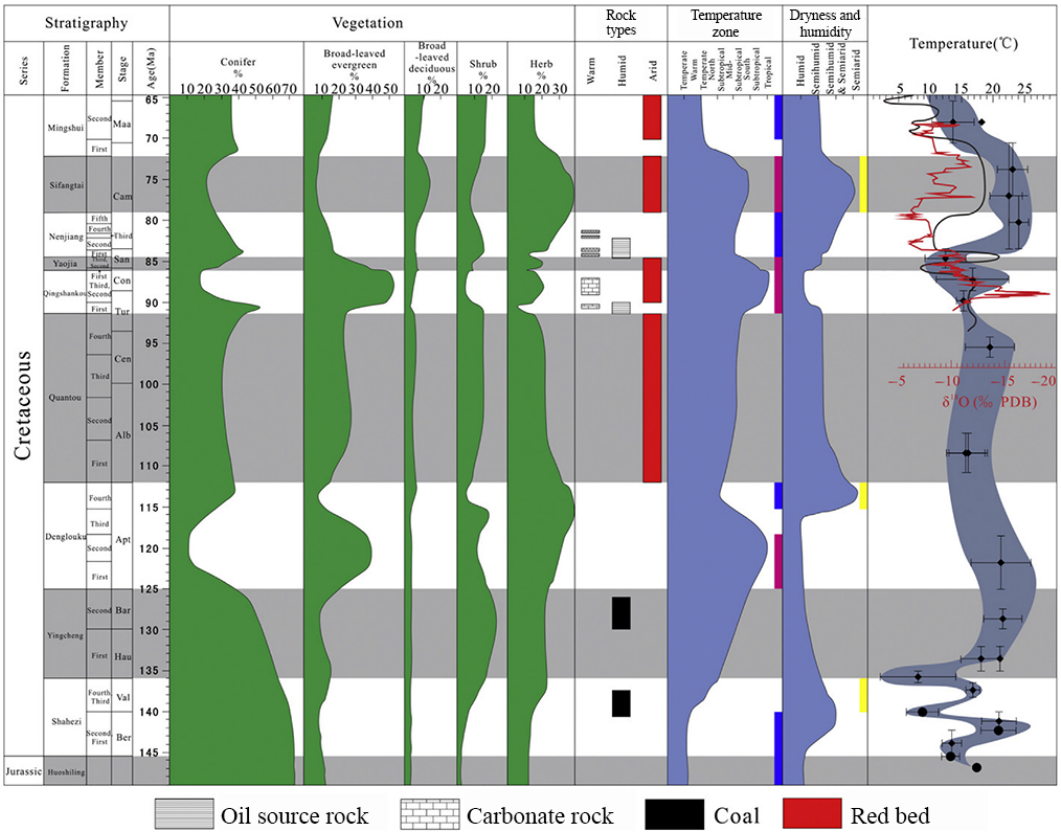

Figure 21. Cretaceous paleoclimate evolution of the Songliao Basin. Spore/pollen relative abundances, paleotemperature zones, and paleohumidity are from Gao et al. (2009). Those of the Far East are from Zakharov et al. (1999). The oxygen isotope data are from Chamberlain et al. (2013). The red bars indicate warming stages, the blue bars indicate cooling stages, and the yellow bars indicate semiarid stages.

6.2 Preliminary progress of the Songliao Basin Drilling Project

The newly finished SK-1 borehole has recovered Upper Cretaceous strata in the Songliao Basin, which offered an unprecedented chance to decipher the Cretaceous terrestrial climate change. The core samples reflect many facets of paleoenvironmental and climate changes during the Late Cretaceous in eastern China, which have attracted a wide range of Earth scientists to compare with other areas in the world.

Base-level cycles are driven either by relative sea level or by tectonic changes. In marine basins eustasy alters accommodation space as sea level rises and falls. In intracontinental basins tectonics drive both basin subsidence and depositional cycles. Core samples from the SK-1 indicate that the Songliao Basin was isolated from the ocean except for two brief periods in the late Turonian of the Qingshankou Formation and in the early Campanian in the lower part of the Nenjiang Formation (Xi et al., 2011). Paleoclimate research has shown that astronomical forcing drove global climate change in the Earth's history and may be recorded in both continental and marine sedimentary strata. The orbitally forced cycles are recorded in Cretaceous marine successions around the world, which provide a calibration tool of the Cretaceous timescale. Milankovitch cycles were recently identified in Late Cretaceous terrestrial strata in the Songliao Basin (Wang et al., 2013a).

High-resolution sequence stratigraphy of the Upper Cretaceous section cored in the SK-1 (Fig. 19) was based on centimeter-by-centimeter description integrated with well logs, seismic data, and well-to-well correlation in the Songliao Basin. Upper Cretaceous of the Songliao Basin can be subdivided into sequences of 2 second order, 6 third order, 72 fourth order, 527 fifth order and 1601 sixth order (Gao et al., 2009; Wang et al., 2013b).

Cyclostratigraphic analyses on the Quantou, Qingshankou, Yaojia, and Nenjiang Formations in the SK-1 south well confirmed the excellent preservation of astronomically driven sedimentary cycles, including long and short eccentricity, obliquity, and precession cycles constrained by four high-resolution SIMS U–Pb zircon ages (Fig. 20).

The climate history of the Songliao Basin is based on pollen and spore ratios (Fig. 21) using more than 20 000 samples from more than 500 cores. The Cretaceous vegetation landscape of the basin fluctuated between a conifer forest and an herbaceous-broadleaved forest. Climates of the Songliao

Basin are compared with the marine oxygen isotopic data of Far East (Zakharov et al., 1999) (Fig. 21). The classification of temperature zones is based on the species of spore/pollen spectra that define the tropical, tropical–subtropical, subtropical, tropical–temperate, and temperate, as well as the oxygen isotopic trends of the Songliao Basin. The dryness and humidity are based on species of parent plants of spore/pollen fossils subdivided into xerophyte, mesophyte, hygrophyte, helophyte, and hydrophyte, which correspond to arid, semiarid, semihumid and semiarid, semihumid, and humid, respectively.

Partially based on the successful SK-1 borehole, the ICDP approved the SK-2 drilling proposal in September 2009. The SK-2 borehole is to recover Lower Cretaceous strata with an estimated drilling depth of nearly 7000 m. Hence, the SK-1 and SK-2 boreholes can provide continuous sedimentary records of the Cretaceous in the Songliao Basin. The drilling operation of SK-2 started in April 2014, because Chinese engineers developed new drilling equipment for a superdeep borehole of $\sim$10 000 m. The SK-2 borehole also adopted "one-well, two-hole" design (Fig. 18). The west hole SK-2w is located in Changyuan of Daqing City and will recover the Quantou–Denglouku Formation. The east hole SK-2e is located in the Xujiaweizi Fault Depression, and will recover the Yingcheng Formation–Huoshiling Formation. The two holes will be interconnected and correlated by the T4 seismic reflection interface. The east and west holes of SK-2 will become the main wells of the proposed deep underground laboratory. The target depth of the east hole SK-2e is 6400 m, which will be the deepest one in the Songliao Basin and in eastern China. More comprehensive understanding of paleoenvironmental and climatic change for the Cretaceous Songliao Basin would be achieved after the accomplishment of the SK-2. Compared with drilling projects in the ocean, loess plateau, and modern lakes, scientific drilling projects in giant paleolakes should be an indispensable part to understand the paleoenvironments and climatic changes from the terrestrial realm.

7 Conclusions

Accompanied with growth of the ICDP, each project of the CCSD Program has a struggle history with expected and unexpected difficulties, and recorded the development in science and technology. The increasing international cooperation in the CCSD Program demonstrates that curiosity of scientists has no borders, and the science-driven policy of the ICDP is highly appreciated.

Data availability. Data used for this work can be found in An et al. (2011, 2012), Li et al. (2013), Xu et al. (2009b), and Xue et al. (2013).

Competing interests. The authors declare that they have no conflict of interest.

Acknowledgements. We are grateful to the ICDP, the Ministry of Land Resources of China, the Ministry of Science and Technology of China, and Natural Science Foundation of China for providing continuous support to the CCSD Program. We thank all crews, drilling team members, and lab technicians in the CCSD Program, and thank all scientists for making exciting discoveries from these boreholes. Constructive review of two anonymous reviewers and the editor T. Wiersberg is appreciated.

Edited by: T. Wiersberg
Reviewed by: two anonymous referees

References

An, Z. S., Wang, P., Shen, J., Zhang, Y., Zhang, P., Wang, S., Li, X., Sun, Q., Song, Y., Ai, L., Zhang, Y., Jiang, S., Liu, X., and Wang, Y.: Geophysical survey on the tectonic and sediment distribution of Qinghai Lake basin, Sci. China, Ser. D Earth Sci., 49, 851–861, 2006.

An, Z. S., Clemens, S. C., Shen, J., Qiang, X., Jin, Z., Sun, Y., Prell, W.L., Luo, J., Wang, S., Xu, H., Cai, Y., Zhou, W., Liu, X., Liu, W., Shi, Z., Yan, L., Xiao, X., Chang, H., Wu, F., Ai, L., and Lu, F.: Glacial-interglacial Indian summer monsoon dynamics, Science, 333, 719–723, 2011.

An, Z. S., Colman, S. M., Zhou, W., Li, X., Brown, E., Jull, A. J. T., Cai, Y., Huang, Y., Lu, X., Chang, H., Song, Y., Sun, Y., Xu, H., Liu, W., Jin, Z., Liu, X., Cheng, P., Liu, Y., Ai, L., Li, X., Liu, X., Yan, L., Shi, Z., Wang, X., Wu, F., Qiang, X., Dong, J., Lu, F., and Xu, X.: Interplay between the Westerlies and Asian monsoon recorded in Lake Qinghai sediments since 32 ka, Sci. Rep., 2, 619, doi:10.1038/srep00619, 2012.

Bornemann, A., Norris, R. D., Friedrich, O., Beckmann, B., Schouten, S., Damste, J. S. S., Vogel, J., Hofmann, P., and Wagner, T.: Isotopic evidence for glaciation during Cretaceous supergreenhouse, Science, 319, 189–192, 2008.

Chamberlain, C. P., Wan, X., Graham, S. A., Carroll, A. R., Doebbert, A. C., Sageman, B. B., Blisniuk, P., Kent-Corson, M. L., Wang, Z., and Wang, C. S.: Stable isotopic evidence for climate and basin evolution of the Late Cretaceous Songliao basin, China, Palaeogeogr. Palaeoclimatol. Palaeoecol., 385, 106–124, 2013.

Cong, B. L.: Ultrahigh-pressure Metamorphic Rocks in the Dabieshan-Sulu Region of China, Science Press, Beijing, 224 pp., 1996.

Dong, S. W., Li, T. D., Lü, Q. T., Gao, R., Yang, J. S., Chen, X. H., Wei, W. B., Zhou, Q., and SinoProbe team: Progress in deep lithospheric exploration of the continental China: A review of the SinoProbe, Tectonophysics, 606, 1–13, 2013.

Feng, Z., Wang, C., Graham, S., Koeberl, C., Dong, H., Huang, Y., and Gao, Y.: Continental Scientific Drilling Project of Cretaceous Songliao Basin: Scientific objectives and drilling technology, Palaeogeogr. Palaeoclimatol. Palaeoecol., 385, 6–16, 2013.

Fu, C. F., An, Z. S., Qing, X. K., Bloemendal, J., Song, Y. G., and Chang, H.: Magnetostratigraphic determination of the age of an-

cient Lake Qinghai, and record of the East Asian monsoon since 4.63 Ma, Geology, 41, 875–878, 2013.

Gao, Y., Wang, P., Cheng, R., Wang, G., Wan, X., Wu, H., Wang, S., and Liang, W.: Description of Cretaceous sedimentary sequence of the first member of the Qingshankou Formation recovered by CCSD-SK-I s borehole in Songliao Basin: lithostratigraphy, sedimentary facies and cyclic stratigraphy, Earth Sci. Front., 16, 314–323, 2009 (in Chinese with English abstract).

Hacker, B. R., Ratschbacher, L., Webb, L., Ireland, T., Walker, D., and Dong, S. W.: U/Pb zircon ages constrain the architecture of the ultrahigh-pressure Qinling-Dabie Orogen, China, Earth Planet. Sci. Lett., 161, 215–230, 1998.

Hay, W.: Can humans force a return to a 'Cretaceous' climate?, Sediment. Geol., 235, 5–26, 2011.

Hermann, J. and Rubatto, D.: Subduction of continental crust to mantle depth: geochemistry of ultrahigh-pressure rocks, Treatise Geochemistry, 4, 309–340, 2014.

Kern, H., Jin, Z. M., Gao, S., Popp, T., and Xu, Z. Q.: Physical properties of ultrahigh-pressure metamorphic rocks from the Sulu terrain, eastern central China: implications for the seismic structure at the Donghai (CCSD) drilling site, Tectonophysics, 354, 315–330, 2002.

Kuo, L. W., Li, H., Smith, S., Smith, S. A. F., Di Toro, G., Suppe, J., Song, S., Nielsen, S., Sheu, H. S., and Si, J.: Gouge graphitization and dynamic fault weakening during the 2008 Mw 7.9 Wenchuan earthquake, Geology, 42, 47–50, 2014.

Li, H. B., Fu, X. F., Van der Word, J., Si, J. L., Wang, Z. X., Hou, L. W., Qiu, Z. L., Li, N., Wu, F. Y., Xu, Z. Q., and Tapponnier, P.: Co-seisimic surface rupture and dextral-slip oblique thrusting of the Ms 8.0 Wenchuan earthquake, Acta Geological Sinica, 82, 1623–1643, 2008 (in Chinese with English abstract).

Li, H. B., Wang, H., Xu, Z. Q., Si, J., Pei, J., Li, T., Huang, Y., Song, S., Kuo, L., Sun, Z., Chevalier, M. L., and Liu, D.: Characteristics of the fault-related rocks, fault zones and the principal slip zone in the Wenchuan Earthquake Fault Scientific Drilling Project Hole-1 (WFSD-1), Tectonophysics, 584, 23–42, 2013.

Li, H. B., Xu, Z. Q., Niu, Y., Kong, G., Huang, Y., Wang, H., Si, J., Sun, Z., Pei, J., and Gong, Z.: Structural and physical property characterization in the Wenchuan Earthquake Fault Scienti?c Drilling project – hole 1 (WFSD-1), Tectonophysics, 619–620, 86–100, 2014.

Li, S. G., Jagoutz, E., Chen, Y. Z., and Li, Q. L.: Sm-Nd and Rb-Sr isotopic chronology and cooling history of ultrahigh pressure metamorphic rocks and their country rocks at Shuanghe in the Dabie Mountains, Central China, Geochim Cosmochim Acta, 64, 1077–1093, 2000.

Liou, J. G., Ernst, W. G., Zhang, R. Y., Tsujimori, T., and Jahn, J. G.: Ultrahigh-pressure minerals and metamorphic terranes – the view from China, J. Asian Earth Sci., 35, 199–231, 2009.

Liou, J. G., Tsujimori, T., Yang, J. S., Zhang, R. Y., and Ernst, W. G.: Recycling of crustal materials through study of ultrahigh-pressure minerals in collisional orogens, ophiolites, and mantle xenoliths: A review, J. Asian Earth Sci., 96, 386–420, 2014.

Liu, D. Y., Jian, P., Kröner, A., and Xu, S. T.: Dating of prograde metamorphic events deciphered from episodic zircon growth in rocks of the Dabie-Sulu UHP complex, China, Earth Planet. Sci. Lett., 250, 650–666, 2006.

Liu, F. L. and Liou, J. G.: Zircon as the best mineral for P-T-time history of UHP metamorphism: A review on mineral inclusions and U-Pb SHRIMP ages of zircons from the Dabie-Sulu UHP rocks, J. Asian Earth Sci., 40, 1–39, 2011.

Liu, F. L., Xu, Z. Q., Katayama, I., Yang, J. S., Maruyama, S., and Liou, J. G.: Mineral inclusions in zircons of para- and orthogneiss from pre-pilot drillhole CCSD-PP1, Chinese Continental Scientific Drilling Project, Lithos, 59, 199–215, 2001.

Liu, F. L., Xu, Z. Q., and Xue, H.: Tracing the protolith, UHP metamorphism, and exhumation ages of orthogneiss from the SW Sulu terrane (eastern China): SHRIMP U–Pb dating of mineral inclusion-bearing zircons, Lithos, 78, 411–429, 2004a.

Liu, F. L., Xu, Z. Q., Liou, J. G., and Song, B.: SHRIMP U–Pb ages of ultrahigh-pressure and retrograde metamorphism of gneisses, south-western Sulu terrane, eastern China, J. Metamorphic Geol., 22, 315–326, 2004b.

Liu, F. L., Xu, Z. Q., Liou, J. G., Dong, H. L., and Xue, H. M.: Ultrahigh-pressure mineral assemblages in zircons from the surface to 5158 m depth in cores of the main drill hole, Chinese Continental Scientific Drilling Project, southwestern Sulu belt, China, Int. Geol. Rev., 49, 454–478, 2007.

Liu, S. S., Weber, U., Glasmacher, U. A., Xu, Z., and Wagner, G. A.: Fission track analysis and thermotectonic history of the main borehole of the Chinese Continental Scientific Drilling project, Tectonophysics, 475, 318–326, 2009.

Liu-Zeng, J., Zhang, Z., Wen, L., Tapponnier, P., Sun, J., Xing, X., Hu, G., Xu, Q., Zeng, L., Ding, L., Ji, C., Hudnut, K. W., and van der Woerd, J.: Co-seismic ruptures of the 12 May 2008, Ms 8.0 Wenchuan earthquake, Sichuan: East–west crustal shortening on oblique, parallel thrusts along the eastern edge of Tibet, Earth Planet. Sci. Lett., 286, 355–370, 2009.

Okay, A. I., Xu, S. T., and Sengor, A. M. C.: Coesite from the Dabie Shan eclogites, central China, Eur. J. Mineral., 1, 595–598, 1989.

Si, J., Li, H., Kuo, L., Pei, J., Song, S., and Wang, H.: Clay mineral anomalies in the Yingxiu–Beichuan fault zone from the WFSD-1 drilling core and its implication for the faulting mechanism during the 2008 Wenchuan earthquake (Mw 7.9), Tectonophysics, 619, 171–178, 2014.

Wang, C. S., Feng, Z., Wu, H., Wang, P., Kong, F., Feng, Z., Ren, Y., Yang, G., Wan, X., Huang, Y., and Zhang, S.: Preliminary Achievement of the Chinese Cretaceous Continental Scientific Drilling Project SK-I, Acta Geologica Sinica, 82, 9–20, 2008 (in Chinese with English abstract).

Wang, C. S., Feng, Z., Zhang, L., Huang, Y., Cao, K., Wang, P., and Zhao, B.: Cretaceous paleogeography and paleoclimate and the setting of SKI borehole sites in Songliao Basin, northeast China, Palaeogeogr. Palaeoclimatol. Palaeoecol, 385, 17–30, 2013a.

Wang, C. S., Scott, R. W., Wan, X., Graham, S. A., Huang, Y. J., Wang, P. J., Wu, H. C., Dean, W. E., and Zhang, L. M.: Late Cretaceous climate changes recorded in Eastern Asian lacustrine deposits and North American Epieric sea strata, Earth Sci. Rev., 126, 275–299, 2013b.

Wang, Q., Ji, S. C., Salisbury, M. H., Pan, M. B., Xia, B., and Xu, Z. Q.: Pressure dependence and anisotropy of P-wave velocities in ultrahigh-pressure metamorphic rocks from the Dabie–Sulu orogenic belt (China): implications for seismic properties of subducted slabs and origin of mantle reflections, Tectonophysics, 398, 67–99, 2005a.

Wang, Q., Ji, S. C., Salisbury, M. H., Xia, B., Pan, M., and Xu, Z. Q.: Shear wave properties and Poisson's ratios of ultrahigh-pressure metamorphic rocks from the Dabie-Sulu orogenic belt, China:

implications for the crustal composition, J. Geophys. Res., 110, B08208, doi:10.1029/2004JB003435, 2005b.

Wang, X. M., Liou, J. G., and Mao, H. K.: Coesite-bearing eclogites from the Dabie Mountains in central China, Geology, 17, 1085–1088, 1989.

Wang, Y., Xia, Y., Dong, X., Dong, H., Yang, K., Dong, Z., and Huang, L.: Quantitative analysis of two uncultured bacterial species from the terrestrial deep subsurface by real-time PCR, Acta Petrologica Sinica, 22, 2103–2106, 2006 (in Chinese with English abstract).

Wu, Y.-B., Zheng, Y. -F., Zhao, Z. F., Gong, B., Liu, X. M., and Wu, F. Y.: U-Pb, Hf and O isotope evidence for two episodes of fluid-assisted zircon growth in marble-hosted eclogites from the Dabie orogeny, Geochim. Cosmochim. Acta, 70, 3743–3761, 2006.

Xi, D., Wan, X., Feng, Z., Li, S., Feng Z., Jia Z., Jing, X., and Si, W.: Discovery of Late Cretaceous foraminifera in the Songliao Basin: evidence from SK-1 and implications for identifying seawater incursions, Chin. Sci. Bull., 56, 253–256, 2011.

Xu, S. T., Okay, A. I., Ji, S. Y., Sengor, A. M. C., Su, W., Liu, Y. C., and Jiang, L. L.: Diamond from the Dabie Shan metamorphic rocks and its implication for tectonic setting, Science, 256, 80–82, 1992.

Xu, Z. Q., Yang, W., Ji, S., Zhang, Z., Yang, J., Wang, Q., and Tang, Z.: Deep root of a continent-continent collision belt: Evidence from the Chinese Continental Scientific Drilling (CCSD) deep borehole in the Sulu ultrahigh-pressure (HP–UHP) metamorphic terrane, China, Tectonophysics, 475, 204–219, 2009a.

Xu, Z. Q., Wang, Q., Tang, Z. M., and Chen, F. Y.: Fabric kinematics of the ultrahigh-pressure metamorphic rocks from the main borehole of the Chinese Continental Scientific Drilling Project: Implications for continental subduction and exhumation, Tectonophysics, 475, 235–250, 2009b.

Xue, L., Li, H., Emily, B., Xu, Z., Kano, Y., Wang, H., Mori, J. J., Si, J., Pei, J., Zhang, W., Yang, G., Sun, Z., and Huang, Y.: Continuous permeability measurements record healing inside the Wenchuan Earthquake Fault Zone, Science, 340, 1555–1559, 2013.

Yang, J. S., Dobrzhinetskaya, L., Bai, W., Fang, Q., Robinson, P. T., Zhang, J., and Green, H. W.: Diamond- and coesite-bearing chromitites from the Luobusa ophiolite, Tibet, Geology, 35, 875–878, 2007.

Yang, J. S., Robinson, P. T., and Dilek, Y.: Diamonds in ophiolites, Elements, 10, 127–130, 2014.

Yang, W. C.: The crust and upper mantle of the Sulu UHPM belt, Tectonophysics, 475, 226–234, 2009.

Zakharov, Y. D., Boriskina, N. G., Ignatyev, A. V., Tanabe, K., Shigeta, Y., Popov, A. M., Afanasyeva, T. B., and Maeda, H.: Palaeotemperature curve for the Late Cretaceous of the northwestern circum-Pacific, Cretac. Res., 20, 685–697, 1999.

Zhang, P. Z., Shen, Z. K., Wang, M., Burgmannet, R., Molnar, P., Wang, Q., Niu, Z. J., Sun, J., Wu, J., Sun, H., and You, X.: Continuous deformation of the Tibetan Plateau from global positioning system data, Geology, 32, 809–812, 2004.

Zhang, Z. M., Shen, K., Wang, J. L., and Dong, H. L.: Petrological and geochronological constraints on the formation, subduction and exhumation of the continental crust in the southern Sulu orogen, eastern-central China, Tectonophysics, 475, 291–307, 2009.

Zheng, Y.-F.: A perspective view on ultrahigh-pressure metamorphism and continental collision in the Dabie-Sulu orogenic belt, Chinese Science Bulletin, 53, 3081–3104, 2008.

Zheng, Y.-F.: Metamorphic chemical geodynamics in continental subduction zones, Chem. Geol., 328, 5–48, 2012.

Zhou, M., Robinson, T., Malpas, J., and Li, Z.: Podiform chromitites in the Luobusa ophiolite (southern Tibet): Implications for melt–rock interaction and chromite segregation in the upper mantle, J. Petrol., 37, 3–21, 1996.

Zhou, Y. and Littke, R.: Numerical simulation of the thermal maturation, oil generation and migration in the Songliao Basin, Northeastern China, Mar. Pet. Geol., 16, 771–792, 1999.

Sci. Dril., 22, 19–28, 2017
www.sci-dril.net/22/19/2017/
doi:10.5194/sd-22-19-2017

Scientific Drilling
Open Access

Progress Reports

GONAF – the borehole Geophysical Observatory at the North Anatolian Fault in the eastern Sea of Marmara

Marco Bohnhoff[1,2], Georg Dresen[1], Ulubey Ceken[3], Filiz Tuba Kadirioglu[3], Recai Feyiz Kartal[3], Tugbay Kilic[3], Murat Nurlu[3], Kenan Yanik[3], Digdem Acarel[1], Fatih Bulut[1], Hisao Ito[4], Wade Johnson[5], Peter Eric Malin[1], and Dave Mencin[5]

[1]GFZ German Research Centre for Geosciences, Section 4.2 "Geomechanics and Rheology", Potsdam, 14473, Germany
[2]Free University Berlin, Department of Earth Sciences, Berlin, 12249, Germany
[3]AFAD Disaster and Emergency Management Presidency, Earthquake Department Ankara, 06510, Turkey
[4]Japan Agency for Marine-Earth Science and Technology (JAMSTEC), Yokohama, 236-0001, Japan
[5]UNAVCO, Boulder, Colorado 80301, USA

Correspondence to: Marco Bohnhoff (bohnhoff@gfz-potsdam.de)

Received: 4 November 2016 – Revised: 2 January 2017 – Accepted: 4 January 2017 – Published: 31 May 2017

Abstract. The Marmara section of the North Anatolian Fault Zone (NAFZ) runs under water and is located less than 20 km from the 15-million-person population center of Istanbul in its eastern portion. Based on historical seismicity data, recurrence times forecast an impending magnitude $M>7$ earthquake for this region. The permanent GONAF (Geophysical Observatory at the North Anatolian Fault) has been installed around this section to help capture the seismic and strain activity preceding, during, and after such an anticipated event.

GONAF (Geophysical Observatory at the North Anatolian Fault) is currently comprised of seven 300 m deep vertical seismic profiling stations and four collocated 100 m deep borehole strainmeters. Five of the stations are located on the land surrounding the Princes Islands segment below the eastern Sea of Marmara and two are on the near-fault Princes Islands south of Istanbul. The 300 m boreholes have 1, 2, and 15 Hz 3-C seismometers near their bottoms. Above this are vertical, 1 Hz, seismometers at ∼ 210, 140, and 70 m depths. The strainmeter boreholes are located within a few meters of the seismometer boreholes and contain horizontal strain tensor sensors and 2 Hz 3-C seismometers at their bottoms. This selection of instruments and depths was made so as to ensure high-precision and broad-frequency earthquake monitoring and vertical profiling, all under low-noise conditions.

GONAF is the first ICDP-driven project with a primary focus on long-term monitoring of fault-zone dynamics. It has already contributed to earthquake hazard studies in the Istanbul area in several ways. Combining GONAF recordings with existing regional seismic stations now allows monitoring of the NAFZ offshore of Istanbul down to magnitudes $M<0$. GONAF also improves the resolution of earthquake hypocenters and source parameters, better defining local fault branches, their seismicity, and earthquake potential. Using its vertical distribution of sensors, it has directly measured depth-dependent seismic side-effects for ground shaking studies. GONAF is starting to address fundamental questions related to earthquake nucleation, rupture dynamics, temporal changes in material properties and strain.

1 Tectonic context: the Marmara seismic gap

The continental North Anatolian Fault Zone (NAFZ) spans some 1200 km, from eastern Anatolia to the northern Aegean Sea (e.g., Barka, 1992; Sengör et al., 2005; Bohnhoff et al., 2016a). It forms the plate boundary between the Anatolian plate in the south and the Eurasian plate in the north. It is one of the most active plate-bounding strike–slip faults in the world, slipping at a rate of 20–30 mm yr^{-1}, with the largest rates at its western end (McClusky et al., 2000; Reilinger et al., 2006). Its kinematic framework is driven by the northward-pushing Arabian plate in the east and the

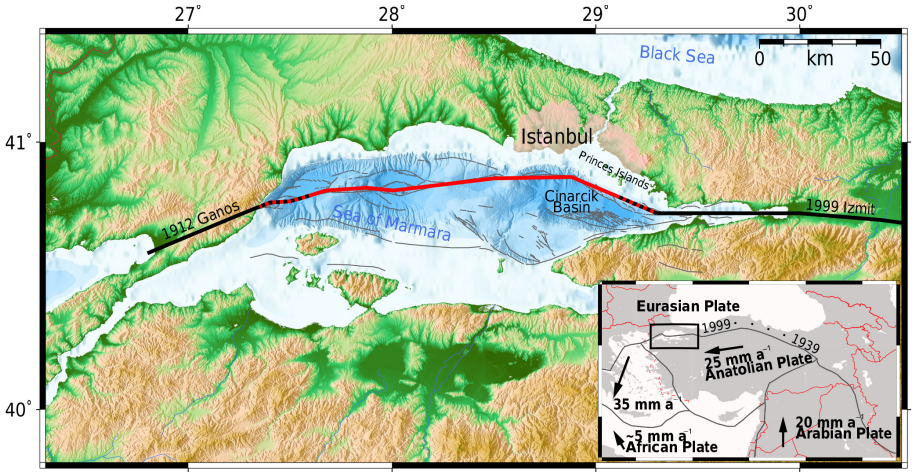

Figure 1. The Marmara region in northwestern Turkey with the main strand of the North Anatolian Fault Zone (NAFZ). The offshore Marmara section (red) is bounded by the two last major ruptures of the region, the 1912 Ganos event to the west and the 1999 Izmit event to the east (both indicated in black). The Marmara section is the last segment of the entire NAFZ that has not been activated since 1766. It hosts the potential of generating an earthquake magnitude M of up to 7.4 in the near future and within a distance of only 20 km to the Istanbul metropolitan area. The location map on the lower right shows the main tectonic plates and their average GPS-derived horizontal velocity with respect to fixed Eurasia.

southward-pulling rollback of the Hellenic subduction zone in the west, forcing the Anatolian plate to rotate counterclockwise (Flerit et al., 2004; Bohnhoff et al., 2005; Bulut et al., 2012).

In the last century, almost the entire NAFZ ruptured in a series of $M>7$ earthquakes, starting with the 1912 Ganos event west of the Sea of Marmara. The next major event then occurred in Erzincan, eastern Anatolia, in 1939, and was followed by a systematic westward propagation of earthquakes (Stein et al., 1997; Sengör et al., 2005). This sequence ended with the M7.4 İzmit and M7.1 Düzce earthquakes in 1999, just east of the Sea of Marmara (Tibi et al., 2001; Barka et al., 2002; Bohnhoff et al., 2016b).

Currently, the NAFZ section below the Sea of Marmara is the only portion of the entire fault zone that has not failed in a major earthquake since 1766 (Fig. 1). The Marmara section has produced several earthquakes as large as $M \sim 7.4$ in historic times, at an average recurrence time of 200–250 years (Parsons, 2004; Bohnhoff et al., 2016a). It would appear then that it is currently in the final stage of its seismic cycle, with a 35–70 % probability of a $M>7$ earthquake occurring by 2034 (Parsons, 2004; Murru et al., 2016).

Unfortunately, the eastern part of this section – the Princes Islands segment – runs within 20 km of the 15+ million inhabitants of the Istanbul metropolitan area. Aside from the potential for a tragic loss of lives, this region also accounts for about 45 % of the national production and about 23 % of the total Turkish gross national product. For these reasons, significant efforts are being made by the Turkish authorities to assess these earthquake hazards and mitigate their risks. Current estimates of damage from an expected $M = 7.5$ earthquake below the Sea of Marmara suggest up to 90 000 fatalities. Up to 800 000 people might be affected and immediate economic losses could be up to USD 40 billion (Bas and Yagci, 2008).

In such a complex natural and urban setting, high-resolution seismic monitoring under low-noise conditions is of central relevance. It presents a critical need to conduct research in refining potential rupture scenarios, identifying potential nucleation points, and rupture directivity models for the pending earthquake. In this paper we summarize the objectives and implementation of the GONAF observatory. We also document our achievements in earthquake detection, waveform quality improvement, and detection of strain by using the downhole seismic arrays and strainmeters.

2 Scientific objectives

The NAFZ is a right-lateral strike–slip fault. However, the transtensional setting of the broader Marmara region also produces surprisingly large normal faulting events, e.g., a M_S 6.3 earthquake along the Çınarcık segment below the eastern Sea of Marmara in 1963 (Ayhan et al., 1981). There is an ongoing debate on whether the pending Marmara event will be pure strike–slip or might include a normal component with consequent tsunami potential (Yalciner et al., 2002; LePichon et al., 2001; Armijo et al., 1999, 2005). Accordingly, for all the risk factors we have cited, it is a pressing matter to resolve the dominant kinematic setting along the Marmara section. This is especially true for the Princes Islands segment just offshore from Istanbul.

Two equally important objectives are to identify potentially creeping and locked fault patches (asperities) – the

latter as potential nucleation points for a large rupture with subsequent directivity effects and ground shaking. The installation of seismometer arrays in boreholes allows not only relatively noise-free waveform recordings, but also studies of near-surface ground motion amplification effects. Fault creep observed on borehole strainmeters provides strong constraints on the accumulation of unreleased strain, both in terms of the amount of fault slip and its areal distribution.

The fact that the entire Marmara section of the NAFZ is under water makes high-resolution seismic and geodetic monitoring of its seismicity and potential creep a challenging task. Our first step in this regard was to install the surface-based PIRES seismic network on the Princes Islands in 2006. The PIRES network has lowered the magnitude of completeness for local microseismicity by 1 order of magnitude to ~ 1.7 (Bulut et al., 2009, 2011). Based on a 4-year PIRES seismicity catalog, Bohnhoff et al. (2013) were able to identify a ≥ 30 km long aseismic fault patch along the Princes Islands segment extending down to a depth of 10 km. The authors concluded that this segment is currently locked and thus represents a potential nucleation point for the next Marmara event. This view is also supported by Global Positioning Satellite (GPS) data (Ergintav et al., 2014).

Beyond the PIRES network, better monitoring of the eastern Sea of Marmara and the Princes Islands segment would be difficult to achieve with surface instruments due to the area's ubiquitous anthropogenic noise. Moreover, near-fault, subareal locations only exist on the Princes Islands. Given these boundary conditions, the GONAF concept of borehole-based geophysical instrumentation surrounding the eastern Sea of Marmara region was conceived and developed in the context of an International Continental Drilling Program (ICDP) project.

Overall, the goal of the GONAF project is a substantially better characterization of the seismic gap first identified by the PIRES and other associated networks. In the long run, outside of any pending significant earthquake, this objective will allow scientific correlations with the findings of other strike–slip faults, such as the San Andreas fault in California. In addition to the study of brittle failures in the form of seismic events, GONAF is also addressing the role of aseismic deformation processes through strain monitoring. These processes included fault creep and slow earthquakes, which are now recognized as playing equally fundamental roles in the seismomechanics of the earth's crust.

3 Strategy

GONAF is a joint research venture between GFZ in Potsdam, Germany, and the AFAD Disaster and Emergency Management Presidency of Turkey, headquartered in Ankara. It is co-funded by GFZ, AFAD, the Turkish Ministry of Development, the International Scientific Drilling Program (ICDP), the German Helmholtz Association (HGF), and the NSF through UNAVCO, a non-profit US university-governed consortium dedicated to supporting geodetic studies. Key aspects of a scientific and technical program for a long-term geophysical observatory for the NAFZ were discussed at an ICDP-funded workshop in Istanbul in 2007 (Dresen et al., 2008). A consensus was reached that the eastern Marmara NAFZ is unique as a segment of a major transform fault, one that is nearing the end of its seismic cycle. It was also considered a worthy technical challenge, in that deep borehole observatories represent the only possibility of obtaining low-noise geophysical data in such a densely populated region.

Following the workshop, an implementation plan was developed that resulted in an ICDP full proposal (Bohnhoff et al., 2010). This was followed by further refinement of the borehole observatory concept, all pointing towards a first ICDP-driven "fault zone seismic monitoring project". Significantly, the initial concept of one or two 2 km deep instrumented boreholes was modified towards a multi-borehole network of several 300 m deep vertical seismic arrays (Fig. 2). The aim of this revision was that even a 2 km deep borehole would not have allowed one to measure crustal stresses of sufficient quality due to the influence of the ~ 1 km escarpment down to the Cinarcik Basin a few kilometers offshore of the near-fault islands and to allow for homogenous low-detection threshold seismic monitoring throughout the eastern Sea of Marmara following the concept of, e.g., the Parkfield High Resolution Seismic Network (HRSN). Following several years of GONAF downhole seismic monitoring along the Princes Islands segment, the potential for eventually drilling individual deeper drill holes will then be re-evaluated.

The first GONAF borehole station was drilled and completed in 2012 on the Tuzla peninsula in eastern Istanbul (Fig. 2). This site combined good access to a secure location on land and the vicinity of a prominent seismicity cluster (Bulut et al., 2011; Prevedel et al., 2015; Raub et al., 2016; Fig. 3). Further GONAF stations were then implemented during 2013–2015. The current seismic observatory now consists of seven borehole seismic stations. Each station is equipped with a vertically distributed array of seismometers, including a selection of different natural-frequency seismometers at the bottom of the boreholes (Figs. 2 and 4). Two of the GONAF borehole arrays are located on the islands of Sivriada and Büyakada. These two sites are less than 5 km from the Princes Islands segment of the NAFZ. The remaining four GONAF stations are located on the Armutlu Peninsula south of the Cinarcik Basin (Fig. 2). This network of borehole stations provides a nearly complete azimuthal coverage for microseismicity occurring below the eastern Sea of Marmara.

In addition to the seven 300 m wells drilled for the seismic arrays, four 100 m deep boreholes were drilled for the installation of UNAVCO Plate Boundary Observatory instruments. These are collocated with four seismometer array stations: Sivriada, Büyükada, Esenköy, and Bozburun (Fig. 2).

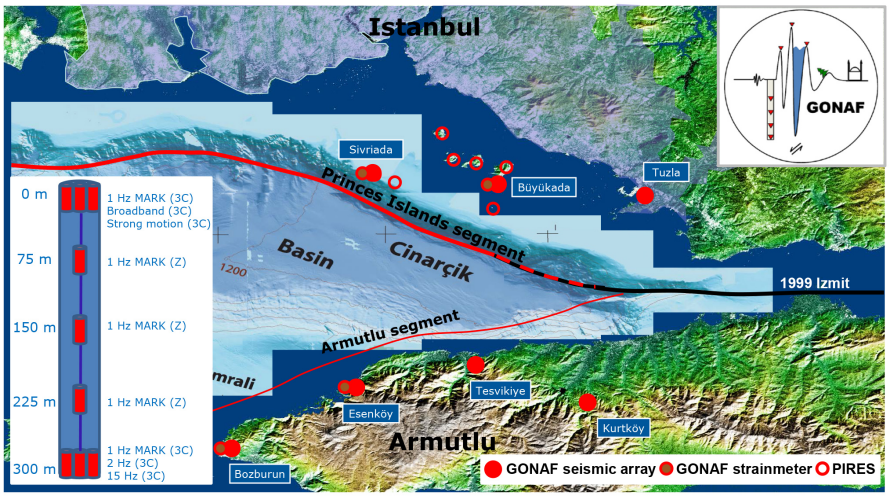

Figure 2. The eastern Marmara region with the Princes Islands segment as the main NAFZ fault trace in this region. Bold red dots indicate locations of the ICDP-GONAF observatory where seismometer arrays were deployed in 300 m deep boreholes. Brown dots indicate locations with additional 100 m deep strainmeter wells. The inset on the lower left shows the sensor distribution in the GONAF wells including multiple seismic sensors of different natural frequencies to sample the entire frequency band of the seismic wavefield (see text for details). Open red circles are surface-based stations of the PIRES seismic network on the Princes Islands.

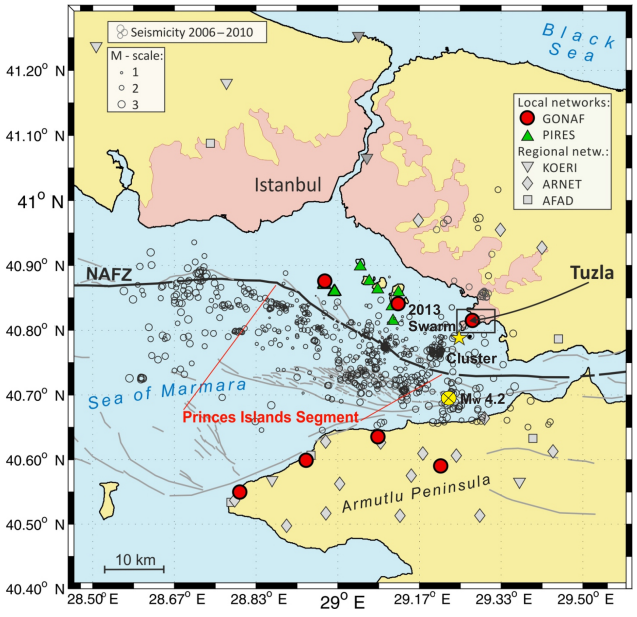

Figure 3. Seismicity map for the eastern Sea of Marmara region for the time period 2006–2010 from surface recordings of the PIRES, AFAD and KOERI stations (Bohnhoff et al., 2013; Prevedel et al., 2015). The yellow star indicates the location of the 2013 microseismic swarm recorded by GONAF-Tuzla seismometers (Prevedel et al., 2015; Raub et al., 2016). The yellow circle indicates the location of the Yalova 25 June 2016 M_w4.2 earthquake of which waveforms obtained at the GONAF-Tesvikiy (TESV; see Fig. 2 for location) vertical seismic array are shown in Figs. 5–7.

These instruments were added to the GONAF plan in order to extend its sensitivity to the long-period deformations of fault creep and slow earthquakes, both below the passband of the seismic sensors. The final monitoring concept foresees that each of the GONAF stations will also be equipped with a set of short-period, broadband, and strong motion sensors at the well head (Fig. 2).

4 Site selection, sensors, installation, and well completion

Borehole seismic installations have to take into account borehole diameter and tilt, temperature profile, and lithology. Long-term permitting, accessibility, and the availability of electrical power and mobile data transmission infrastructure complete the requirements for a permanent observatory such as GONAF.

In the case of GONAF, with target depths of 300 m and a regional geothermal gradient of $\sim 30\,^{\circ}\mathrm{C\,km^{-1}}$, temperature was not an issue with respect to long-term functionality of the downhole equipment. Bottom hole temperatures found during logging were around 25 °C, well below the 50 °C limit beyond which standard operation of the 1 and 2 Hz sensors could become an issue. Conventionally drilled boreholes are claimed to be vertical, but are commonly found to deviate by as much as 5–15°. Accordingly, the drilling company was contracted to keep all GONAF boreholes within 3° from the vertical. This deviation was then checked as part of the logging program.

To find sites in the study area that could provide a more-or-less uniform detection threshold, approximate locations

Figure 4. Upper part: GONAF downhole seismic instruments prior to deployment at the Kurtkoy station on the Armutlu Peninsula. The 300 m deep, gimbaled 1 Hz 3-C L4 seismometer sonde is on the right. In the middle is the combined 300 m deep 3-C 15 Hz DS200 and gimbaled 2 Hz HS-1 sonde. The other three sondes are the vertically distributed, gimbaled 1-C 1 Hz L4 seismometers. For redundancy each sonde has its own waterproof signal cable with an internal Kevlar stress member. Lower part: the 10 ft containers used to cover each station and to house the special low-noise Guralp CMG-DM recorders, telemetry systems, and their support equipment.

for GONAF stations were pre-defined on maps. The center pieces of this exercise were the Princes Islands, the only location with short distances to the NAFZ. The island sites on Sivriada and Büyukada were decided upon based on their closest proximity to the target fault section (Fig. 2). The remaining five on-land sites were then optimized after pre-site surveying. For these sites we sought hard-rock conditions to ensure good coupling of the sensors and therefore more faithful recording of the seismic wave field. Permitting issues related to land ownership as well as local electricity and data communication infrastructure were then evaluated.

On the northern shore of the Sea of Marmara, the Tuzla site is located outside the main Istanbul population center but still in an urbanized area. It is the closest station to the Tuzla seismicity cluster (Fig. 3). Along the southern shore of the Sea of Marmara – the northern shore of the Armutlu Peninsula – remote spots were easy to find. However, well-consolidated rock conditions were rare. As a result, their locations were determined primarily by sites that seemed to provide the best rock within the spacing and azimuths needed for the overall network.

The seismic sensors deployed in the GONAF borehole are all passive sensors and were selected to cover the entire frequency range intended to be studied. This is primarily defined by the local seismicity that occurs down to the base of the seismogenic layer at $\sim$ 18 km, resulting in signal frequencies up to a few tens of Hertz (Bohnhoff et al., 2013). However, it is also intended to cover higher frequencies of events occurring near individual wells as well as to detect potentially occurring low-frequency events. All GONAF stations are equipped with a 24-channel Guralp 24-bit data logger with variable gain and integrated pre-amplifiers.

The Tuzla station as the first completed GONAF array has three Sercel 1 Hz L4 vertical component sensors placed at depths of 71, 144, and 215 m, and also Geospace 2 Hz HS-1 and 15 Hz DS2500 three-component sensors at a depth of 288 m. (The L4 sensor were formerly manufactured under the name of Mark Products.) The other six stations with vertically distributed seismic arrays include three vertical 1 Hz L4 seismometers at nominal 70–75 m spacing starting at $\sim$ 70–75 m downhole. At the bottom of each well, at 285–295 m depths, are 3-C, gimbaled 1 Hz L4s, gimbaled Geospace 2 Hz HS-1s, and fixed Geospace 15 Hz DS2500s (Figs. 2 and 4). The L4s were selected as they are widely used in local and regional surface seismic networks worldwide, forming something of an international standard. In order to achieve successful installation of them, both a large diameter, internally gimbaled pressure case, and even a larger drill hole were needed. The former requirement is due to the tilt sensitivity of all seismographs with natural frequencies below about 12 Hz. At 1 Hz, even 1° of tilt effectively removes a horizontal component from scientific analysis due to signal distortion.

To achieve a borehole-tilt tolerance of up to $\sim$ 8°, a gimbaled case with an outer diameter of $\sim$ 205 mm was required. To allow for a comfortable amount of space for this sonde plus a 60 mm outer diameter (OD) cementing trim tube, a 349 mm borehole was selected for the borehole inner diameter (ID). With the available space and novelty of placing 1 Hz sensors at 300 m, it was decided to include the 2 and 15 Hz units, both for comparison and backup. All sensors were cemented in the boreholes to ensure good coupling and long-term cable stability. The seismic waveform data are currently sampled at 500 Hz by 18-channel Guralp CMG-DM recorders. These recorders are specially equipped with 0.1×10^{-6} V self-noise pre-amplifiers in order to exceed the self-noise of downhole sensors. The data are then transmitted in real time to GFZ and AFAD headquarters for archiving and analysis.

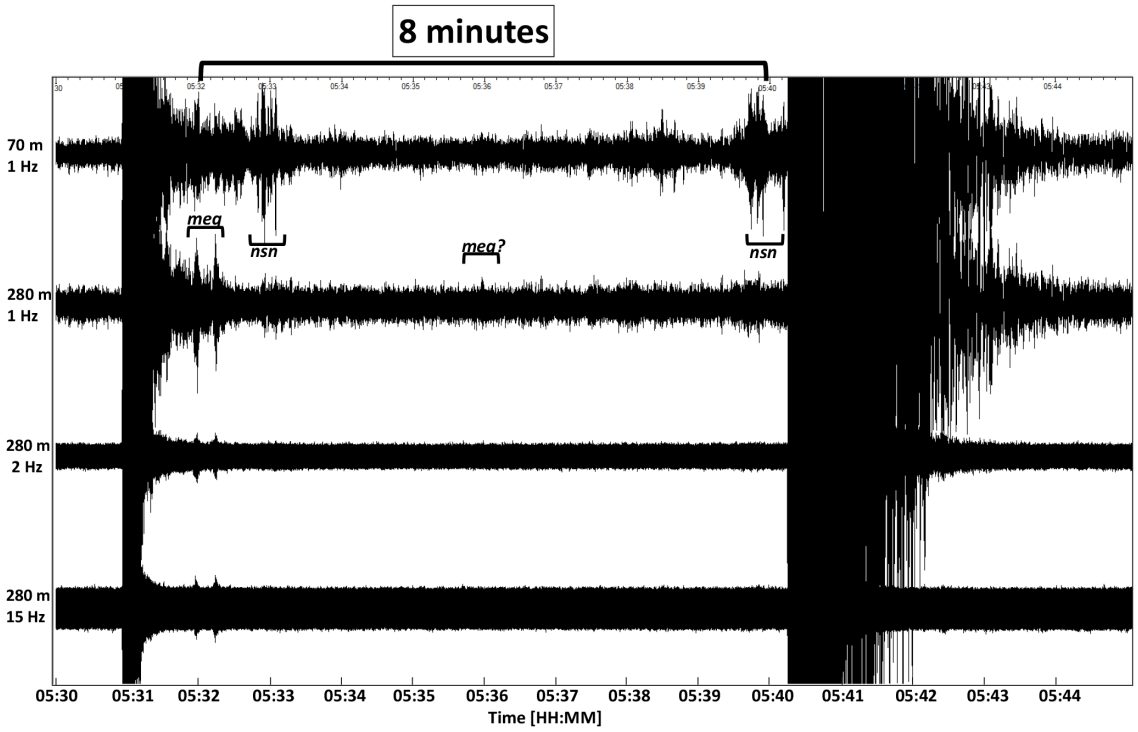

Figure 5. Vertical component seismograms of the Yalova 25 June 2016 foreshock (∼ 05:31) and M_w4.2 (∼ 05:40) earthquakes as recorded at the Tesvikiye (TESV) borehole station of the GONAF network. The depth and natural frequency of the TESV sensors are shown on the left. The seismograms were recorded at 500 samples / second and have a usable bandwidth of 0.1 to 200 Hz. The amplitudes of each trace have been normalized to matching maximum values. The times of some near-surface noise (*nsn*) and smaller earthquakes (*meq*) are shown with upward and downward facing brackets. These two signals can be easily identified by comparing their signal-to-noise ratios (S/Ns) as a function of 1 Hz sensor depth: near-surface noise ratios decrease with depth, while earthquake ratios increase. For example, the microearthquakes that took place just before and above the left end of the 8 min bar are clearly evident on the ∼ 300 deep sensor, but are buried in near-surface scattering noise at ∼ 75 m. The S/N for the near-surface noises just after these events is reversed: the large signals at ∼ 75 m are nearly gone on the ∼ 300 m sensor. In between the latter times are a number of events with roughly equivalent S/Ns (∼ 1) at both depths. As is shown in Fig. 6, in many cases it is possible to determine their origin by comparing frequency contents at ∼ 75 and ∼ 300 m. The 8 min long bracket along the time axis shows the data window used for this analysis in Fig. 6.

All the seismic sensors were tested prior to deployment. Individual sensors were then attached to the 60 mm cementing trim tube and lowered into the borehole. Once the entire string was lowered into the borehole, the entire well was cemented from the bottom up. Each GONAF station is covered with a 10 ft container to house the 18-channel data logger and its support equipment (Fig. 4).

The four GONAF strainmeter installations were completed after the seismic stations were in place. The main sensors in these installations are GTSM strainmeters, each with three horizontal strain gauges placed at 120° separations along with a fourth redundant gauge offset 30° from the principal axis (Gladwin, 1984; Gladwin and Hart, 1985). A 3-C Geospace 2 Hz HS-1 seismometer is included as a standard part of these systems. Their 100 m deep wells were first logged to find the most competent rock sections. Then, using the same installation methods as developed for the US Plate Boundary Observatory, the sensors were lowered into a pre-loaded slug of expansive grout at the selected depth.

5 Technical and first scientific achievements

The scientific goals set for GONAF required successful completion of its promised improvements in event detection and waveform quality – all dependent on the technical aspects of the still-emerging field of borehole seismology for earthquake research. The first indication that these goals were likely to be met came from the Tuzla site (e.g., Prevedel et al., 2015). This site detected, along with the existing regional surface network, an $M \sim 1.6$ event immediately to its south. Using this event as a correlation template, the Tuzla data in the days surrounding this event were checked for additional weaker events missed by the surface stations. A total of 114 additional events from the same location were identified in the Tuzla GONAF downhole data by these means, all with relative coda magnitudes less than $M \sim 1.6$. The smallest of these events was found to be about $M \sim -1$. Subsequently, at the Tesvikiye GONAF station on the southern Sea of Marmara shore, a pair of events, one with $M \sim 0$

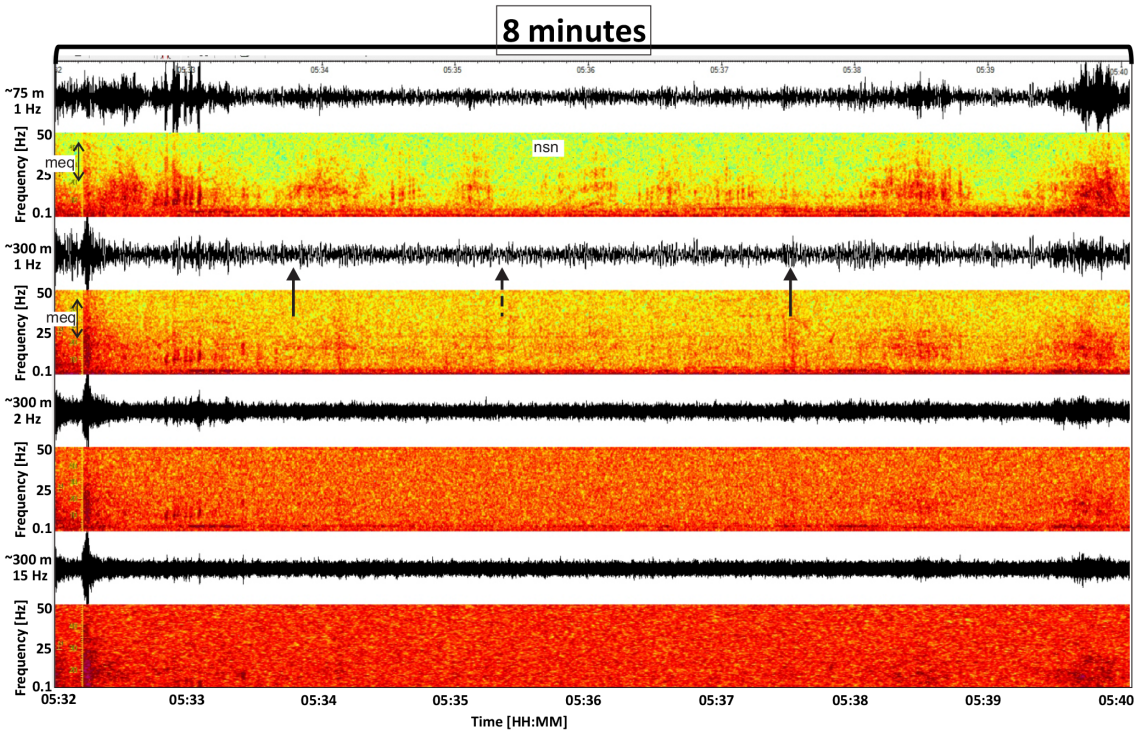

Figure 6. Seismograms and spectrograms illustrating the increasing attenuation of near-surface noise with depth and the increasing microearthquake signals with depth. The depth and natural frequency of the vertical component sensors used to record these motions are shown on the left. The data window is for the 8 min between the main foreshock and the M_w4.2 Yelova earthquake, as shown in Fig. 5. The 500 samples / second seismograms have been band pass filtered between 0.1 and 50 Hz, and normalized to matching maximum values. The spectrogram bandwidths shown are also between 0.1 and 50 Hz, and their color scales were adjusted to matching maximum values and ranges. Examples of the difference between downgoing near-surface noise (*nsn*) and upcoming microearthquake signal (*meq*) attenuation are labeled. For example, the near-surface noise recorded during the lower time bar on the ~ 75 m deep 1 Hz vertical is nearly absent on the ~ 300 m deep sensors; likewise for the signals on either side at the time of 05:33:00. In contrast, the high-frequency microearthquake signal at the beginning of the record on the ~ 300 m 1 Hz is similarly reduced on the ~ 75 m deep sensor. Potential smaller microearthquakes not evident on the ~ 75 m deep recording are indicated by black arrows on the ~ 300 m 1 Hz spectrogram, and are at the detection limit of the GONAF stations. The self-noise floor and sensitivity of the 1 Hz sensor are clearly evident in these plots: the higher-frequency sensors pick up the first microearthquake event, but the other events are buried by their overall system-response characteristics.

and the other with $M \sim -1$, were also recorded. Except for their amplitudes and signal-to-noise ratios, the initial half seconds of the waveforms of these two events are nearly identical (Prevedel et al., 2015). Judging from their S–P time of ~ 0.3 s, these events occurred roughly 2.5 km away. So, based on the smaller event's signal-to-noise ratio of ~ 10, it would appear that the detection limit of the 300 m deep 1 Hz sensors approaches a relative magnitude $M \sim -1.3$ to -1.4 event at this distance.

The occurrence of a M_w4.2 (AFAD Earthquake Department) event several kilometers northeast of the Tesvikiye GONAF station on 25 June 2016 also helped establish several GONAF seismic station technical achievements, including (1) the improved detection threshold of the ~ 300 m deep sensors, (2) the near-surface noise discrimination value of the vertical array, and (3) the relative performance of the three different natural frequency sensors, 1, 2, and 15 Hz (Figs. 5, 6, and 7).

None of the Tesvikiye sensors appears to have clipped during either the foreshock or main event, which were roughly 15 km away based on their S–P times of ~ 2 s. The relative sizes of the aftershock events show that the detection threshold for earthquakes at this distance from this station is around $M \sim 0$. This suggests that the combined detection, location, and unclipped dynamic range of the seven-station network will be at least between $M \sim 0$ and 4.5 or so. By comparing signals and signal-to-noise ratios between the near-surface and deep sensors, the task of separating microearthquakes from cultural noises is greatly facilitated, as demonstrated by the waveform examples shown in Figs. 5 and 7.

Comparison of the codas of the foreshock and the M_w4.2 event as recorded on the three different frequency sensors at ~ 300 m shows the well-known apparent "reverse dispersion" of scattered seismic waves: the higher frequencies of the coda cut off earlier than lower ones. The relative signal-to-noise ratios between these sensors accords mainly with

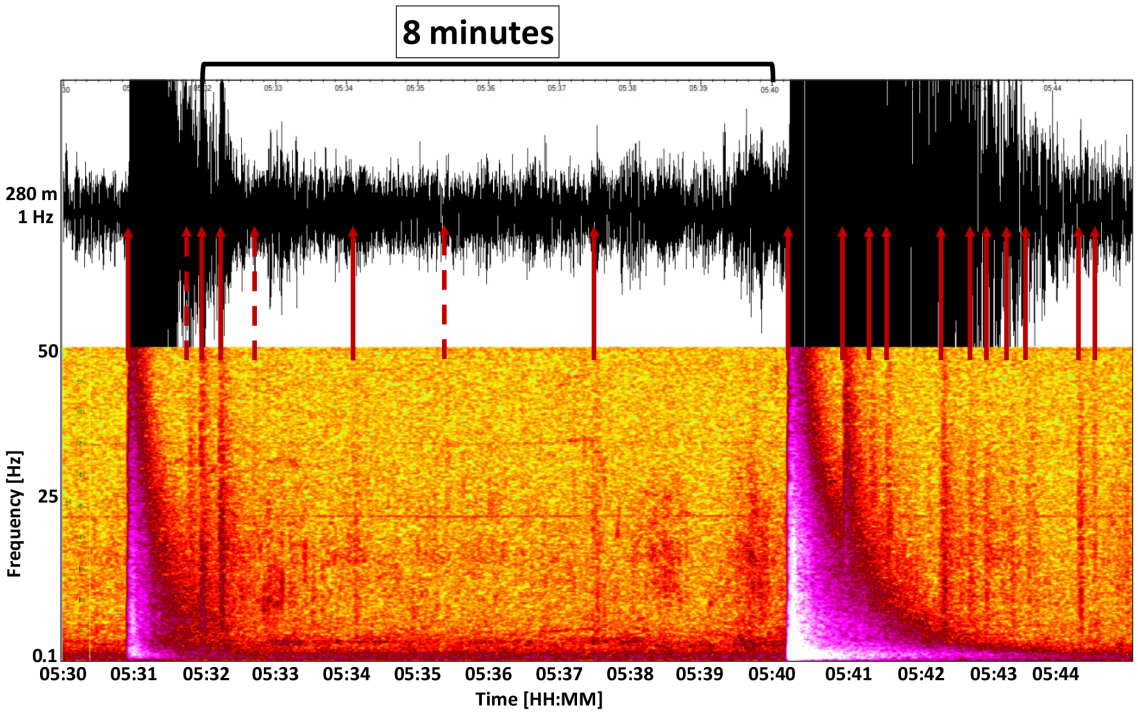

Figure 7. This figure shows the times of earthquakes identified at the ~ 300 m deep 1 Hz GONAF-TESV sensor by their spectra in the 15 min interval from 05:00:00 to 05:15:00 on 25 June 2016. The solid arrows indicate events with S–P time within 0.1 s of the fore- and main-shocks, the latter arriving at 05:30:56 and 05:40:15. The dashed arrows are events that do not have this S–P time or could not be confidently identified and measured in the waveform data themselves.

their generator constants. Because of its size and consequent combination of coil and magnetic proof mass, the 1 Hz sensor puts out several times the voltage for equivalent motion as the other two sensors. Hence this sensor overcomes many of the electrical interferences generated by the signal cable and recorder. Ordinarily one would hence select this type of sensor, until one recalls the size of the internally gimbaled sonde and drill hole needed to successfully install them.

Several earthquake research studies have been performed with data from the PIRES and more recently also from the GONAF stations over the last few years. One study focused on using the improved detection limit of these stations to study the microseismic activity along the Princes Islands segment (Bohnhoff et al., 2013). Consistent with previous studies, but now with a much more definitive result, the conclusion is that this crucial portion of the Marmara seismic gap is indeed locked. This view has also been confirmed by GPS data (Ergintav et al., 2014). Therefore, the need to consider it as a potential nucleation point of the pending $M > 7$ earthquake has been further substantiated due to better network resolution (Raub et al., 2016). Data from the Tuzla GONAF site have allowed determination of the near-surface structure around the borehole, a key prerequisite for local seismic hazard and risk assessment (Raub et al., 2016). These studies are being extended to all other GONAF sites.

As shown in Fig. 7, the downhole data from the 25 June, 2016, M_w4.2 event have revealed microearthquakes – potentially triggered aftershocks – hidden in the coda of the near-surface Tesvikiye sensor. As this also appears true for the observed foreshock, all the GONAF seismic data are currently being examined for the time interval surrounding the M_w4.2 mainshock.

6 Conclusions

The recently implemented Geophysical Observatory at the North Anatolian Fault (GONAF) in northwestern Turkey aims at monitoring the eastern portion of the NAFZ below the Sea of Marmara. This section of the North Anatolian Fault is currently overdue for a $M > 7$ earthquake and runs underwater at less than 20 km from the 15-million-person population center of Istanbul. GONAF provides low-noise recordings covering the entire frequency band of signals generated by seismic and creeping processes.

The GONAF observatory currently comprises seven 300 m deep vertical seismic profiling stations and four collocated 100 m deep borehole strainmeters. Five of the stations are located on the land surrounding the Princes Islands segment below the eastern Sea of Marmara; two are on the near-fault Princes Islands south of Istanbul. The 300 m boreholes have 1, 2, and 15 Hz 3-C seismometers near their bottoms. Above

this are vertical, 1 Hz, seismometers at ∼ 210, 140, and 70 m depths. The strainmeter boreholes are located within a few meters of the seismometers and contain horizontal strain tensor sensors and 2 Hz 3-C seismometers at their bottoms.

GONAF is the first ICDP-driven project with a primary focus on long-term monitoring of fault-zone dynamics. It has already contributed to earthquake hazard studies in the Istanbul area in several ways. Combining GONAF recordings with existing regional seismic stations now allows monitoring of the NAFZ offshore of Istanbul down to magnitudes $M < 0$. This has improved the resolution of earthquake hypocenters and source parameters, better defining local fault branches, their seismicity, and earthquake potential along the Princes Islands fault segment. Thus, GONAF contributes to addressing fundamental questions related to earthquake nucleation, rupture dynamics, temporal changes in material properties and strain along active transform faults.

7 Data availability

Seismic waveform data from the GONAF project will be made available with a 3-year retention period. Strainmeter data are available in real-time through UNAVCO. The waveform recordings shown in Figs. 5–7 are freely available.

Competing interests. The authors declare that they have no conflict of interest.

Acknowledgements. We thank GFZ Potsdam, AFAD Turkey, the Turkish Ministry of Development, the International Scientific Drilling Program (ICDP), the German Helmholtz Association (HGF), and NSF/UNAVCO for funding of the GONAF observatory. We are thankful for logistical support from the AFAD branches and offices in Yalova and İstanbul and acknowledge the hard work performed by the drillers from Bütün Ltd. and G&M Engineering Ltd. We thank Mustafa Aktar and Haluk Eyidogan for their engagement during the initial phase of the GONAF project. The seismic instrumentation was designed and built at the former Institute of Earth Science and Engineering, University of Auckland, Aotearoa. The ICDP-OSG (Operational Support Group) performed the logging at the Tuzla site. We acknowledge geological interpretation of the well logs by Esen Apart. Christopher Wollin and Christina Raub helped compile Figs. 1 and 3.

Edited by: T. Wiersberg
Reviewed by: L. Chiaraluce and S. Roy

References

AFAD Earthquake catalogue: Prime Ministry, Disaster and Emergency Management Presidency, Earthquake Department, On-line Catalogue, http://www.deprem.gov.tr, 2007–present.

Armijo, R., Meyer, B., Hubert, A., and Barka, A.: Westward propagation of the North Anatolian fault into the northern Aegean: Timing and kinematics, Geology, 27, 267–270, 1999.

Armijo, R., Pondard, N., Meyer, B., Uçarkus, G., de Lépinay, B. M., Malavieille, J., Dominguez, J., Gustcher, M.-A., Schmidt, S., Beck, C., Çagatay, N., Çakir, Z., Imren, C., Eris, K., Natalin, B., Özalaybey, S., Tolun, L., Lefèvre, I., Seeber, L., Gasperini, L., Rangin, C., Emre, O., and Sarikavak, K.: Submarine fault scarps in the Sea of Marmara pull-apart (North Anatolian fault): Implications for seismic hazard in Istanbul, Geochem. Geophy. Geosy., 6, 1–29, doi:10.1029/2004GC000896, 2005.

Ayhan, E., Alsan, E., Sancaklı, N., and Üçer, S. B.: Turkey and Surrounding Earthquake Catalogue 1881–1980, Boğaziçi University Publications, 1981.

Barka, A. A.: The North Anatolian fault zone, Annales Tectonicae, Spec. Iss. VI, 164–195, 1992.

Barka, A. A., Akyüz, H., Altunel, E., Sunal, G., Cakir, Z., Dikbas, A., Yerli, B., Armijo, R., Meyer, B., de Chabalier, J., Rockwell, T., Dolan, J., Hartleb, R., Dawson, T., Christofferson, S., Tucker, A., Fumal, T., Langridge, R., Stenner, H., Lettis, W., Bachhuber, J., and Page, W.: The Surface Rupture and Slip Distribution of the 17 August 1999 Izmit Earthquake (M7.4), North Anatolian Fault, B. Seismol. Soc. Am., 92, 43–60, 2002.

Bas, M. and Yagci, M. Ö.: Disaster Prevention Mitigation Studies for a Safer Urban Life. Measures for Preventing Disaster of Istanbul Metropolitan Municipality, in: Istanbul Megacity Project Report, Municipality Disaster Management Center (AKOM), edited by: Erdik, M. and Zschau, J., Istanbul, Turkey, 22 October, 2008.

Bohnhoff, M., Harjes, H.-P., and Meier, T.: Deformation and stress regimes in the Hellenic subduction zone from focal Mechanisms, J. Seismol., 9, 341–366, 2005.

Bohnhoff, M., Dresen, G., Aktar, M., Bulut, F., Eyidogan, H., and Ito, H.: GONAF: A deep Geophysical Observatory, Full Proposal to the International Continental Scientific Drilling Program (ICDP), 2010.

Bohnhoff, M., Bulut, F., Dresen, G., Malin, P. E., Eken, T., and Aktar, M.: An earthquake gap south of Istanbul, Nature Commun., 4, 1999, doi:10.1038/ncomms2999, 2013.

Bohnhoff, M., Martínez-Garzón, P., Bulut, F., Stierle, E., and Ben-Zion, Y.: Maximum earthquake magnitudes along different sections of the North Anatolian fault zone, Tectonophysics, 674, 147–165, doi:10.1016/j.tecto.2016.02.028, 2016a.

Bohnhoff, M., Ickrath, M., and Dresen, G.: Seismicity distribution in conjunction with spatiotemporal variations of coseismic slip and postseismic creep along the combined 1999 Izmit-Düzce rupture, Tectonophysics, 686, 132–145, doi:10.1016/j.tecto.2016.07.029, 2016b.

Bulut, F., Bohnhoff, M., Ellsworth, W. L., Aktar, M., and Dresen, D.: Microseismicity at the North Anatolian Fault in the Sea of Marmara offshore of Istanbul, NW Turkey, J. Geophys. Res., 114, 1–16, doi:10.1029/2008JB006244, 2009.

Bulut, F., Ellsworth, W. L., Bohnhoff, M., Aktar, M., and Dresen, G.: Spatiotemporal Earthquake Clusters along the North Anatolian Fault Zone Offshore Istanbul, B. Seismol. Soc. Am., 101, 1759–1768, 2011.

Bulut, F., Bohnhoff, M., Eken, T., Janssen, C., Kilic, T., and Dresen, G.: The East Anatolian Fault Zone: Seismotectonic setting and spatiotemporal characteristics of seismicity based on

precise earthquake locations, J. Geophys. Res., 117, B07304, doi:10.1029/2011JB008966, 2012.

Dresen, G., Bohnhoff, M., Aktar, M., and Eyidogan, H.: Drilling the North Anatolian Fault, Sci. Dril., 6, 58–59, doi:10.2204/iodp.sd.6.10.2008, 2008.

Ergintav, S., Reilinger, R. E., Cakmak, R., Floyd, M., Cakir, Z., Dogan, U., King, R. W., McClusky, S., and Ozener, H.: Istanbul's Earthquake Hot Spots: Geodetic Constraints on Strain Accumulation along Faults in the Marmara Seismic Gap, Geophys. Res. Lett., 41, 5783–5788, doi:10.1002/2014GL060985, 2014.

Flerit, F., Armijo, R., King, G., and Meyer, B.: The mechanical interaction between the propagating North Anatolian Fault and the back-arc extension in the Aegean, Earth Planet. Sc. Lett., 224, 347–362, 2004.

Le Pichon, X., Sengör, A. M. C., Demirbag, E., Rangin, C., Imren, C., Armijo, R., Görür, N., Cagatay, N., Mercier, de Lepinay, B., Meyer, B., Saatcilar, R., and Tok, B.: The active Main Marmara Fault, Earth Planet. Sc. Lett., 192, 595–616, 2001.

Gladwin, M. T.: High-precision multicomponent borehole deformation monitoring, Rev. Sci. Instrum., 55, 2011–2016, 1984.

Gladwin, M. T. and Hart, R.: Design parameters for borehole strain instrumentation, PAGEOPH, 123, 59–80, 1985.

McClusky, S., Balassanian, S., Barka, A., Demir, C., Ergintav, S., Georgiev, I., Gurkan, O., Hamburger, M., Hurst, K., Kahle, H., Kastens, K., Kekelidze, G., King, R., Kotzev, V., Lenk, O., Mahmoud, S., Mishin, A., Nadariya, M., Ouzounis, A., Paradissis, D., Peter, Y., Prilepin, M., Reilinger, R., Sanli, I., Seeger, H., Tealeb, A., Toksöz, M. N., and Veis, G.: Global Positioning System constraints on plate kinematics and dynamics in the eastern Mediterranean and Caucasus, J. Geophys. Res., 105, 5695–5719, 2000.

Murru, M., Akinci, A., Falcone, G., Pucci, S., Console, R., and Parsons, T.: $M \geq 7$ earthquake rupture forecast and time-dependent probability for the sea of Marmara region, Turkey, J. Geophys. Res.-Sol. Ea., 121, 2679–2707, doi:10.1002/2015JB012595, 2016.

Parsons, T.: Recalculated probability of $M \geq 7$ earthquakes beneath the Sea of Marmara, J. Geophys. Res., 109, B05304, doi:10.1029/2003JB002667, 2004.

Prevedel, B., Bulut, F., Bohnhoff, M., Raub, C., Kartal, R. F., Alver, F., and Malin, P. E.: Downhole Geophysical Observatories: Best Installation Practices and a Case History from Turkey, Int. J. Earth Sci. (Geol. Rundsch.), 104, 1537–1547, doi:10.1007/s00531-015-1147-5, 2015.

Raub, C., Bohnhoff, M., Petrovic, B., Parolai, S., Malin, P. E., Yanik, K., Kartal, R. F., and Kiliç, T.: Seismic wave propagation in shallow layers at the GONAF-Tuzla site, Istanbul, Turkey, B. Seismol. Soc. Am., 106, 912–927, doi:10.1785/0120150216, 2016.

Reilinger, R., McClusky, S., Vernant, P., Lawrence, S., Ergintav, S., Cakmak, R., Ozener, H., Kadirov, F., Guliev, I., Stepanyan, R., Nadariya, M., Hahubia, G., Mahmoud, S., Sakr, K., ArRajehi, A., Paradissis, D., Al-Aydrus, A., Prilepin, M., Guseva, T., Evren, E., Dmitrotsa, A., Filikov, S. V., Gomez, F., Al-Ghazzi, R., and Karam, G.: GPS constraints on continental deformation in the Africa-Arabia-Eurasia continental collision zone and implications for the dynamics of plate interactions, J. Geophys. Res., 111, B05411, doi:10.1029/2005JB004051, 2006.

Sengör, A. M. C., Tuysuz, O., Imren, C., Sakinc, M., Eyidogan, H., Gorur, N., Le Pichon, X., and Rangin, C.: The North Anatolian Fault: a new look, Annu. Rev. Earth Pl. Sc., 33, 37–112, 2005.

Stein, R. S., Barka, A. A., and Dieterich, J. H.: Progressive failure on the North Anatolian fault since 1939 by earthquake stress triggering, Geophys. J. Int., 128, 594–604, 1997.

Tibi, R., Bock, G., Xia, Y., Baumbach, M., Grosser, H., Milkereit, C., Karakisa, S., Zünbül, S., Kind, R., and Zschau, J.: Rupture processes of the 1999 August 17 Izmit and November 12 Düzce (Turkey) earthquakes, Geophys. J. Int., 144, F1–F7, 2001.

Yalciner, A. C., Alpar, B., Altinok, Y., Özbay, I., and Imamura, F.: Tsunamis in the Sea of Marmara: Historical documents for the past, models for the future, Mar. Geol., 190, 445–463, 2002.

Sci. Dril., 22, 29–33, 2017
www.sci-dril.net/22/29/2017/
doi:10.5194/sd-22-29-2017

Scientific Drilling
Open Access

Facility for testing ice drills

Dennis L. Nielson[1], Chris Delahunty[1], John W. Goodge[2], and Jeffery P. Severinghaus[3]

[1]DOSECC Exploration Services, LLC, 2075 S. Pioneer Rd., Salt Lake City, UT 84104, USA
[2]Department of Earth and Environmental Sciences, University of Minnesota Duluth, Duluth, MN 55812, USA
[3]Scripps Institution of Oceanography, UC San Diego, 9500 Gilman Drive no. 0244, La Jolla, CA 92093, USA

Correspondence to: Dennis L. Nielson (dnielson@dosecc.com)

Received: 12 July 2016 – Revised: 31 January 2017 – Accepted: 13 February 2017 – Published: 31 May 2017

Abstract. The Rapid Access Ice Drill (RAID) is designed for subsurface scientific investigations in Antarctica. Its objectives are to drill rapidly through ice, to core samples of the transition zone and bedrock, and to leave behind a borehole observatory. These objectives required the engineering and fabrication of an entirely new drilling system that included a modified mining-style coring rig, a unique fluid circulation system, a rod skid, a power unit, and a workshop with areas for the storage of supplies and consumables. An important milestone in fabrication of the RAID was the construction of a North American Test (NAT) facility where we were able to test drilling and fluid processing functions in an environment that is as close as possible to that expected in Antarctica. Our criteria for site selection was that the area should be cold during the winter months, be located in an area of low heat flow, and be at relatively high elevation. We selected a site for the facility near Bear Lake, Utah, USA.

The general design of the NAT well (NAT-1) started with a 27.3 cm (10.75 in.) outer casing cemented in a 152 m deep hole. Within that casing, we hung a 14 cm (5.5 in.) casing string, and, within that casing, a column of ice was formed. The annulus between the 14 and 27.3 cm casings provided the path for circulation of a refrigerant. After in-depth study, we chose to use liquid CO_2 to cool the hole. In order to minimize the likelihood of the casing splitting due to the volume increase associated with freezing water, the hole was first cooled and then ice was formed in increments from the bottom upward. First, ice cubes were placed in the inner liner and then water was added. Using this method, a column of ice was incrementally prepared for drilling tests. The drilling tests successfully demonstrated the functioning of the RAID system. Reproducing such a facility for testing of other ice drilling systems could be advantageous to other research programs in the future.

1 Introduction

Characterizing and mapping continental bedrock beneath the Antarctic ice sheets is a fundamental objective of the US National Science Foundation's Antarctic Program (Goodge and Severinghaus, 2016). However, drilling through thick ice using existing ice-coring equipment is a slow process that has required multiple working seasons, and these systems were not designed for recovery of sub-glacial bedrock samples. The development of a mechanical drilling system that can rapidly drill through ice and core the base of the ice sheet and underlying bedrock is a high priority for the scientific community (Clow and Koci, 2002; Gerasimoff, 2012). Other priorities include finding the oldest ice in Antarctica in order to enhance our understanding of past global climate changes by linking changes recorded in the polar ice sheets with complementary marine sediment records.

The goal of the Rapid Access Ice Drill (RAID) is to rapidly drill a thick section (up to 3300 m) of Antarctic ice and to collect core samples of the transition zone and underlying bedrock. We expect to drill five or six holes in a 2-month drilling season. To accomplish this, we need to achieve penetration rates through the ice of 3 m min^{-1}. In addition, existing equipment is only designed to core ice, whereas RAID is the first system to focus on coring the transition zone and underlying bedrock. RAID will operate autonomously in remote regions of Antarctica and therefore must be highly mobile. It includes five different components: drill skid, rod

skid, fluid re-circulation system (FRS), power unit, and shop and supply container.

To mitigate the risks associated with the performance of this new drilling system, a series of bench and field tests were designed to evaluate individual components and system integration before deployment to Antarctica. The North American Test (NAT) was the first integrated RAID system test where drilling and fluid circulation functions were tested under conditions that were as close as possible to those expected in Antarctica. The RAID is designed to use ESTISOL-140 (ESTISOL) as a drilling fluid because it has a density similar to that of ice, it has a low freezing point, and it has good transparency, allowing the hole to be logged optically following drilling (Sheldon et al., 2014). The FRS processes the returned ESTISOL and included ice chips, separates the ice, and re-circulates the ESTISOL down the hole. RAID utilizes pressurized reverse circulation to drill through the ice; i.e., ESTISOL is pumped down the annulus between the rods and ice, and the returned fluid and ice cuttings flow up the inside of the drill rods. This is done to mitigate the risk of cuttings freezing in the small annulus between the ice and the drill rod. The FRS is a key component of the fluid circulation system, and is a unique development under this project. As with all prototype equipment, it requires comprehensive testing under expected operating conditions.

In order to accomplish the RAID system test, we designed and built a facility where we could drill ice and test the rig's drilling and coring capabilities as well as the functioning of the FRS. In brief, the NAT facility consisted of a hole where we froze a column of ice and conducted a series of system tests. Other test facilities for testing ice drilling include a 60 m deep hole at CRREL (National Research Council, 1986) and a 13 m deep facility at the University of Alaska (Das and Jois, 1994). A 76 m deep well at the University of Wisconsin was established as part of the IceCube development and was used in early 2016 to test the ASIG drill (K. Slawney, personal communication, 2017).

The NAT facility was established on private land near Bear Lake, Utah, and was permitted through the Utah Division of Oil Gas and Mining. This site met a number of criteria. First, this region is often one of the coldest areas in the lower continental United States. We wanted to replicate temperatures that the equipment and personnel would experience in Antarctica. Second, operations in Antarctica are expected to take place at elevations of 3000 to 4000 m. These elevations will impact the performance of both machinery and personnel; the elevation at the NAT site is 1824 m above sea level. Lastly, since we wished to freeze a column of ice to a depth of 137 m, we were working against natural heat flow. Therefore, we chose a region in northeastern Utah that has relatively low heat flow (60–80 $\mathrm{mW\,m^{-2}}$; Edwards and Chapman, 2013; Nielson et al., 2016).

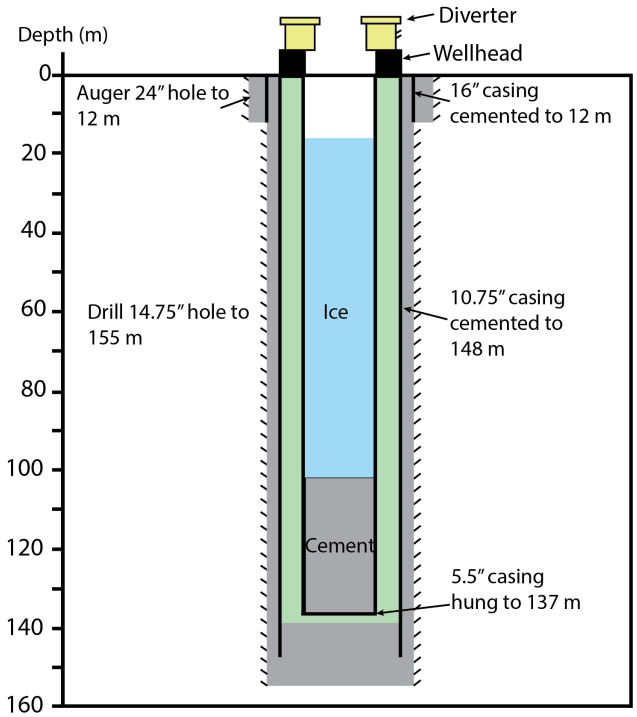

Figure 1. Schematic diagram of the North American Test facility.

2 Facility construction

Drilling was initiated in January, 2015, by augering a 61 cm (24 in.) hole to a depth of 12 m (40 ft). A 40.6 cm (16 in.) diameter conductor casing was cemented in place. A 37.5 cm (14.75 in.) hole was then drilled to total depth of 155 m by an Atlas Copco RD-20 rotary drill, utilizing air and foam. Then, a 27.3 cm (10.75 in., L-80, 45.5 $\mathrm{lb\,ft^{-1}}$) high-strength low-carbon steel casing was cemented in place to 152 m. The 27.3 cm casing was designed to separate the test hole from the bedrock to eliminate the possibility of contamination from ESTISOL. Throughout the planning process, we were concerned about the behavior of steel at very low temperature, and the volume change associated with the water to ice transition that could potentially split the casing. As a result, we chose casing that was as strong as practical. Charpy V-notch testing confirmed an average toughness rating of 177.6 J at −50 °C.

A 14 cm (5.5 in., L-80, 17 $\mathrm{lb\,ft^{-1}}$) casing string was designed to host the ice, and a cement plug at the bottom simulated the ice–bedrock transition. The Charpy V-notch testing on this casing produced 99.8 J at −50 °C. The 14 cm casing was centralized and hung inside the 27.3 cm casing using a standard oil field wellhead. The annular space between these two casing strings formed the space for the circulation of coolant. A diverter was attached to the 5.5 in. casing to control the flow of the circulation fluid. Figure 1 shows the final, as-built NAT facility.

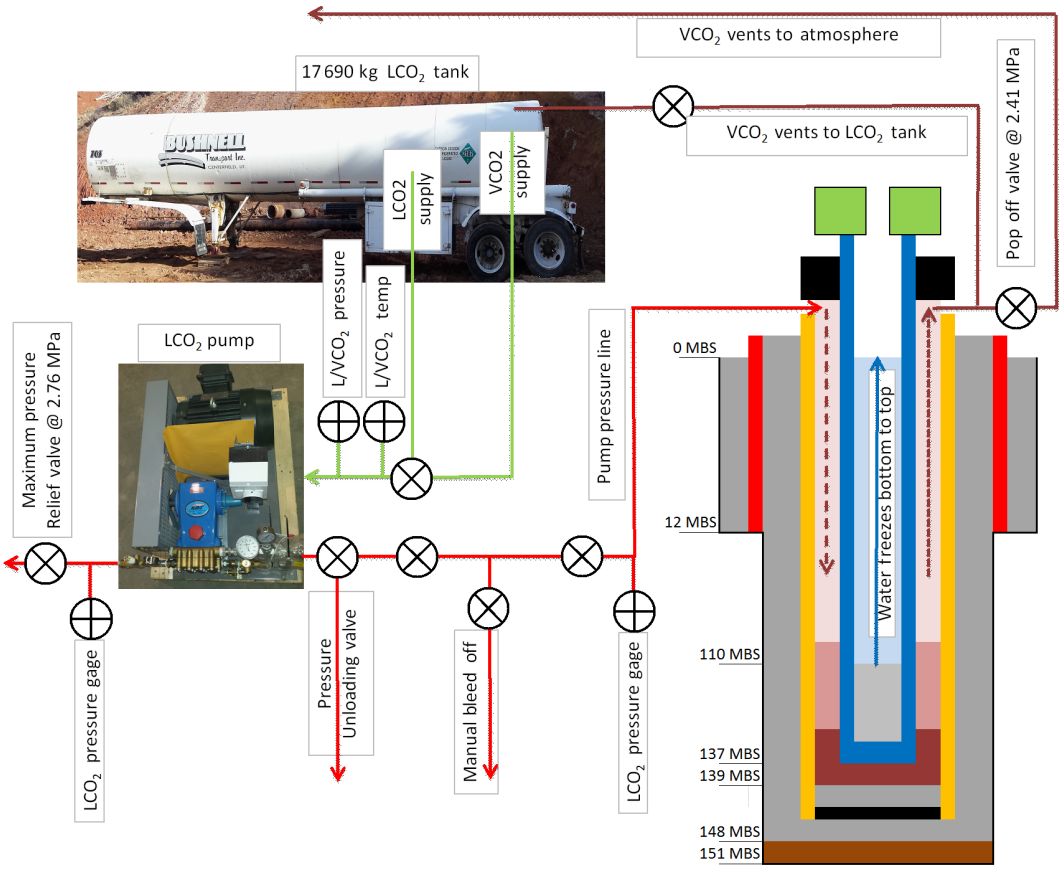

Figure 2. Cooling process diagram for the NAT facility.

A thermistor string was critical for monitoring the temperature of the well during the testing activities. A Geokon thermistor string with digital read-out at 15 m intervals was installed in the annular space between the 27.3 and 14 cm casing strings.

Liquid CO_2 (LCO_2) was selected as the refrigerant after an extensive review of different options. The basis of this selection was that LCO_2 is relatively inexpensive, readily available, and pumps easily. The wellhead had choke and kill lines through which we introduced LCO_2 and allowed CO_2 vapor to exit. By controlling the pressure at the outlet, we were able to manage the temperatures during the cooling process. The cooling system for the facility (Fig. 2) included a 17 690 kg (39 000 lb.) insulated LCO_2 storage tank that held LCO_2 at −20 °C and 1.72 MPa (250 psi). From this supply tank an insulated 2.5 cm line was connected to the suction side of the LCO_2 pump. The pump could generate up to 8.27 MPa (1200 psi) and moved the liquid from the supply tank to the inlet of the wellhead. Prior to pumping LCO_2 into the well, a vapor line was connected to the well from the top of the supply tank allowing the hole to flood with CO_2 vapor. This removed oxygen and moisture from the annular space and started the cooling process. The supply temperature and pressure were monitored at the pump using analog gauges. The pump had a maximum pressure relief valve on the distribution manifold that was set to 2.76 MPa (400 psi). The first time we loaded the hole with LCO_2 and exceeded 3.10 MPa (450 psi), we experienced pressure that was large enough to lift the 14 cm casing out of the hanger wedges. This broke the seal around the 14 cm casing, and CO_2 leaked from the annular space. To correct this issue, we used a set of chains and binders to hold the diverter down, which in turn held the 14 cm casing in place.

As LCO_2 was introduced into the well, it absorbed heat, flashed to vapor, and the surrounding area experienced a temperature drop. Therefore, the hole cooled from the top down (Fig. 3). Once the temperature of the well was lowered to the saturation curve (equilibrium between liquid and vapor), the CO_2 will remain in a two-phase liquid–vapor state. Cycling the injection allowed the annular space to be flooded by LCO_2. Releasing the pressure on the hole allowed the LCO_2 to flash, resulting in a decrease in temperature. Using this method, we were able to cool the entire hole. Due to the natural heat flux, it was necessary to constantly introduce LCO_2 into the hole to maintain the temperature required.

Figure 3 shows the cooling history of NAT-1 starting on 5 February 2015 and following completion of the test facility. On 9 February, CO_2 vapor was introduced into the annulus to

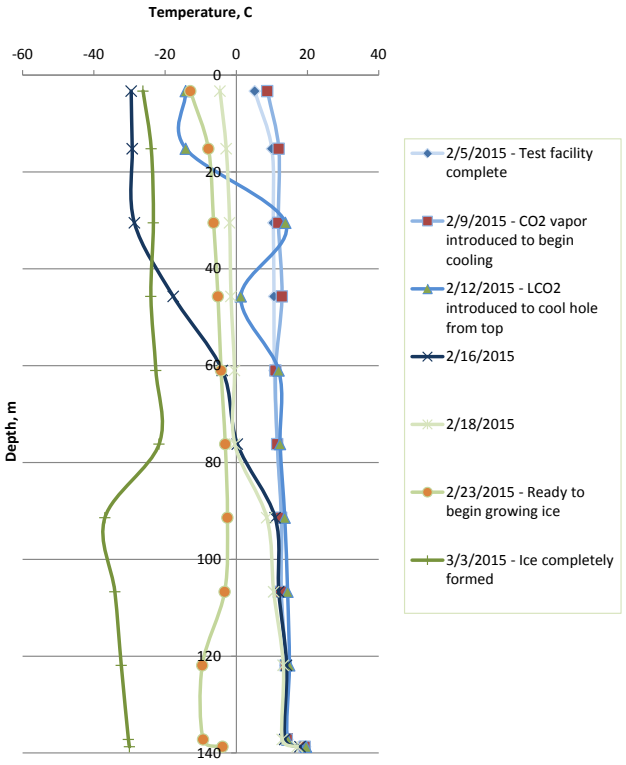

Figure 3. Temperature with depth showing the cooling history of the North American Test facility.

displace air and begin the cooling process. On 12 February, we began introducing LCO_2 and cooling the hole from the top. The curve from February 23 shows the temperature profile of the hole just before we started to grow ice in the 14 cm casing. The final curve from 3 March shows the temperature profile once ice was formed in the 14 cm casing.

On several occasions we ran out of LCO_2 from the main supply tank, or needed to stop cycling in order to do maintenance. This resulted in the temperature in the hole rebounding rapidly, and the cooling process had to be repeated.

Freezing water produces roughly 207 MPa (30 000 lbs in.$^{-2}$) of force on the walls of a confining vessel. We were concerned that if the 14 cm liner burst during the freezing process, we might only get one opportunity to drill the ice. In addition to selecting steel that was as strong as possible, we decided to introduce cubed ice from the surface and then add liquid water to fill the gaps between the cubes. Although time-consuming, we believed this method would efficiently establish an ice column and reduce the strain on the liner by about 75 % compared to filling it with water alone.

To calibrate the process, we added 3.2 kg of cubed ice to a piece of 14 cm casing and then added water. Together, 3.2 kg of ice and 2.5 L of water filled approximately 50 cm of the 14 cm casing. In the borehole, ice cubes were allowed to free fall to the bottom. The water, however, was a more difficult problem since it needed to be delivered to the bottom of the hole without freezing to the casing. A simple fluid dispenser was devised based on a reverse-bailer concept that would introduce approximately 53 L of water to the bottom of the hole using the drill's wireline. Impact of the fluid dispenser with the top of the ice released a rubber plug, and the water flowed into the ice. The freezing process then took place in 3.3 m increments, and the duration of a complete freezing cycle was 3 to 4 h. A video log was run at the end of each ice–water loading cycle to verify placement and the correct depth of the ice.

3 Testing and lessons learned

Details of the testing procedure will be covered separately; however, the principal objectives were to evaluate bit design, to exchange a face-centered bit for coring assembly, to drill at different rates, and to confirm the functioning of the FRS. The RAID is designed to be capable of drilling rapidly through the ice in order to maximize the number of holes that can be drilled in an Antarctic summer field season. To achieve this objective, the rate of penetration is of paramount importance. The range of components that affect the penetration rate introduces too many variables to accurately determine the rate mathematically and therefore must be tested to see how hard the systems can be pushed to maximize ice drilling speed while ensuring a high degree of safety. The drilling process used an 88.9 mm bit and NRQ V-wall core rod (69.85 mm; 2.75 in. OD). The main parameters that have a direct effect on penetration rate are rotation speed, flow rate of the fluid circulation system, capacity of the FRS system to process debris and ice cuttings and return a clean drilling fluid, pressure exerted on the borehole to maintain the fluid flow required, and the cutting capacity of the drill bit.

Achieving progressively higher penetration rates was the chief factor guiding our testing sequence. The underlying rationale for this testing approach was that if the drill can operate successfully at its maximum penetration rate (3.0 m min^{-1}), then all supporting systems are in fact functioning within specifications. A step-wise approach with progressively higher penetration rates allowed us to validate operation of each sub-system. Phase I tests at a quarter of the desired maximum speed (0.75 m min^{-1}) were intended to first establish successful drilling into the ice column, and to become familiar with the system before pushing its limits. Succeeding phases were designed to validate operation at successively higher penetration rates: at half-speed (1.5 m min^{-1}) and at full speed (3.0 m min^{-1}). The next phase focused on coring into the cement plug at the bottom of the ice in order to simulate bedrock coring.

Video logs were run in the hole following each test. The logs revealed an unanticipated problem with the ice-forming process. In the process of adding ice cubes and then saturating the ice with water, we observed that the top 50 % of

the 3.3 m segment formed compact ice, and the bottom 50 % of the volume was loosely bonded ice cubes. Attempting to freeze a 3.3 m section was too aggressive. Water did not flow completely through the cubed ice, resulting in a section of completely frozen ice that drilled smoothly and an underlying section where the ice would break off in pre-formed cubes during drilling.

After completion of the half-speed testing segment, we refroze the hole using only water so that we could attempt to drill the full-speed test in as pristine ice as possible. We did this in increments of about 1.5 m, and the time to freeze these segments was about 4–5 h.

Frequently, the drill bit came into contact with the casing wall, resulting in damage to the cutters on the bit. Drilling with an 88.9 mm outer-diameter bit in a 124.2 cm inner-diameter casing provided too little space for the bit to wander, and any future work should consider using a larger inner-casing string.

The coring tools were tested and we were able to retrieve core, though not of the length we desired. The concrete placed at the bottom of the 14 cm casing was powdered by the extreme cold and was not an appropriate analog for hard rock.

Designing NAT-1 devoted a considerable amount of study to determine the best mechanism for cooling the hole. We considered the option of using a mechanically pumped coolant, such as Dynalene, in place of LCO_2. LCO_2 was chosen because of lower cost and ability to reach lower temperatures through the control of pressure. However, LCO_2 proved difficult to handle, and a long-term test site should consider use of a circulating refrigerant. Despite the challenges and lessons learned during experimentation, we view the creation of the NAT facility as a success that allowed for the validation of the drilling and fluid circulation components of the RAID. At the completion of the testing, the facility was plugged and abandoned. The RAID system has been shipped to Antarctica and will undergo field trials at Minna Bluff in November–December, 2016.

Competing interests. The authors declare that they have no conflict of interest.

Acknowledgements. This project was funded by the US National Science Foundation through grants 1242027 and 1419935 to the University of Minnesota Duluth. We would like to express our appreciation to Dan McClellan, Philippe Wyffels, Blaise Stephanus, and John Eckels for their contributions to the project.

Edited by: T. Wiersberg
Reviewed by: A. Pyne and one anonymous referee

References

Clow, G. D. and Koci, B.: A fast mechanical-access drill for polar glaciology, paleoclimatology, geology, tectonics and biology, Mem. Nat. Inst. Polar Research, 56, 5–37, 2002.

Das, D. K. and Jois, S. S.: Thermal modeling of ice cores and boreholes via the finite element technique, Proceedings Forth International Workshop on Ice Drilling Technology, Tokyo, Mem. Nat. Inst. Polar Research, 49, 256–280, 1994.

Edwards, M. C. and Chapman, D. S.: Geothermal resource assessment of the Basin & Range province in western Utah, University of Utah, Department of Geology and Geophysics, 112 pp., 2013.

Gerasimoff, M. D.: Prospectus for a Rapid Access Ice Drill: a drilling system equipped for rapid transit of glacial ice, equipped for on-the-fly ice coring and suitable for regional geological mapping and glaciology, Ice Drilling Design and Operations report, University of Wisconsin, Madison, 57 pp., 2012.

Goodge, J. W. and Severinghaus, J.: Rapid Access Ice Drill: a new tool for exploration of the deep Antarctic ice sheets and subglacial geology, J. Glaciol., 62, 1049–1064, doi:10.1017/jog.2016.97, 2016.

National Research Council: Recommendations for a US ice coring program, National Academy Press, Washington, DC, 1986.

Nielson, D. L., Delahunty, C., Goodge, J. W., and Severinghaus, J. P.: Rapid Access Ice Drill (RAID), Arctic Technology Conference, St. John's, Newfoundland, OTC Paper 27324, 2016.

Sheldon, S. G., Popp, T. J., Hansen, S. B. and Steffensen, J. P.: Promising new borehole liquids for ice-core drilling on the East Antarctic high plateau, Ann. Glaciol., 55, 260–270, 2014.

Sci. Dril., 22, 35–42, 2017
www.sci-dril.net/22/35/2017/
doi:10.5194/sd-22-35-2017

Scientific Drilling
Open Access

A comparison of the use of X-ray and neutron tomographic core scanning techniques for drilling projects: insights from scanning core recovered during the Alpine Fault Deep Fault Drilling Project

Jack N. Williams[1], **Joseph J. Bevitt**[2], **and Virginia G. Toy**[1]

[1]Department of Geology, University of Otago, PO Box 56, Dunedin 9054, New Zealand
[2]Australian Centre for Neutron Scattering, Australian Nuclear Science and Technology Organisation, Lucas Heights NSW 2234, Australia

Correspondence to: Jack Williams (jack.williams@otago.ac.nz)

Received: 20 September 2016 – Revised: 17 December 2016 – Accepted: 16 January 2017 – Published: 31 May 2017

Abstract. It is now commonplace for non-destructive X-ray computed tomography (CT) scans to be taken of core recovered during a drilling project. However, other forms of tomographic scanning are available, and these may be particularly useful for core that does not possess significant contrasts in density and/or atomic number to which X-rays are sensitive. Here, we compare CT and neutron tomography (NT) scans of 85 mm diameter core recovered during the first phase of the Deep Fault Drilling Project (DFDP-1) through New Zealand's Alpine Fault. For the instruments used in this study, the highest resolution images were collected in the NT scans. This allows clearer imaging of some rock features than in the CT scans. However, we observe that the highly neutron beam attenuating properties of DFDP-1 core diminish the quality of images towards the interior of the core. A comparison is also made of the suitability of these two scanning techniques for a drilling project. We conclude that CT scanning is far more favourable in most circumstances. Nevertheless, it could still be beneficial to take NT scans over limited intervals of suitable core, where varying contrast is desired.

1 Introduction

The value of core obtained in drilling projects can be significantly enhanced through the application of non-destructive tomographic scanning techniques. These techniques permit high resolution imaging of the internal structure of the core and allow the identification of features that would not be apparent during visual inspection of the core alone. They may also allow assessment of bulk material properties, such as porosity and permeability (e.g. Grader et al., 2000; Wennberg et al., 2009; Voorn et al., 2015), and act as a historical record of the core once it has been subsampled. For these reasons and others, it is now common to obtain X-ray computed tomographic (CT) scans of core upon its recovery during drilling projects (Rothwell and Rack, 2006; Withjack et al., 2003).

Tomography refers to the cross-sectional imaging of an object through the transmission or reflection of an incident wave penetrating the object from multiple directions. In the case of CT scanning, the internal structure of an object is visualised based on the extent to which it attenuates X-rays. Data like these have demonstrably contributed to the scientific outcomes of drilling projects (e.g. Keren and Kirkpatrick, 2016; Sills, 2013; Withjack et al., 2003). However, the applicability of CT scanning can be limited. For example, if the core does not contain materials that possess significant contrasts in X-ray attenuation, then features within the core will not be observed in the scans. In these cases, other forms of non-destructive tomographic core scanning may be more useful, such as neutron tomography (NT) or nuclear magnetic resonance (NMR) imaging. These techniques use different incident waves from CT scanning, so they are sen-

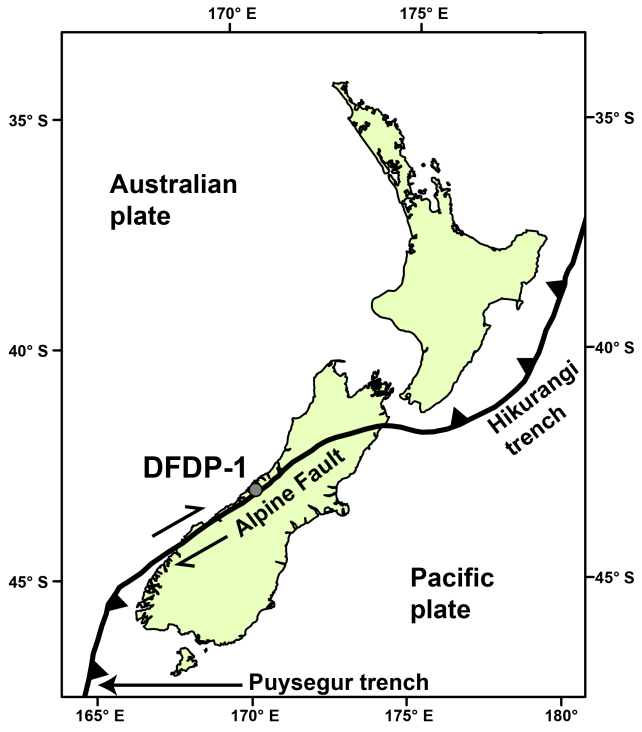

Figure 1. Location of the Alpine Fault and the DFDP-1 boreholes in the context of the Australian–Pacific plate boundary through New Zealand.

sitive to different material properties. Therefore, they can image features that may be poorly resolved in CT images.

In this contribution, we compare and contrast CT and NT scans taken of core collected from phase 1 of the Deep Fault Drilling Project (DFDP-1) through New Zealand's Alpine Fault zone (Fig. 1). Previous assessments have been made of the quality of images derived from CT and NT scanning of geologic materials (Schwarz et al., 2005; Vontobel et al., 2005), including drillcore (Christe et al., 2007). Herein, we provide the first comparison of (1) CT and NT images in samples from an active fault zone and (2) the practicality of these scanning techniques within the constraints of a drilling project.

2 Experimental set-up of CT and NT scanning of DFDP-1 core

The Alpine Fault accommodates approximately 70 % of the motion between the Australian and Pacific plates in the South Island of New Zealand (Fig. 1). Several criteria, such as its late interseismic state (Berryman et al., 2012; Sutherland et al., 2007), well-determined Quaternary slip rates (Norris and Cooper, 2001), and the fact that it currently exhumes a suite of deformed rocks with features representative of deformation processes still occurring today, make the Alpine Fault a globally unique target for scientific drilling (Townend et al., 2009). The Alpine Fault Deep Fault Drilling Project (DFDP, http://alpine.icdp-online.org) was initiated in 2011 with its first phase, resulting in the completion of two vertical boreholes, DFDP-1A and DFDP-1B, drilled to depths of $\sim$100 and 152 m respectively. Both holes intercepted the principal slip zone gouges of the Alpine Fault (Sutherland et al., 2012).

Within several weeks of the completion of the DFDP-1 boreholes, 23.2 m of PQ (i.e. diameter 85 mm) core from DFDP-1A and 50.5 m from DFDP-1B were CT scanned. In this technique, the attenuation of the X-ray signal is mainly a result of interaction between the X-ray photon and the electrons of an atom's shell (Schwarz et al., 2005; Vontobel et al., 2005). Attenuation reflects the density and the atomic number (Z) of the material it passes through. The raw intensity data are converted linearly to a CT number, which are typically represented visually by a greyscale value (Ketcham and Carlson, 2001).

CT scans were collected at the Oncology Department of Dunedin Hospital, New Zealand. A Philips accolade scanner was operated at 200 mA and X-ray tube voltage 120 kVp, which gives a half value layer of 8.4 mm. The horizontal slice spacing was 1 mm, the field of view was 250 mm, and the image size was 1024×1024 pixels. This results in a voxel size of $0.244 \times 0.244 \times 1$ mm in the x, y, and z directions respectively. To reconstruct the CT image stack into three-dimensional images and two-dimensional slice images of the core, OsiriX imaging software (http://www.osirix-viewer.com/) was used.

NT scans of DFDP-1 core were collected using the thermal neutron tomography instrument, DINGO, at the Australian Centre for Neutron Scattering, Australian Nuclear Sciences and Technology Organisation (ANSTO) in Sydney, Australia (Garbe et al., 2011). Neutrons mainly interact with matter through absorption and scattering with atomic nuclei, so neutron beam attenuation is strongly affected by the presence of light atoms, which present a small cross-sectional area to the neutron flux (Christe et al., 2007). Therefore, NT scans are able to resolve features that contain contrasts in the concentration of light elements, such as hydrogen, boron, and lithium.

The set-up used to scan DFDP-1 core is shown in Fig. 2. Core was wrapped in aluminium foil, which is highly transparent to neutrons. During the scan, the core was rotated around its axis through 180 or 360° while the neutron beam was passing through it. The scintillation screen of DINGO, and thus the field of view, is 20 cm × 20 cm. The 100 µm thick scintillation screen consists of an aluminium sheet, which is coated with a thin layer of the scintillation material ZnS/6LiF (Garbe et al., 2011). It is possible to translate the sample stage in the z direction (up and down) so that scans are taken in two separate fields of view. In this way, it is possible to scan a core of < 40 cm in length or two different core samples of < 40 cm in total length at one time (e.g. Scan 1, Table 1). In these cases, two separate scans are collected that later require stitching together.

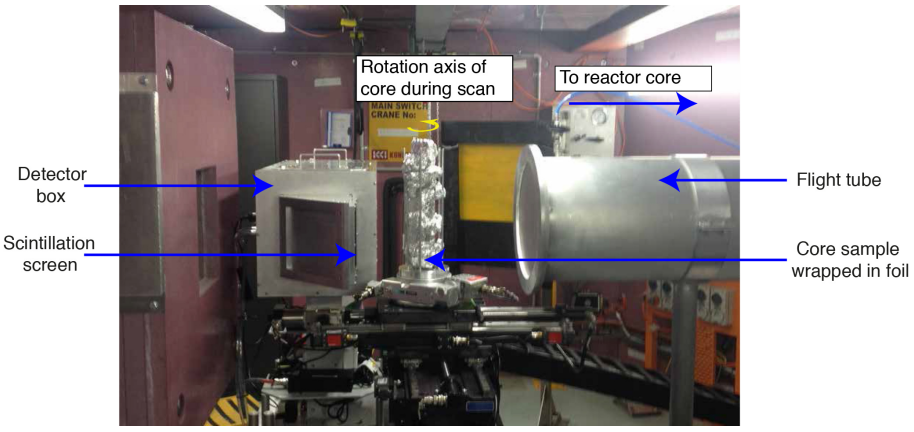

Figure 2. Set-up of DINGO for NT scanning of DFDP-1 core. The field of view is approximately 2.5 m across.

We selected ten subsamples of DFDP-1 core of < 25 cm in length. The selection of these samples was based on (1) whether they contained noteworthy fault rock fabrics and (2) ensuring that a range of the lithologies described in DFDP-1 core (Toy et al., 2015) was scanned. Nine samples were whole core and, for comparison, one was split along its length. In 5 days, we were able to perform nine scans (Table 1), which amounted to a total length of 2.26 m of scanned core.

All core samples were scanned with a low-intensity, low-divergent neutron beam with a collimation ratio of $L/D = 1000$, where L is the collimator length and D is the neutron aperture diameter (ASTM, 2013). For comparison, two scans of core were also taken with a high-intensity and more divergent beam ($L/D = 500$). When allowing for the collection of reference images of the empty beam, the typical run time for < 20 cm of core was ∼ 5 h. For scanning intervals of core from 20 to 40 cm, which required the automated height adjustment of the scintillation screen, the run times were ∼ 10 h. The raw image files collected from the scan were reconstructed into an image stack comprising slices perpendicular to the rotation axis using Octopus Reconstruction (https://octopusimaging.eu/octopus/octopus-reconstruction). In this step, a beam hardening correction was applied to the images. The actual correction applied was chosen subjectively, since noise can be added to images in which a beam hardening correction is too harsh. Image stacks were then viewed using the software Avizo (http://www.fei.com/software/avizo3d/), after the application of Avizo's Non-Local Means smoothing image filter.

3 CT and NT image comparison

Broadly speaking, the DFDP-1 cores scanned comprise two types of lithology: ultramylonites (Units 1 and 2 of Toy et al., 2015) and cataclasites (Units 3, 4 and 6 of Toy et al., 2015). Ultramylonites contain a foliation defined by alternating millimetre–centimetre quartzofeldspathic and phyllosilicate-rich (biotite, muscovite, and chlorite) layers. Cataclasites are found to contain millimetre–centimetre quartzofeldspathic clasts surrounded by a phyllosilicate matrix. All lithologies are cross-cut by millimetre–centimetre thick clay-enriched fractures, which contain quartz, albite, muscovite, chlorite, calcite, and smectite, that constitute the damage zone of the Alpine Fault (Caine et al., 1996; Schleicher et al., 2015; Toy et al., 2015; Williams et al., 2016).

Figures 3 and 4 present a comparison of CT and NT scans of ultramylonite units and cataclasite units respectively. In addition, we include 180° of unrolled Geotek images of the same interval of core. Both scanning techniques are capable of imaging the core features described above, in particular clay-enriched fractures. In NT scans, these fractures appear bright white, indicating high neutron attenuation and therefore relatively high concentrations of hydrogen. This may reflect the fact that the clays contain bonded water in their mineralogical structure. Open and partially open fractures were more successfully imaged by CT scanning (Fig. 3c).

The voxel size in NT scans is 0.000870 mm^3 (3 s.f.), which is ∼ 70 times smaller than the voxel size of the CT scans (0.0595 mm^3 3 s.f. – significant figures). This allows better characterisation of the morphology of the fractures, the identification of some fractures not identified in the CT scans (e.g. Fig. 3b), and more precise imaging of the cataclastic fabric (Fig. 4a). However, we note that industrial CT instruments may permit higher spatial resolution (100–200 µm) than the medical CT instrument used in this study (Kyle and Ketcham, 2015; Masschaele et al., 2013). In addition, the resolution of the CT scans will depend on core diameter and density. Therefore, the higher resolution of the NT scans in this study will not necessarily be realised in all cases.

DFDP-1 core was found to be highly neutron attenuating and therefore posed considerable challenges in imaging the centre of the drillcore, even after the application of a beam hardening correction. In Fig. 4c and d, it can be observed that it is difficult to trace features that are well defined near

Table 1. Summary of core samples and acquisition parameters for the NT scans performed on DFDP-1 core on the NT instrument DINGO at ANSTO.

Scan	Sample a	Sample b	Rotation (°)	Rotation increment (°)	Intensity	Images	Exposure (s) scanned (cm)	Length of core
1	DFDP-1A 1A_55-2	DFDP-1B_35-1	180	0.25	Low	721	20	15
2	DFDP-1B_35-1		180	0.25	Low	721	20	20
3	DFDP-1B_49-1	DFDP-1A_58-1	180	0.225	Low	1602	22	42
4	DFDP-1B_43-1		180	0.225	Low	801	22	23
5	DFDP-1A_63-2	DFDP-1B_58-2	180	0.225	Low	1602	22	35
6	DFDP-1A_59-2	DFDP-1B_66-1	180	0.225	Low	1602	22	35
7	DFDP-1B_65-2		180	0.225	Low	801	22	23
8	DFDP-1A_63-2		360	0.2	High	1801	4	20
9	DFDP-1A_63-2	DFDP-1A_55-2	360	0.2	High	1801	4	13

Table 2. A comparison of the practicality of CT and NT scanning in the framework of a drilling project.

	X-ray computed tomography scanning	Neutron tomography scanning
(i) Applicability to geologic materials	Broadly applicable to all geological materials	Not recommended for wet (i.e. H-rich) samples; Better suited to dry, dense geological materials
(ii) Availability and portability of scanner	Widely available at major hospitals and scientific institutions; Portable, so can be brought onto a drill site or ship	Requires neutron source, limited availability
(iii) Scanning rate	12 m h^{-1}	~ 50–200 cm day^{-1}, depending on scanner set-up
(iv) Maximum length of core scanned	~ 1.5 m	40 cm
(v) Resolution	100–1000 µm, depending on direction	~ 25–200 µm, independent of direction
(vi) Sensitive to	Contrasts in density and atomic number	Presence of hydrogen and other light elements
(vii) Penetration	10–50 cm, depending on sample composition, X-ray energy and desired image quality	10–50 cm, depending on sample composition
(viii) Cost, per metre of drillcore	USD 15/m[a]	USD 2640–10 560/m[b]

[a] Calculated assuming that it is possible to scan 12 m of core per hour (i.e. each scan of a 1 m core section takes 5 min); pricing structure at the Dunedin Hospital Oncology Department.
[b] Based on a scanning rate of 50–200 cm day^{-1} and the commercial pricing for use of the DINGO facility at ANSTO (http://www.ansto.gov.au/ResearchHub/Bragg/Users/Requestingbeamtime/CommercialPrices/index.htm).

the outer surface of the core, into its centre. This problem is exemplified in Fig. 5., which shows unrolled images of the CT and NT scans generated using a script in Fiji (https://fiji.sc/). To obtain these, the image stack is loaded in Fiji and a circle is drawn around the core in an axial-perpendicular slice. This is then used to a define a path around which the image is constructed for all slices perpendicular to the core axis. In this way, we can generate circumferential images of the outer surface of the core and also of surfaces within the core interior.

In the case of the NT scans, this shows that it is possible to resolve more features that are closer to the outer surface of the core, where there has been less absorption and scattering of the neutron beam, than in an interior surface of the core (Fig. 5). This result was found regardless of whether the core was scanned using a low- or high-intensity neutron beam. Therefore, the most successful imaging of the interior of highly neutron attenuating core will be acquired in split core samples, such as in Fig. 4a, with a thickness of 3.5 cm. Similar problems with neutron penetration were also encountered by Christe et al. (2007); however, a correction to account for neutron scattering could mitigate this to an extent (Hassanein et al., 2005, 2006). No such penetration issues were found when CT scanning DFDP-1 core.

4 Applying CT and NT scanning during drilling projects

Table 2 outlines a list of criteria that may be applied when deciding which scanning technique to employ during a drilling project. Based on these criteria, CT scanning is more advantageous than NT scanning. For example, whereas CT scanning is suitable for a wide range of geological samples, NT scanning may not be appropriate for wet samples as the high amounts of H they contain will mean they have strongly neutron attenuating properties (Table 2i). Furthermore, whereas CT scanners are widespread and portable – to the extent that they can be brought onto a drill site or ship (Freifeld et al.,

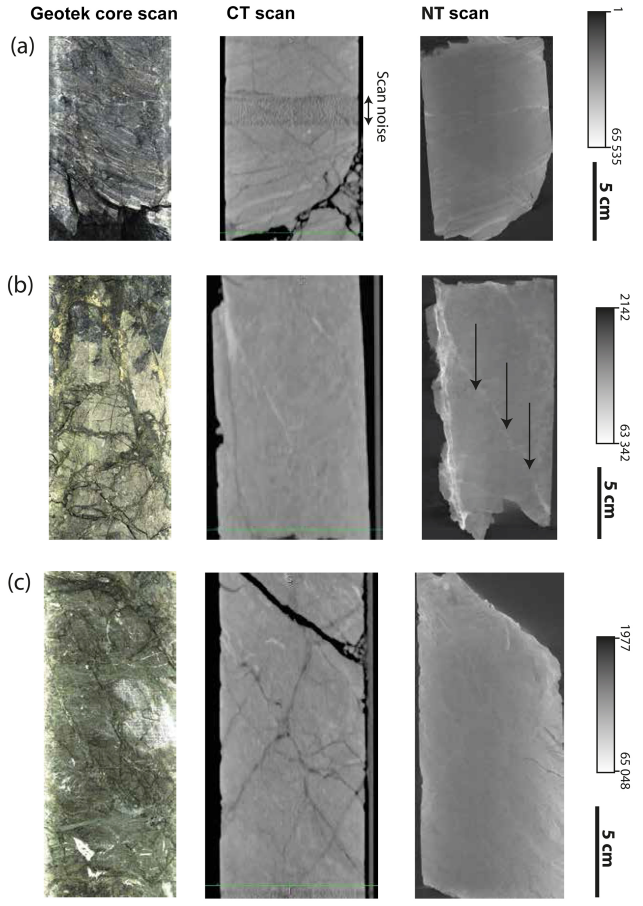

Figure 3. Comparison of 180° unrolled Geotek images and 2-D core axial-parallel CT and NT slice images of DFDP-1 for ultramylonite intervals. For core section intervals (borehole_core run and section_depth interval from the top of the core section in cm) **(a)** DFDP-1A_55-1_82-95 (depth interval 75.82–75.95 m), **(b)** DFDP-1B_49-1_35-50 (115.85–116.00 m), and **(c)** DFDP-1B_35-1_70-88 (102.57–102.75 m). Arrows in **(b)** identify a clay-enriched fracture in the NT image that is not identified in the CT images. Greyscale refers to NT images, and all CT images have a greyscale of CT 500–4000.

2006) – NT scanners require a neutron source, of which only a handful are available worldwide (Table 2ii).

When designing a core flow plan for a drilling project, it is often critical that the rate of core scanning is equal to or exceeds the rate at which core is recovered. This is in order to prevent the accumulation of unscanned core, which can lead to delays in other aspects of the core flow plan. In this respect, CT scanning is preferable as core can be scanned more rapidly than the rate at which it is recovered (Table 2iii, assuming an average core recovery rate of 1 m per hour). In CT scanning, the X-ray source and detector can be moved rapidly around the long axis of a fixed sample (Ketcham and Carlson, 2001; Schwarz et al., 2005). Conversely, in the case of NT scanning, the neutron source and detector are fixed whilst the sample is rotated through 180 or 360°. In addition, once the NT scans have been taken, further processing of the raw sinograms is required to construct the image stack. Moreover, in our experience of scanning DFDP-1 core, it was also necessary that the core be quarantined for 1–2 weeks at the scanning facility before their radiation decayed to safe background levels.

The current set-up of DINGO limits the maximum length of core that can be scanned to 40 cm (Table 2iv). This limit is imposed by the maximum vertical movement of the sample stage relative to the scintillation screen. In future, it is conceivable that a continuous scan of whole core sections >40 cm in length may be carried out on DINGO if core is mounted on a horizontal axis rotation stage (as opposed to the current vertical rotation set-up, Fig. 2) so that core is translated horizontally past the scintillation screen between measurements. In such a set-up, the field of view will still be 20 cm, so the generation of a continuous image stack of the entire core section will require that the individual scans be stitched together.

Given the above considerations, in the framework of a drilling project, CT scanning is more desirable than NT scanning. However, instances exist when it would be desirable to take NT scans, given that they are more sensitive to different material contrasts than CT scans (Table 2vi). We therefore propose the following strategy for scanning core. On site, or immediately after core recovery, all core should be CT scanned. This will provide an excellent "bulk" dataset of the core and, along with visual core descriptions, allow the determination of noteworthy intervals. We advocate that these selected intervals should then be imaged by NT as this allows the identification of features that may not have been resolved during CT scanning. The most successful NT imaging will be performed for core samples that contain localised amounts of hydrogen or other light elements, which are surrounded by only weakly interacting materials, such as in the case of DFDP-1 core. In cases of cores that contain a relatively high amount of strongly neutron attenuating elements, successful imaging can still be achieved if the core is split before NT scanning or if smaller diameter core is collected at the outset.

5 Conclusions

We have reviewed the use of X-ray computed tomography (CT) and neutron tomography (NT) to scan core recovered during the first phase of the Deep Fault Drilling Project (DFDP-1) through New Zealand's Alpine Fault. Both scanning techniques successfully imaged millimetre–centimetre core features, such as clay-enriched fractures and cataclasite fabrics. The morphology of these features was more adequately captured by the NT scanning as it is capable of higher resolution imaging than the CT scans; however, because of the highly neutron attenuating properties of DFDP-1 core,

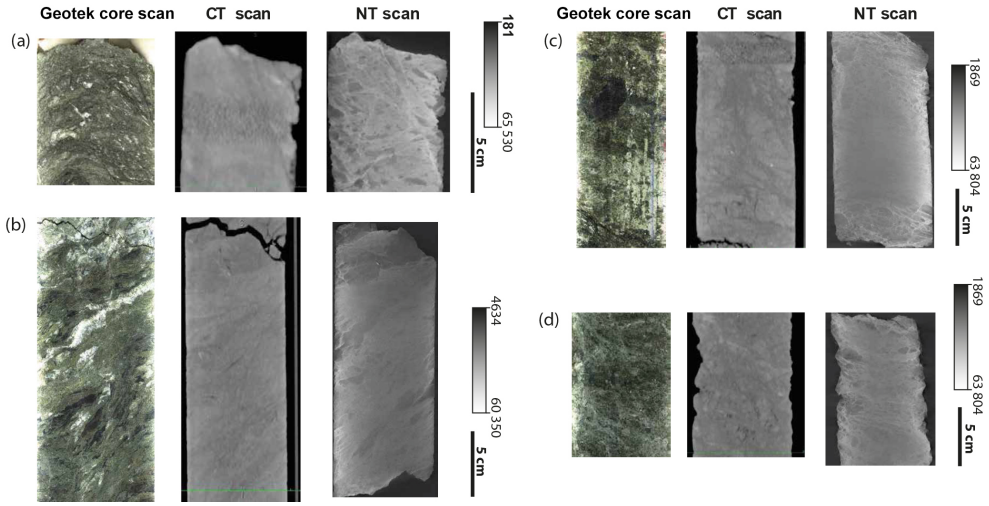

Figure 4. As for Fig. 3, but for cataclasite units. For core section intervals (borehole_core run and section_depth interval from the top of the core section in cm) **(a)** DFDP-1B_58-2_0-8 (depth interval 127.93–128.01 m), **(b)** DFDP-1A_63-2_47-70 (86.48–86.71 m), **(c)** DFDP-1A_59-2_8-27 (80.01–80.20 m), and **(d)** DFDP-1B_66-1_40-53 (138.50–138.63 m). Note that **(a)** is the split core sample.

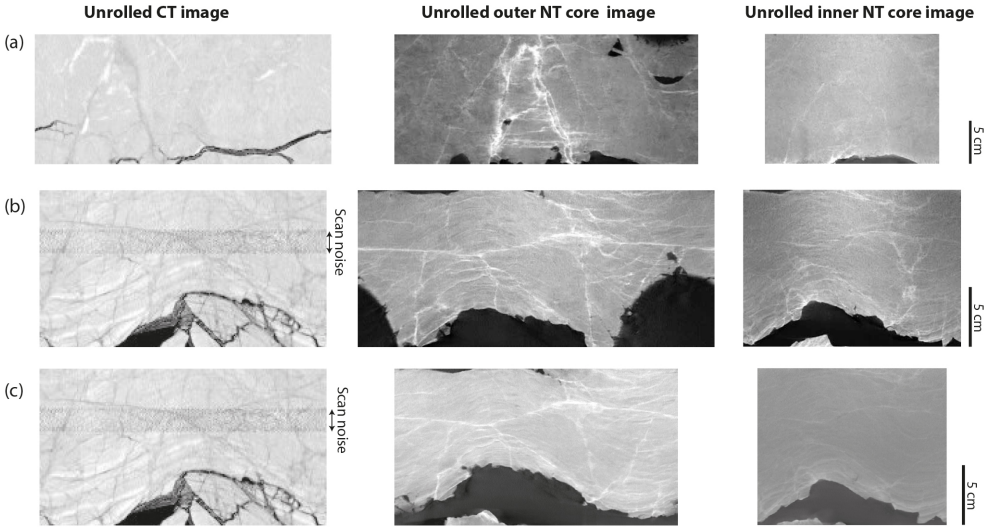

Figure 5. Comparison of unrolled images of core taken from CT and NT scans. Outer and inner core images are constructed from the NT scans to depict the difference in image quality between the outer core surface and the core interior. For core section intervals (borehole_core run and section_depth interval from the top of the core section in cm) **(a)** DFDP-1B_49-1_35-50 (depth interval 115.85–116.00 m), **(b)** at low-intensity mode DFDP-1A_55-1_82-95 (75.82–75.95 m), and **(c)** at high-intensity mode DFDP-1A_55-1_82-95 (75.82–75.95 m).

these features are poorly resolved towards the centre of the core in NT scans.

In the workflow typically encountered during a drilling project, CT scanning offers considerable advantages in terms of scanning rate, availability of scanners, applicability to a wide range of geologic materials, and cost. We thus recommend that this is used to generate a bulk dataset of the 3-D internal structure of the core. Nevertheless, NT scans have the potential to provide a complementary dataset to these CT scans over limited intervals of core.

6 Data availability

Data are available on request from the corresponding author.

Competing interests. The authors declare that they have no conflict of interest.

Acknowledgements. DFDP-1 was funded by the following: GNS Science; Victoria University of Wellington; the University of Otago; the University of Auckland; the University of Canterbury;

Deutsche Forschungsgemeinschaft and the University of Bremen; Natural Environment Research Council grants NE/J024449/1, NE/G524160/1 and NE/H012486/1 and the University of Liverpool; and the Marsden Fund of the Royal Society of New Zealand. The International Continental Scientific Drilling Program provided extensive support. The DINGO thermal neutron instrument is supported by the Australian Government's National Collaborative Research Infrastructure & Strategy (NCRIS) scheme. Steven Mills (University of Otago) provided the script in Fiji to generate unrolled core images. Jack N. Williams was supported by a University of Otago doctoral scholarship. This paper was significantly improved by reviews from Christian Scheffzuek and an anonymous reviewer.

Edited by: J. Behrmann
Reviewed by: C. Scheffzuek and one anonymous referee

References

ASTM: (American Society for Testing, Materials), E803-91, Standard Test Method for Determining the L/D Ratio of Neutron Radiography Beams, 2013.

Berryman, K. R., Cochran, U. A., Clark, K. J., Biasi, G. P., Langridge, R. M., and Villamor, P.: Major earthquakes occur regularly on an isolated plate boundary fault, Science, 336, 1690–1693, 2012.

Caine, J. S., Evans, J. P., and Forster, C. B.: Fault zone architecture and permeability structure, Geology, 24, 1025–1028, 1996.

Christe, P., Bernasconi, M., Vontobel, P., Turberg, P., and Parriaux, A.: Three-dimensional petrographical investigations on borehole rock samples: A comparison between X-ray computed- and neutron tomography, Acta Geotech., 2, 269–279, doi:10.1007/s11440-007-0045-9, 2007.

Freifeld, B. M., Kneafsey, T. J., and Rack, F. R.: On-site geological core analysis using a portable X-ray computed tomographic system, Geol. Soc. London, Spec. Publ., 267, 165–178, 2006.

Garbe, U., Randall, T., and Hughes, C.: The new neutron radiography/tomography/imaging station DINGO at OPAL, in Nuclear Instruments and Methods in Physics Research, Sectio En A: Accelerators, Spectrometers, Detectors and Associated Equipment, 651, 42–46, 2011.

Grader, A. S., Balzarini, M., Radaelli, F., Capasso, G., and Pellegrino, A.: Fracture-Matrix Flow: Quantification and Visualization Using X-Ray Computerized Tomography, in: Dynamics of Fluids in Fractured Rock, edited by: Faybishenko, B., Witherspoon, P. A., and Benson, S. M., 157–168, doi:10.1029/GM122p0157, 2000.

Hassanein, R., Lehmann, E., and Vontobel, P.: Methods of scattering corrections for quantitative neutron radiography, in: Nuclear Instruments and Methods in Physics Research, Section A: Accelerators, Spectrometers, Detectors and Associated Equipment, 542, 353–360, 2005.

Hassanein, R., de Beer, F., Kardjilov, N., and Lehmann, E.: Scattering correction algorithm for neutron radiography and tomography tested at facilities with different beam characteristics, Phys. B Condens. Matter, 385–386, 1194–1196, doi:10.1016/j.physb.2006.05.406, 2006.

Keren, T. T. and Kirkpatrick, J. D.: The damage is done: Low fault friction recorded in the damage zone of the shallow Japan Trench décollement, J. Geophys. Res. Sol. Ea., 121, 3804–3824, doi:10.1002/2015JB012311, 2016.

Ketcham, R. A. and Carlson, W. D.: Acquisition, optimization and interpretation of X-ray computed tomographic imagery: applications to the geosciences, Comput. Geosci., 27, 381–400, available at: http://ac.els-cdn.com/S0098300400001163/1-s2.0-S0098300400001163-main.pdf?_tid=47f3eb96-5bd4-11e3-86fc-00000aab0f6b&acdnat=1386045485_e323788eaa9cc76ba255f3fba7abec66, 2001.

Kyle, J. R. and Ketcham, R. A.: Application of high resolution X-ray computed tomography to mineral deposit origin, evaluation, and processing, Ore Geol. Rev., 65, 821–839, doi:10.1016/j.oregeorev.2014.09.034, 2015.

Masschaele, B., Dierick, M., Van Loo, D., Boone, M. N., Brabant, L., Pauwels, E., Cnudde, V., and Van Hoorebeke, L.: HECTOR: A 240kV micro-CT setup optimized for research, J. Phys. Conf. Ser., 463, 12012, doi:10.1088/1742-6596/463/1/012012, 2013.

Norris, R. J. and Cooper, A. F.: Late Quaternary slip rates and slip partitioning on the Alpine Fault, New Zealand, J. Struct. Geol., 23, 507–520, 2001.

Rothwell, R. G. and Rack, F. R.: New techniques in sediment core analysis: an introduction, Geol. Soc. London, Spec. Publ., 267, 1–29, 2006.

Schleicher, A. M., Sutherland, R., Townend, J., Toy, V. G., and van der Pluijm, B. A.: Clay mineral formation and fabric development in the DFDP-1B borehole, central Alpine Fault, New Zealand, New Zeal. J. Geol. Geophys., 58, 13–21, 2015.

Schwarz, D., Vontobel, P., Lehmann, E. H., Meyer, C. A., and Bongartz, G.: Neutron Tomography of Internal Structures of Vertebrate Remains?: a Comparison With X-Ray Computed Tomography, Palaeontol. Electron., 8, 11 pp., 2005.

Sills, D. W.: The fabric of clasts, veins and foliations within the actively creeping zones of the San Andreas Fault at SAFOD: implications for deformation processes, 2013.

Sutherland, R., Eberhart-Phillips, D., Harris, R. A., Stern, T., Bevan, J., Ellis, S., Henrys, D., Cox, S., Norris, R. J., Berryman, K. R., Townend, J., Bannister, S., Pettinga, J., Leitner, B., Wallace, L., Little, T. A., Cooper, A. F., Yetton, M., and Stirling, M.: Do great earthquakes occur on the Alpine fault in central South Island, New Zealand?. A continental plate boundary: tectonics at South Island, New Zealand, edited by: Okaya, D., Stern, T., and Davey, F., American Geophysical Union, Washington D.C., 2007.

Sutherland, R., Toy, V. G., Townend, J., Cox, S. C., Eccles, J. D., Faulkner, D. R., Prior, D. J., Norris, R. J., and Mariani, E.: Drilling reveals fluid control on architecture and rupture of the Alpine fault, New Zealand, Geology, 40, 1143–1146, doi:10.1130/G33614.1, 2012.

Townend, J., Sutherland, R., and Toy, V.: Deep Fault Drilling Project – Alpine Fault, New Zealand, Sci. Dril., 8, 75–82, doi:10.2204/iodp.sd.8.12.2009, 2009.

Toy, V. G., Boulton, C. J., Sutherland, R., Townend, J., Norris, R. J., Little, T. A., Prior, D. J., Mariani, E., Faulkner, D., Menzies, C. D., Scott, H., and Carpenter, B. M.: Fault rock lithologies and architecture of the central Alpine fault, New Zealand, revealed by DFDP-1 drilling, Lithosphere, 7, 155–173, doi:10.1130/L395.1, 2015.

Vontobel, P., Lehmann, E., and Carlson, W. D.: Comparison of X-ray and neutron tomography investigations of geological materials, IEEE T. Nucl. Sci., 52, 338–341, 2005.

Voorn, M., Exner, U., Barnhoorn, A., Baud, P., and Reuschlé, T.: Porosity, permeability and 3D fracture network characterisation of dolomite reservoir rock samples, J. Pet. Sci. Eng., 127, 270–285, doi:10.1016/j.petrol.2014.12.019, 2015.

Wennberg, O. P., Rennan, L., and Basquet, R.: Computed tomography scan imaging of natural open fractures in a porous rock; geometry and fluid flow, Geophys. Prospect., 57, 239–249, 2009.

Williams, J. N., Toy, V. G., Massiot, C., McNamara, D. D., and Wang, T.: Damaged beyond repair? Characterising the damage zone of a fault late in its interseismic cycle, the Alpine Fault, New Zealand, J. Struct. Geol., 90, 76–94, doi:10.1016/j.jsg.2016.07.006, 2016.

Withjack, E. M., Devier, C., and Michael, G.: The Role of X-Ray Computed Tomography in Core Analysis, Soc. Pet. Eng., SPE Western Regional/AAPG Pacific Section Joint Meeting, 19–24 May, Long Beach, California, doi:10.2118/83467-MS, 2003.

Sci. Dril., 22, 43–48, 2017
www.sci-dril.net/22/43/2017/
doi:10.5194/sd-22-43-2017

Scientific Drilling
Open Access

Scientific Drilling at Lake Tanganyika, Africa: A Transformative Record for Understanding Evolution in Isolation and the Biological History of the African Continent, University of Basel, 6–8 June 2016

Andrew S. Cohen[1] **and Walter Salzburger**[2]

[1]Department of Geosciences, University of Arizona, Tucson, AZ 85721, USA
[2]Zoologisches Institut, Universität Basel, 4051 Basel, Switzerland

Correspondence to: Andrew S. Cohen (cohen@email.arizona.edu)

Received: 12 July 2016 – Revised: 1 September 2016 – Accepted: 19 September 2016 – Published: 31 May 2017

Abstract. We report on the outcomes of a workshop held to discuss evolutionary biology, paleobiology and paleoecology questions that could be addressed by a scientific drilling project at Lake Tanganyika, the largest, deepest and oldest of the African Rift Valley lakes. Lake Tanganyika is of special significance to evolutionary biologists as it harbors one of the most spectacular endemic faunas of any lake on earth, with hundreds of unique species of fish, molluscs, crustaceans and other organisms that have evolved over the lake's long history. Most of these groups of organisms are known from fossils in short cores from the lake, raising the possibility that both body fossil and ancient DNA records might be recovered from long drill cores. The lake's sedimentary record could also provide a record of African terrestrial ecosystem history since the late Miocene. This 3-day workshop brought together biological and geological specialists on the lake and its surroundings to prioritize paleobiological, ecological and microbiological objectives that could ultimately be incorporated into an overall drilling plan for Lake Tanganyika and to consider how biological objectives can effectively be integrated into the paleoclimate and tectonics objectives of a Lake Tanganyika drilling project already considered in prior workshops.

1 Introduction

Understanding how ecosystems are assembled and altered through time, and understanding how the interplay between speciation, dispersal and extinction shapes species assemblages and communities, have been fundamental problems in both ecological and evolutionary sciences going back to the time of Darwin (1859). Evolutionary – in many cases adaptive – radiations in quasi-insular settings provide outstanding laboratories to address these questions (Losos and Ricklefs, 2009). Integral to advancing our understanding of the dynamics of the processes that underlie diversification is a need for long and highly resolved time series of community and habitat structure and individual species characteristics (morphological and genetic) that can supplement the short-term "snapshots" we obtain from studying extant species and species interactions alone (e.g., Vermeij, 1994). It has long been understood that the incorporation of fossil information fundamentally improves the accuracy of phylogenetic trees, and our testable hypotheses of how groups of organisms have diversified (or disappeared) through time (e.g., Donoghue, 1989), while in-depth knowledge of past environmental conditions allows the identification of possible triggers of diversification events. Fossil records from the deposits of ancient lakes provide an important way to obtain such information. With their combination of long-term, continuous sedimentation providing environmental context and in situ speciation, the fossils and sediments of ancient lakes are ideal building blocks for making fundamental advances in understanding the processes underlying adaptive radiation, extinction and the development of complex species interactions (Rossiter and Kawanabe, 2000; Cohen, 2012; Wilke et al., 2016).

Among the ancient lakes of the world, Lake Tanganyika stands out as an ideal site for such a study. It is the oldest

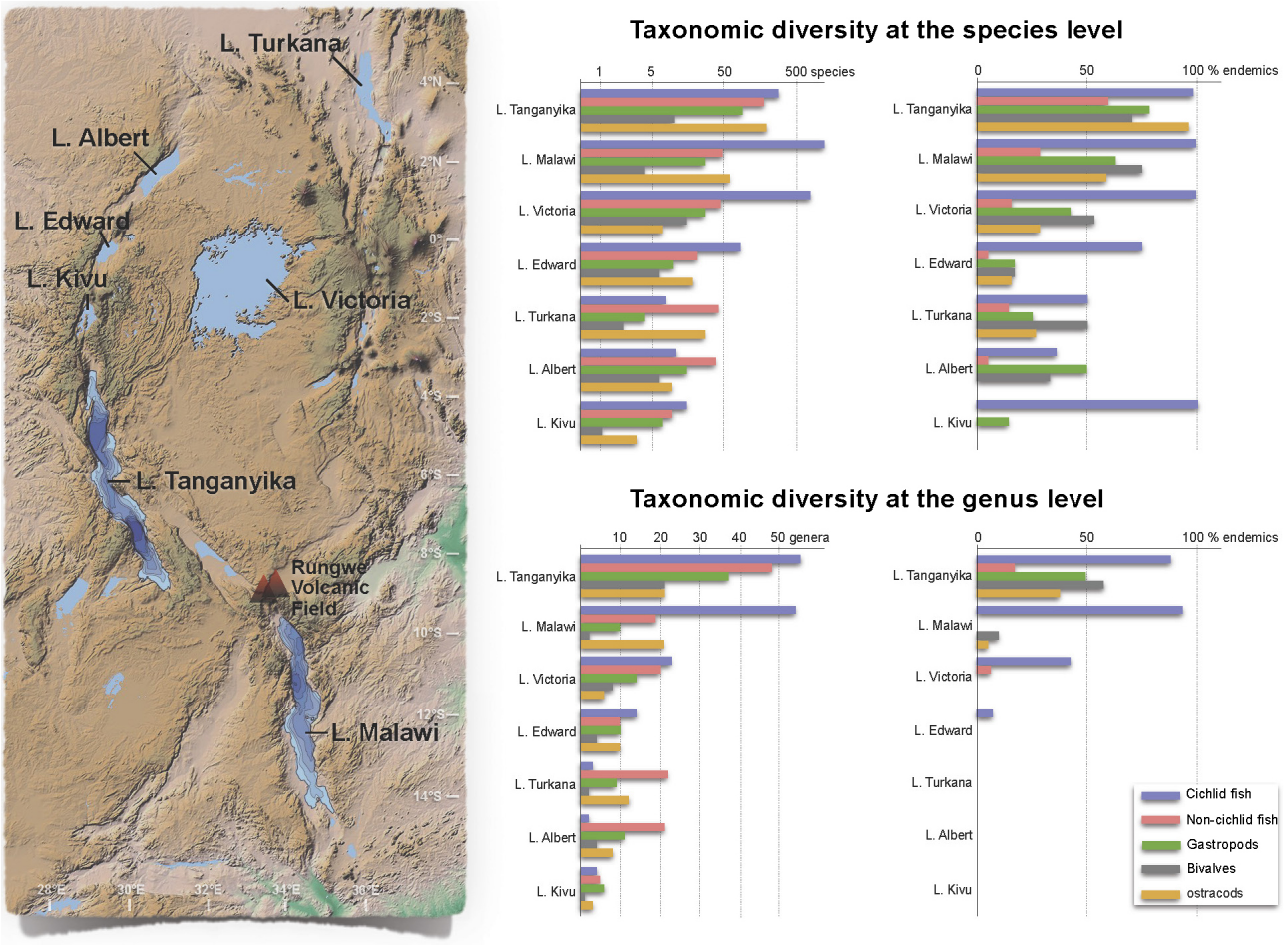

Figure 1. Taxonomic diversity of the African Great Lakes. The figure illustrates the unique characteristics of Lake Tanganyika's endemic diversity, where the age and persistence of the lacustrine environment is reflected in the large numbers and percentages of endemic genera among many groups of organisms in comparison to other lakes.

(∼ 9–12 Ma, Cohen et al., 1993), deepest (∼ 1470 m), and most voluminous (18 900 km^3 volume, 32 600 km^2 area) of the African Rift Valley lakes. The combination of its antiquity and size probably accounts for its extraordinary biodiversity, not only in sheer numbers of species found nowhere else in the world, but also in their morphological and behavioral distinctiveness and phylogenetic distance from their nearest relatives (Salzburger et al., 2014 and Fig. 1). This endemic biodiversity cuts across multiple large groups of animals, notably the cichlid fishes, and various groups of molluscs and crustaceans. Furthermore, all of these organisms have left interpretable records in fossils buried in the lake's sediments (e.g., Palacios-Fest et al., 2005).

Lake Tanganyika has previously been identified as a prime target for scientific drilling, and is the highest priority ancient lake still undrilled in Africa, based on its potential to also yield a unique and long record of tropical paleoclimate and tectonic processes in a very seismically active portion of the rift. Prior workshops have been held to consider these other science objectives of a Lake Tanganyika drilling campaign (Russell et al., 2012; McGlue and Scholz, 2016 workshop report). The combination of a long tectonic and climatic history of this lake has created an environmental framework of basin evolution and lake-level changes that in turn are likely primary drivers of the fascinating biological evolution observed in this lake.

2 Workshop goals

Over the course of a 3-day workshop held at the University of Basel, Switzerland, an international group of 25 biologists, paleoecologists and geologists considered the specifics of how a scientific drilling campaign at Lake Tanganyika might further advance our understanding of the lake's and its watershed's biotic history, and in turn make fundamental and transformative advances in our more general understanding of evolution in isolation and adaptive radiation among organisms. The workshop, sponsored by the Swiss National Sci-

ence Foundation and the University of Basel, provided a first opportunity for specialists to consider specific strategies for drilling, core recovery and sampling of Lake Tanganyika's sedimentary record that would maximize the scientific impact of such an endeavor.

3 Evolutionary biology and paleoecology objectives of a Lake Tanganyika Scientific Drilling Project

An initial set of talks laid out some of the major paleobiological themes that could be pursued by a Lake Tanganyika Scientific Drilling Project (LTSDP) and set the stage for intensive discussions that occupied most of the workshop. Andy Cohen (University of Arizona) provided an overview of the project and the synergistic relationship of evolutionary biology/paleobiology objectives of the project to its other goals in paleoclimatology (Russell et al., 2012) and tectonics (McGlue and Scholz, 2016). Chris Scholz (Syracuse University) discussed our current understanding of subsurface seismic stratigraphy in Lake Tanganyika, which will be critical for identifying appropriate drilling targets to answer paleobiological questions (which are not necessarily the same as those optimal for paleoclimatology), as well as practical considerations for a drilling project in that lake. Because of its great depth and lack of seasonal overturn, Lake Tanganyika today is a stratified lake, oxygenated only within its upper layer (100–250 m), which limits the depth of benthic animal biodiversity. Besides, it has a surprisingly simplified pelagic ecosystem in comparison to the extraordinary diversity near its shores. Thus identifying drilling targets, which have regularly experienced lake floor oxygenation yet also are zones of quasi-continuous sedimentation, will be of paramount importance. James Russell (Brown University) discussed the potential of Lake Tanganyika as a long paleoclimate record of the Afrotropics. Lake Tanganyika's sensitivity to regional/global climate variability is well documented (Tierney et al., 2008; Otto-Bliesner et al., 2014), and this variability also forces changes in the lake's ecosystem over long timescales.

Walter Salzburger (University of Basel) focused on the cichlid fish fauna of the lake, which, while not the most diverse in terms of numbers of species within a single African lake, undoubtedly contains the greatest breadth of morphological, ecological and behavioral variation of any lake in the world, rendering Lake Tanganyika's cichlids iconic examples of evolution in isolation and adaptive radiation (Fryer and Iles, 1972). The availability of a continuous paleoecoological record of the lake and of fish fossils, which are abundant in the lake's sediments, raises the possibility that our understanding of cichlid evolution could be greatly enhanced through scientific drilling. An especially exciting prospect, the collection of ancient DNA from fossil fish or other organisms in Lake Tanganyika, was discussed by Moritz Muschick (EAWAG). Obtaining an ancient DNA (aDNA) record of cichlids from older species, especially with an accompanying high-resolution paleoenvironmental record, would allow scientists for the first time to truly understand the dynamics and drivers of adaptive radiation. This would be a truly transformative advance for all of evolutionary biology. Although the current temporal range of successful aDNA studies is only a small fraction of the age of Lake Tanganyika, the field is advancing rapidly and progressively older analyses are being regularly reported (Hofreiter et al., 2014; Wade, 2015). Another promising direction for incorporating fossil materials into phylogenetic studies from Lake Tanganyika may also come from the emerging field of fossil protein sequencing (Service, 2015). Ellinor Michel, Jon Todd (Natural History Museum, London), and Bert Van Bocxlaer (Ghent University) discussed the scientific potential of a fossil record of the extraordinary diversity of molluscs (especially gastropods) of Lake Tanganyika. Understanding the timing and environmental drivers of diversification, and whether other groups of snails have dominated past communities and the context of the innovations in traits (some thought to be the product of coevolution between snails and their predators), would all provide fascinating questions for evolutionary studies. Philip Barker (Lancaster University) discussed the potential for evolutionary ecology studies of diatoms in Lake Tanganyika. While the levels of endemism are lower among single-celled algae compared to animals, diatoms will be critical for understanding the ecosystem dynamics of the lake, and particularly from the standpoint of nutrient cycling, pelagic productivity and potentially in concert with changes occurring in the lake's watershed (i.e., silica delivery as affected by grassland development). The evolution of the pelagic ecosystem and how it might be tracked with a drill core record was discussed in detail by Peter McIntyre (University of Wisconsin) and Catherine Wagner (University of Wyoming). The modern simple pelagic ecosystem actually involves highly specialized and endemic species. Whether this evolved early or late in the lake's history is as yet unknown.

A drill core from Lake Tanganyika would not only inform us about the lake's aquatic biological history, but also that of its watershed through pollen, phytolith and charcoal records. Sarah Ivory (Brown University) discussed how a vegetation record from the lake could give us a much clearer picture of the timing and dynamics of biogeographic assembly of tropical African vegetation. This is not only of theoretical interest, but could also help inform conservation biology strategies for these endangered communities in the future (e.g., Ivory et al., 2016). Rick Potts (Smithsonian Institution) also discussed the importance of a terrestrial environmental record extending back to the late Miocene for improving our understanding of the context of human evolution in Africa. Lake Tanganyika drill cores could provide a continuous record of environmental variability from the time of the human (hominin)/African ape evolutionary split, at a central location between the two major theaters of the hominin fossil record, in southern and eastern Africa. Ishmael Kimirei (Tanzania

Fisheries Research Institute) discussed ways in which a scientific drilling project at Lake Tanganyika could enhance training and collaborative research opportunities for African scientists. It is critical for this project's success and in enhancing its broader impacts to involve African scientists as full partners from its inception.

4 Recommendations of the workshop

The breakout and plenary discussions that followed the presentations provided an opportunity for the group to make specific recommendations on key hypotheses that could be tested in paleoecology and evolutionary biology by drilling Lake Tanganyika and integrating drill core data with existing information from existing biogeographic and phylogenetic information. Specifically, attendees discussed favorable drilling localities and sampling and analytical strategies required to evaluate the hypotheses. Lake Tanganyika is comprised of three major basins (and several additional subsidiary basins, Ebinger, 1989), which may have played a critical role in structuring diversification and biogeography within the lake. Cycles of isolation and reconnection of populations may have been very important as drivers of speciation. Collection of drill cores from more than one basin could allow us to test the idea that the development of these three basins left a biogeographic imprint on evolution that persists today through faunal isolation during low lake stands. Also, it would let us examine how terrestrial vegetation has evolved not only in the southern parts of the basin, where vegetation is dominated by *miombo* woodland, but also further north, where a record of tropical wet forest typical of the Guineo-Congolian vegetation region is more likely to be obtained. Collecting drill cores over this north–south spatial range (Tanganyika is the longest freshwater lake in the world, extending from ~ 3 to 9° S) would have to be weighed against the likelihood that better chronological control on individual cores will be possible further south in the lake in closer proximity to the Rungwe volcanic field, which generates volcanic tephras found in the lake (Tiercelin and Mondeguer, 1991). Considerable discussion centered around the critical need to accurately date interbasinal faunal changes, either directly through tephras and other materials, or by correlation from the more tephra-rich sediments of the southern part of the lake towards the northern basins far from volcanoes. The extent to which additional drill sites for paleobiological objectives can be added into a drilling program will need to be weighed against the necessity for recovery of multiple cores per site to ensure a high-quality chronology for the most stratigraphically continuous sites.

Extensive discussions were also focused on how to best obtain useful paleobiological samples from the drill cores. This may involve approaches to sampling and core handling that are quite different to the more traditional approaches emphasizing paleoclimatic records from lakes. One very promising approach may be continuous computerized tomography (CT) scanning of drill cores to search for well-preserved fossils (Fig. 2). Without prescreening the cores by CT prior to splitting, articulated fish skeletons on bedding planes and macromolluscs throughout the core are both likely to be damaged or unlikely to be observed during core splitting and description. CT scans could also be enormously valuable to this project as a tool for directly quantifying fossil abundances, particularly if automated counting methods can be developed for image analysis of the scans. They may also offer a means of obtaining extremely high-resolution paleobiological data throughout the core records on par with the geochemical and physical properties data that are now routinely obtained from core scanning. Turbidites, which are typically considered a nuisance in lake cores by paleoclimatologists, may actually yield important shallow-water fossils from intervals that are otherwise represented by deep-water sediments devoid of shallow-water taxa. Also, the large amount of core anticipated for a Lake Tanganyika drilling project, coupled with the large number of taxonomic specialists interested in obtaining samples from these highly fossiliferous sediments, will certainly require a different workflow in fossil processing than has occurred in past lake drilling projects. Lake Tanganyika sediments are likely to yield an extraordinary range of fossils (fish, molluscs, diatoms and other siliceous algae, ostracodes, pollen, phytoliths, macroplants, charcoal, chironomids, sponges, crabs and bryozoans are all well documented from the lake as fossils already). Considerable discussion therefore focused on appropriate sampling intervals for the science questions of interest that would allow comparative studies between taxonomic and ecologic groups at identical timescales and resolutions. This would greatly improve our ability to address broader issues such as the evolution of ecosystem complexity in Lake Tanganyika, pelagic/benthic or lake/terrestrial ecosystem coupling, and co-evolutionary questions. Our ability to do this will critically depend on developing a plan for sampling, processing, sharing and allocating limited core materials in an efficient and timely way and ensuring that data management is well organized for the large numbers of sample splits that will inevitably be generated. LacCore (where initial core description will likely be done) already utilizes sample tracking following System for Earth Sample Registration (SESAR) and International Geosample Number (IGSN) standards, but it will be imperative that downstream labs distributing more specialized sample splits also follow these same protocols. Because of the large amount of core expected to be recovered (several kilometers are likely), the group recognized the need for a stratified sampling approach with some evolutionary questions addressed with lower-resolution sampling throughout the record, whereas questions about ecological turnover would be studied at high resolution over targeted but short intervals (e.g., Jackson et al., 2015).

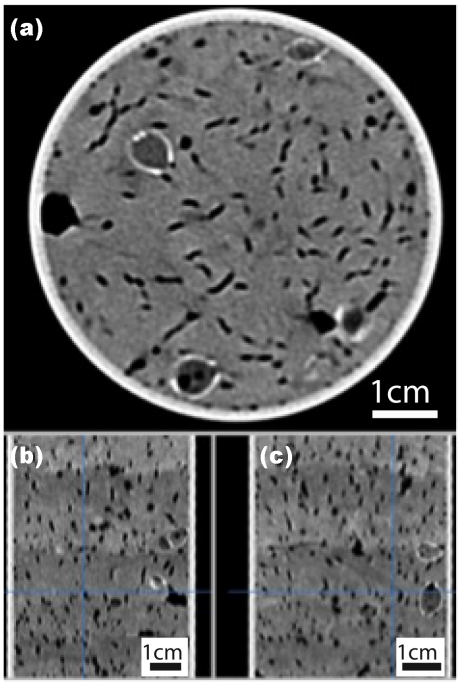

Figure 2. CT scan of a short core from Lake Wohlen (Wohlensee), Switzerland. The image courtesy of Hendrik Vogel and Flavio Anselmetti, and taken by Nicole Schwendener, was taken using the CT scanner at the Institute of Forensic Medicine, University of Bern. High-density bivalve shells appear as light, curved cross sections, whereas low-density voids appear dark, and the homogenous sediment matrix is intermediate in tone. **(a)** Cross-sectional view of the core. **(b)** and **(c)**: lateral views of the core.

Discussions about aDNA and geomicrobiology components were focused on the practicalities of doing these types of studies on Lake Tanganyika cores. A roadmap for geomicrobiology studies exists from prior work at the Dead Sea, Lake Towuti, and other recent projects (e.g., use of fluorescent pigments in drilling fluids to track contamination and a GFZ mobile, on-site laboratory for sediment and porewater collection; see Ariztegui et al., 2015, for a detailed discussion). However, aDNA studies on lake cores are still in their infancy, and preliminary work is needed to determine the effective maximum age of fossil material that can be expected to yield aDNA from these types of tropical lake sediments. In the lead-up to drilling, pilot studies will therefore need to be done to assess the potential of obtaining aDNA from fossils other than fish, to determine ways to minimize the destructive aDNA sampling of valuable fossils, and to develop sequencing data for modern, closely related reference taxa (currently only comprehensively available for cichlid fish). These pilot studies will be critical for defining the exact science questions that can be realistically addressed with this approach as well as the appropriate sampling strategies. Also, aDNA and geomicrobiology samples will fall under a different set of international regulations regarding the export of biological samples than do typical core materials (e.g., the 2010 Nagoya Convention on Biological Diversity, in-country export regulations on biological materials), necessitating careful advance planning. This might provide a stronger impetus for in-country sample processing of geomicrobiological materials if possible. Obtaining optimal (i.e., large/intact) fossils for aDNA research probably should not rely on routine sieved macrofossil sampling of core splits, but should be more targeted. Locating these critical fossils from CT scans for both aDNA and morphological studies would not only ensure obtaining of the best samples for study with the least contamination, but would also avoid compromising the integrity of core materials for other purposes. Sample extraction for aDNA will require cleaner conditions than the initial core description (ICD) norm, involving surface decontamination with UV and bleach and UV treatment of water if sieved samples are to be used. Museum involvement will be critical for ensuring the long-term storage of unique fossil material collected by this project.

A final set of discussions focused on innovative funding, training and outreach opportunities for the biological aspects of a Tanganyika drilling project. As Ishmael Kimirei reiterated, early and continuous involvement with local partners will be critical, particularly given that many of the potential local biology and environmental science collaborators and institutions have no prior experience with scientific drilling. Participants in the workshop already have existing training and research partnerships with a number of institutions that could benefit from knowledge transfer and training opportunities related to this drilling project (e.g., the Tanzanian Fisheries Research Institute, The Hydrobiology Laboratory in Uvira, DRC, the University of Dar es Salaam Departments of Geology and Aquatic Sciences and Fisheries, the University of Zambia in Lusaka and the Department of Fisheries in Zambia, and the University of Burundi). The project would also develop new partnerships with organizations like the new Tanzanian National ICT Broadband Backbone (NICTBB http://www.nictbb.co.tz/index.php), the Tanzania Petroleum Development Corporation, the Nelson Mandela Institution of Science and Technology in Arusha, and the Tanzania National Parks Authority. Involving several of these applied agencies will help introduce the findings of conservation paleobiology obtained from core records into both terrestrial and lake management research strategies. There is also a potential for funding from large international donors for this component since the project is so highly interdisciplinary. Summer schools and training programs drawing on this interdisciplinary approach have already been very successful in training the upcoming generation of African environmental scientists (e.g., the Nyanza Project, www.geo.arizona.edu/nyanza/, and the Volkswagen Foundation Summer School series, http://www.geo.uni-potsdam.de/summer_schools_en/articles/1805.html). These could have drilling science as a focus during the field campaign and ICD work. Numerous outreach/informal education strategies were also

discussed. A Lake Tanganyika drilling project will be a large and highly visible endeavor and will need a strong and comprehensive outreach component that is integrated into project planning from the beginning. Target audiences will include local rural, urban African and international (US/European) people, and outreach strategies could include online multimedia platforms, film or video projects, local (lakeside) museum support, art displays and children's books. The project can draw on lessons learned in the region from prior outreach efforts related to scientific drilling and Lake Tanganyika (e.g., www.youtube.com/watch?v=B1iU0fBTfUw and https://vimeo.com/78232028).

Over the next few years the team members involved in this workshop are looking forward to developing the exciting science prospects that would be provided by a Lake Tanganyika drill core record and developing strong interdisciplinary collaborations with the paleoclimate and tectonics teams of this project. Such an integrated study would truly transform our understanding of the long-term biological and environmental evolution of complex ecosystems.

Acknowledgements. This workshop was funded by grants from the Swiss National Science Foundation (SNF), the University of Basel, and the Center for African Studies of the University of Basel. We thank the Zoological Institute, University of Basel, for providing the venue, the Center for African Studies for assistance with conference travel and organization and all workshop participants for their contributions to this meeting and comments on earlier drafts of this paper. We thank Thomas Wilke and one other anonymous reviewer for many useful suggestions that improved this paper.

Edited by: T. Morishita
Reviewed by: T. Wilke and one anonymous referee

References

Ariztegui, D., Thomas, C., and Vuillemin, A.: Present and future of subsurface biosphere studies in lacustrine sediments through scientific drilling, Int. J. Earth Sci., 104, 1655–1665, 2015.

Cohen, A. S.: Scientific drilling and biological evolution in ancient lakes: lessons learned and recommendations for the future, Hydrobiologia, 682, 3–25, 2012.

Cohen, A. S., Soreghan, M., and Scholz, C.: Estimating the Age of Ancient Lake Basins: An Example from *L. Tanganyika*, Geology, 21, 511–514, 1993.

Darwin, C.: On The Origin Of Species By Means Of Natural Selection, 1st Edn., John Murray, London, 1859.

Donoghue, M. J.: The importance of fossils in phylogeny reconstruction, Ann. Rev. Ecol. Syst., 20, 431–460, 1989.

Ebinger, C.: Tectonic development of the western branch of the East African rift system, Geol. Soc. Am. Bull., 101, 885–903, 1989.

Fryer, G. and Iles, T. D.: The cichlid fishes of the great lakes of Africa: their biology and evolution, Oliver and Boyd, Edinburgh, 641 pp., 1972.

Hofreiter, M., Paijmans, J. L. A., Goodchild, H., Speller, C. F., Barlow, A., Fortes, G. G., Thomas, J. A., Ludwig, A., and Collins, M. J.: The future of ancient DNA: Technical advances and conceptual shifts, Bioessays, 37, 284–293, 2014.

Ivory, S., Regan, E., Sax, D., and Russell, J. M.: Niche expansion and temperature sensitivity of tropical African montane forests, Global Ecol. Biogeogr., 25, 693–703, 2016.

Jackson, L. J., Stone, J. R., Cohen, A. S., and Yost, C. L.: High resolution paleoecological records from Lake Malawi show no significant cooling associated with the Mount Toba supereruption at ca. 75 ka, Geology, 43, 823–826, 2015.

Losos, J. B. and Ricklefs, R. E.: Adaptation and diversification on islands, Nature, 457, 830–836, 2009.

McGlue, M. and Scholz, C.: Lake Tanganyika: A Miocene to Recent source-to-sink laboratory in the African tropics, STEPPE Workshop Report https://steppe.org/wp-content/uploads/reports/Lake_Tanganyika_STEPPE_Workshop_Report_safe.pdf, 2016.

Otto-Bliesner, B., Russell, J. M., Clark, P. U., Liu, Z., Overpeck, J. T., Konecky, B., deMenocal, P. B., Nicholson, S. E., He, F., and Lu, Z.: Coherent changes of Northern and Eastern Equatorial African rainfall during the last deglaciation, Science, 364, 1223–1227, 2014.

Palacios-Fest, M. R., Alin, S. R., Cohen, A. S., Tanner, B., and Heuser, H.: Paleolimnological investigations of anthropogenic environmental change in Lake Tanganyika: IV. Lacustrine paleoecology, J. Paleolimnol., 34, 51–71, 2005.

Rossiter, A. and Kawanabe, H. (Eds.): The Biology of Ancient Lakes, Academic Press, San Diego, 2000.

Russell, J. M., Cohen, A. S., Johnson, T. C., and Scholz, C. A.: Scientific Drilling in the East African Lakes: A strategic planning workshop, Sci. Dril., 14, 49–54, doi:10.2204/iodp.sd.14.08.2012, 2012.

Salzburger, W., Van Bocxlaer, B., and Cohen, A. S.: The ecology and evolution of the African Great Lakes and their faunas, Ann. Rev. Ecol. Syst., 45, 519–545, 2014.

Service, R. F.: Protein Power, Science, 349, 372–373, 2015.

Tiercelin, J. J. and Mondeguer, A.: The geology of the Tanganyika trough, in: Lake Tanganyika and its Life, edited by: Coulter, G. W., Oxford U. Press, London, 7–48, 1991.

Tierney, J. E., Russell, J. M., Huang, Y., Sinninghe Damsté, J. S., Hopmans, E. C., and Cohen, A. S.: Northern Hemisphere Controls on Tropical Southeast African Climate During the Past 60,000 Years, Science, 322, 252–255, 2008.

Vermeij, G. J.: The evolutionary interaction among species: Selection, Escalation and Coevolution, Ann. Rev. Ecol. Syst., 25, 219–236, 1994.

Wade, L.: Breaking a tropical taboo, Science, 349, 370–371, 2015.

Wilke, T., Wagner, B., Van Bocxlaer, B., Albrecht, C., Ariztegui, D., Delicado, D., Francke, A., Harzhauser, M., Hauffe, T., Holtvoeth, J., Just, J., Leng, M. J., Levkov, Z., Penkman, K., Sadori, L., Skinner, A., Stelbrink, B., Vogel, H., Wesselingh, F., and Wonik, T.: Scientific drilling projects in ancient lakes: Integrating geological and biological histories, Glob. Planet. Change, 143, 118–151, 2016.

Sci. Dril., 22, 49–61, 2017
www.sci-dril.net/22/49/2017/
doi:10.5194/sd-22-49-2017

Scientific Drilling
Open Access

IODP workshop: developing scientific drilling proposals for the Argentina Passive Volcanic Continental Margin (APVCM) – basin evolution, deep biosphere, hydrates, sediment dynamics and ocean evolution

Roger D. Flood[1], Roberto A. Violante[2], Thomas Gorgas[3], Ernesto Schwarz[4], Jens Grützner[5], Gabriele Uenzelmann-Neben[5], F. Javier Hernández-Molina[6], Jennifer Biddle[7], Guillaume St-Onge[8], and APVCM workshop participants[*]

[1]School of Marine and Atmospheric Sciences, Stony Brook University, Stony Brook, New York 11794-5000, USA
[2]Argentina Hydrographic Survey, Buenos Aires, C1270ABV, Argentina
[3]GFZ German Research Centre for Geosciences, 14473, Potsdam, Germany
[4]Geological Research Center, University of La Plata – CONICET, B1904DPK, La Plata, Argentina
[5]Alfred-Wegener-Institut Helmholtz-Zentrum für Polar- und Meeresforschung, 27568 Bremerhaven, Germany
[6]Department of Earth Sciences, Royal Holloway, University of London, Egham, Surrey TW20 0EX, UK
[7]School of Marine Science and Policy, University of Delaware, Lewes, Delaware 19958, USA
[8]Institut des Sciences de la Mer de Rimouski, Université du Québec à Rimouski, Rimouski, Québec, G5L 3A1, Canada
[*]A full list of authors and their affiliations appears at the end of the paper.

Correspondence to: Roger D. Flood (roger.flood@stonybrook.edu)

Received: 21 November 2016 – Revised: 9 February 2017 – Accepted: 13 February 2017 – Published: 31 May 2017

Abstract. The Argentine margin contains important sedimentological, paleontological and chemical records of regional and local tectonic evolution, sea level, climate evolution and ocean circulation since the opening of the South Atlantic in the Late Jurassic–Early Cretaceous as well as the present-day results of post-depositional chemical and biological alteration. Despite its important location, which underlies the exchange of southern- and northern-sourced water masses, the Argentine margin has not been investigated in detail using scientific drilling techniques, perhaps because the margin has the reputation of being erosional. However, a number of papers published since 2009 have reported new high-resolution and/or multichannel seismic surveys, often combined with multi-beam bathymetric data, which show the common occurrence of layered sediments and prominent sediment drifts on the Argentine and adjacent Uruguayan margins. There has also been significant progress in studying the climatic records in surficial and near-surface sediments recovered in sediment cores from the Argentine margin. Encouraged by these recent results, our 3.5-day IODP (International Ocean Discovery Program) workshop in Buenos Aires (8–11 September 2015) focused on opportunities for scientific drilling on the Atlantic margin of Argentina, which lies beneath a key portion of the global ocean conveyor belt of thermohaline circulation. Significant opportunities exist to study the tectonic evolution, paleoceanography and stratigraphy, sedimentology, and biosphere and geochemistry of this margin.

Published by Copernicus Publications on behalf of the IODP and the ICDP.

1 Introduction

The Argentine Continental Margin (ACM), one of the largest margins worldwide, is a complex geological feature where geotectonic evolution, as well as the post ocean-opening history, configured three types of margins (Fig. 1): passive volcanic rifted (red line), transcurrent (orange line) and mixed convergent, and sheared (yellow line). Apart from its implications for the evolution of the Southern Ocean, the ACM constitutes a key region in the global oceanographic–climatic system as it is the only place in the Southern Ocean with a net water-mass exchange between the equatorial and southern polar regions (Fig. 2). Strong Antarctic-sourced currents run along the Argentine margin, driven by the Coriolis force, from 56° S and reaching to at least 34° S, or even farther north. Also, waters of Northern Hemisphere origin flow south along the Argentine margin north of about 38° S. The ACM evolution has been affected by climate, current, sea level, and tectonic processes, as well as by sediment input patterns and history along the roughly 5000 km long coast line of Argentina. All of these characteristics, coupled with the fact that this is a critically important, yet under-sampled portion of the World Ocean, makes the ACM an important region for using IODP (International Ocean Discovery Program) scientific drilling to explore and discover the potential benefits of such operations within the "passive" sector of the margin (here called the Argentine Passive Volcanic Continental Margin – APVCM).

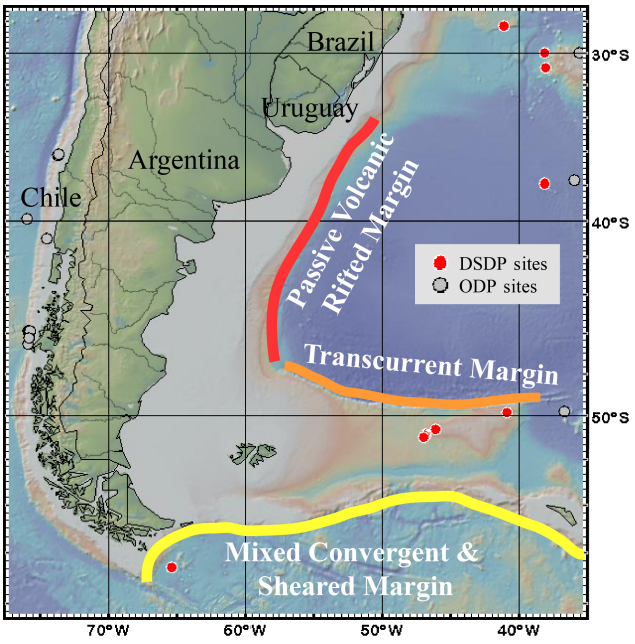

Figure 1. The character of the Argentine Continental Margin. Red: passive volcanic rifted margin; orange: transcurrent margin; yellow: mixed convergent and sheared margin. The passive volcanic rifted margin is termed the APVCM. Red dots indicate DSDP (Deep Sea Drilling Project) sites, gray dots indicate ODP (Ocean Drilling Program) sites. The figure was constructed in GeoMapApp (http://www.geomapapp.org) using the Global Multi-Resolution Topography (GMRT) synthesis (Ryan et al., 2009).

2 Workshop event, topics, sponsorship and seismic Data

The IODP workshop event, Developing Scientific Drilling Proposals for the Argentina Passive Volcanic Continental Margin (APVCM) – Basin Evolution, Deep Biosphere, Hydrates, Sediment Dynamics and Ocean Evolution, was held in Buenos Aires on 8–11 September 2015. The 3.5-day event was conducted in the Ministerio de Relaciones Exteriores Comercio Internacional y Culto (Ministry of Foreign Affairs, International Trade and Worship) in the city of Buenos Aires, comprising 45 scientists from 8 countries and 34 organizations or institutions, who discussed scientific drilling on the APVCM (Fig. 1) to determine the composition of and reconstruct the history of the sedimentary deposits under the impact of climatic and tectonic events. Breakout discussion groups were dedicated to tectonics, paleoceanography, sedimentology and seismic stratigraphy, and deep-Earth life forms, biosphere and geochemistry.

The workshop aimed to bring together a diverse group of scientists to explore and discover the merits of and thereby develop a strategy for scientific drilling operations on the APVCM. The goal of a scientific drilling campaign along and across the APVCM is to significantly contribute to our understanding of the evolution of the South Atlantic and its role and influence on global ocean circulation and the climate history of our planet. Sediments on the APVCM margin range from Late Jurassic–Cretaceous to Holocene in age, and depositional units from approximately the Eocene to Pliocene are particularly well developed. Records from this margin obtained through scientific drilling will be important to resolve key questions of the evolution of Earth's oceans and climate through this period.

IODP workshop topics were introduced to the audience through key note presentations on

- the evolution of the southwestern Atlantic Ocean;
- the structure of the APVCM;
- the nature and timing of rifting and thermal evolution of the margin;
- the nature of sedimentary processes and facies that shaped the margin;
- the margin construction, stability and evolution;
- the climate records, ocean circulation and paleoceanography;
- the history and character of surface and deep circulation along the Argentine margin;

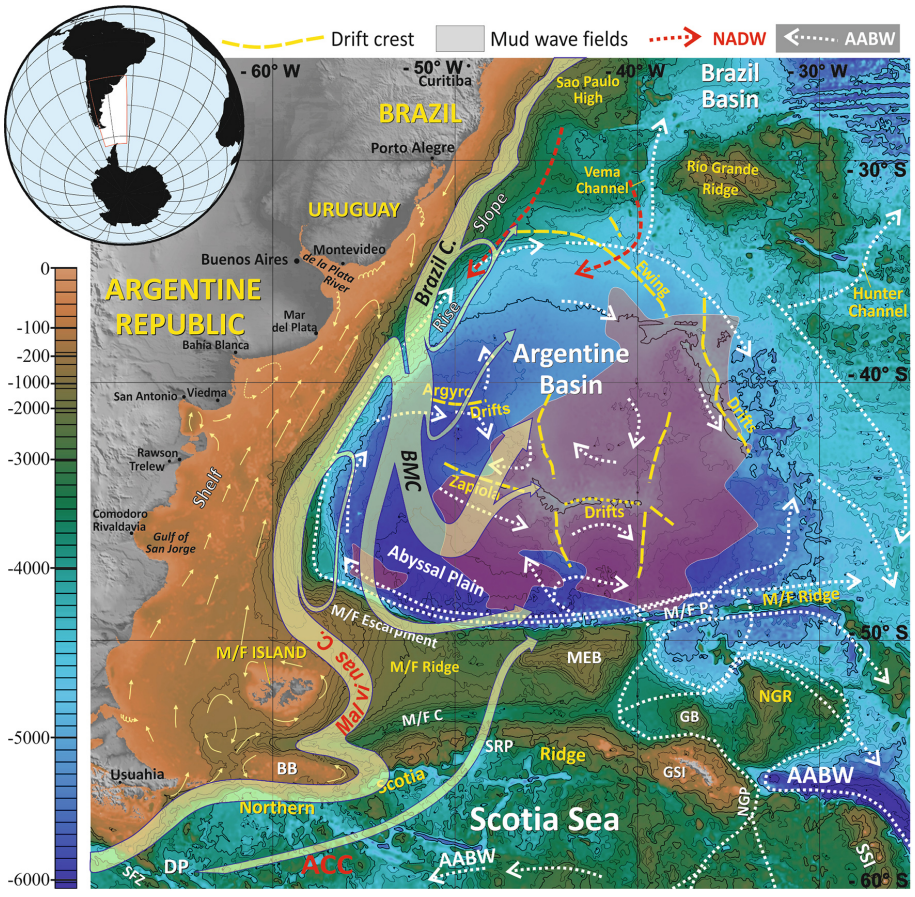

Figure 2. Location of Argentine Basin with regional bathymetric map and general circulation of surface and deep-water masses indicated (after Hernández-Molina et al., 2010). Legend for the physiographic reference points, in alphabetical order: BB: Burdwood Bank; BMC: Brazil–Malvinas Confluence; DP: Drake Passage; M/FI: Malvinas–Falkland Island; M/FE: Malvinas–Falkland Escarpment; M/FP: Malvinas–Falkland Passage; M/FR: Malvinas–Falkland Ridge; GB: Georgia Basin; GP: Georgia Passage; MEB: Maurice Ewing Bank; NGP: Northeast Georgia Passage; NGR: Northeast Georgia Ridge; SG: South Georgia; SFZ: Shackleton Fracture Zone; SRP: Shag Rocks Passage; and SSI: South Sandwich Island. Legend for the water masses: ACC: Antarctic Circumpolar Current; AABW: Antarctic Bottom Water.

- the opportunities for deep biosphere studies on a complex passive margin;
- the data needs for IODP proposals, the capabilities of the R/V *JOIDES* Resolution and the IODP proposal process.

Workshop sponsorship was provided by the National Science Foundation US Science Support Program (USSSP), Argentina's Ministry of Science, Technology and Productive Innovation (MINCYT-CONICET), the Argentine Ministry of Foreign Affairs, COPLA (National Commission of the Outer Limit of the Shelf – CONVEMAR), the Pampa Azul Initiative, YPF S.A. (Argentina's National Petroleum Company), and CIG (Geological Research Center, University of La Plata – CONICET), Argentina. This was also a European Consortium for Ocean Research Drilling (ECORD) MagellanPlus workshop.

Seismic data are particularly important for planning and executing scientific drilling programs, and for the Argentine margin it is appropriate to mention early on in this report that three significant seismic data sets were shown and discussed at the workshop. The primary data set for the Argentine margin consists of mostly dip lines collected by BGR (Bundesanstalt für Geowissenschaften und Rohstoffe) in Hanover, Germany. The second primary data set consists of the primarily dip seismic lines collected by COPLA, which build on the BGR lines by extending the BGR lines offshore and by filling in between the BGR lines where they are widely spaced. The COPLA lines were collected in support of Argentina's application to set the outer limit of the Argentine continental shelf and there will be limited access to these lines, at least until that process has been concluded. Workshop organizers met with members of COPLA several times before the workshop to discuss the goals of the IODP workshop and the kind of data needed to support IODP scientific drilling. We were told that portions of the lines were expected to be available to support scientific drilling on a case-by-case basis. Indeed, four

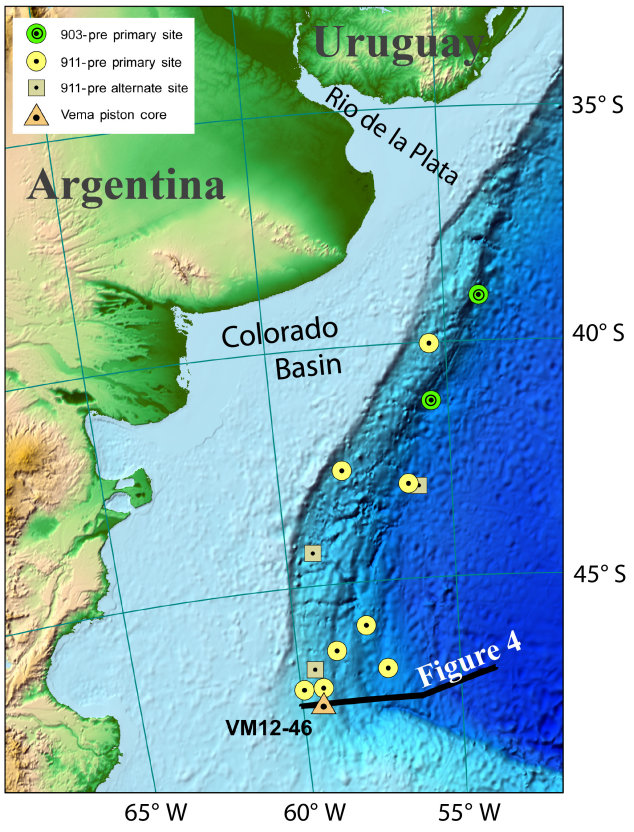

Figure 3. Location of sites proposed by IODP proposals 903-Pre "Argentine margin seaward dipping reflectors" and 911-Pre "Argentine margin paleoceanographic transects". Also shown are the location of core VM12-46 and the location of the seismic profile in Fig. 4. The figure was constructed in ArcMap using the ETOPO1 basemap (http://dx.doi.org/10.7289/V5C8276M).

potential drill sites were proposed during the meeting based on the COPLA lines, and a pre-proposal currently active in the IODP system uses COPLA and BGR lines to define two potential sites (903-Pre, Fig. 3). The ArgentineSPAN-(TM) lines collected on the Argentine margin by ION Geophysical, Inc., were the third set of lines presented and discussed. These deep-penetration, proprietary lines are both strike lines and dip lines, and may also be available to support scientific drilling. Indeed, 911-Pre (Fig. 3) uses ArgentineSPAN-(TM) and BGR lines to define several sites. Other important data sets may exist on the margin, but they were not discussed at this meeting.

3 Background and geological setting

The Argentine margin contains important sedimentological, paleontological and chemical records of regional and local tectonic evolution, sea level, climate evolution and ocean circulation that date from the opening of the South Atlantic in the Late Jurassic–Early Cretaceous as well as of the present-day results of post-depositional chemical and biological alteration. Despite its important location, which underlies the exchange of southern- and northern-sourced water masses, the Argentine margin has not been investigated in detail using scientific drilling techniques (Fig. 1). This low level of scientific drilling activity in the region may in part be due to the reports of Maurice Ewing and co-workers (e.g., Lonardi and Ewing, 1971), which, based on widely spaced and low-resolution seismic profiles, noted that the margin had an erosional character as it was crossed by numerous large canyon systems, some of which were likely altered by strong currents. However, a number of papers published since 2009 reported new high-resolution and/or multichannel seismic surveys (Fig. 4), often combined with multi-beam bathymetric data, which show the common occurrence of layered sediments and prominent sediment drifts on the Argentine and adjacent Uruguayan margins (e.g., Hernández-Molina et al., 2009, 2010, 2015; Violante et al., 2010, Krastel et al., 2011; Lastras et al., 2011; Muñoz et al., 2012; Grützner et al., 2011, 2012, 2016; Preu et al., 2012, 2013; Voigt et al., 2013; Uenzelmann-Neben et al., 2016; see also Hinz et al., 1999). There has also been significant progress studying the climatic records in surficial and near-surface sediments recovered in sediment cores from the Argentine margin (e.g., Chiessi et al., 2007; Bozzano et al., 2011; Govin et al., 2012; Bender et al., 2013; Razik et al., 2013; Razik, 2014; García Chapori et al., 2014, 2015), demonstrating that this margin also contains important modern sedimentary deposits.

Encouraged by these recent results, our 3.5-day IODP workshop in Buenos Aires (8–11 September 2015) focused on opportunities for scientific drilling on the APVCM as a significant contribution to several of IODP's research themes described in the program's Science Plan (IODP-SP) for 2013–2023 *Illuminating Earth's Past, Present and Future* (http://www.iodp.org/program-documents). Future drilling in this region is likely to be of high priority because this margin lies beneath a key portion of the global ocean conveyor belt of thermohaline circulation (Broecker, 1991).

Interest is high in the southern South Atlantic Ocean, and there is currently much being learned about the details of the evolution of this key ocean basin (Torsvik et al., 2009; Moulin et al., 2010; Heine et al., 2013; Granot and Dyment, 2015). The rift phase of the Gondwana breakup extended from the Triassic/Jurassic(?) to the Early Cretaceous. Seaward dipping reflectors (SDRs) are observed on seismic profiles near the continental–ocean boundary (COB), indicating the presence of massive volcanism (a large igneous province, or LIP) at the transition from rifting to drifting (Gladczenko et al., 1997; Hinz et al., 1999). The volcanic layers that make up the SDRs may be subaerial and interbedded with terrestrial sediments. Slumps are observed in the prograding Cretaceous sediment off the Colorado Basin that may thin the sediments over SDRs in some areas. Cretaceous shelf sediments here are expected to be black shales, sandstones and coarser-grained deposits (Loegering et al., 2013) while Cre-

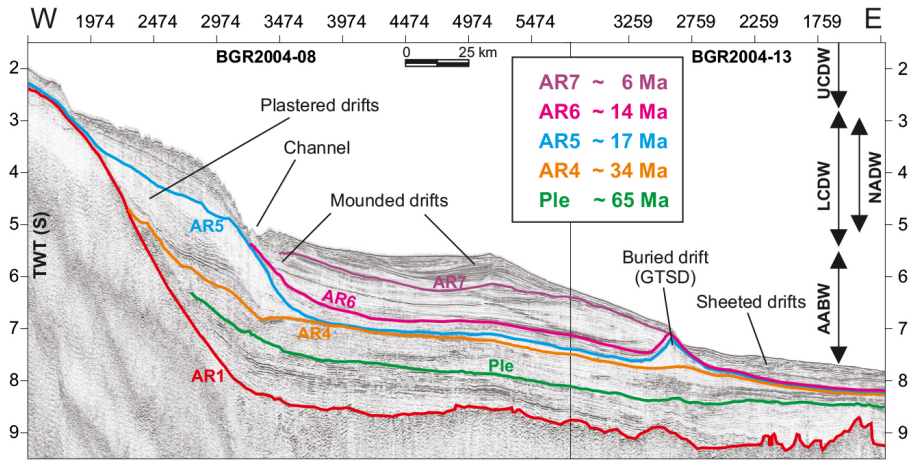

Figure 4. Interpreted seismic line across the Argentine margin featuring distinct drift deposits, channels, and thickness of deposits. Ocean current distribution within the water column: AABW is Antarctic Bottom Water; LCDW is Lower Circumpolar Deep Water; UCDW is Upper Circumpolar Deep Water; NADW is North Atlantic Deep Water (see Grützner et al., 2012). Predicted age and character of the sediment deposits need to be determined through sampling to understand in detail the evolution of the margin in response to climate changes.

taceous sediments in deeper water are likely to be pelagic shales, marls and fine-grained sands (R. Gerster, personal communication, 2015). At about 95 Ma the Equatorial Atlantic Gateway opened, and the gateway continued to enlarge allowing for enhanced exchange of southern waters with the North Atlantic Basin, perhaps leading to a global cooling of bottom water and the end of the Cretaceous greenhouse period (Friedrich et al., 2012; Granot and Dyment, 2015). However, basin-to-basin differences in water properties are not well resolved, including the character of the South Atlantic waters that flooded the North Atlantic Basin (Friedrich et al., 2012).

Hernández-Molina et al. (2010) and Grützner et al. (2012) suggested that sediments from about the Cretaceous–Tertiary boundary to the Eocene–Oligocene boundary are thick along the margin and are characterized by being parallel to subparallel reflections of low to moderate amplitude. This is generally a time of low to moderate bottom current activity and a warm climate.

Lastras et al. (2011) and Muñoz et al. (2012) sampled relatively thick sections of fine-grained Eocene sediments at about 45 to 47° S outcropping at water depths of from 900 to 2500 m in the walls of large canyons. Eocene sediments found in cores from this section of the slope consist of benthic diatoms to the south and a carbonate facies to the north. Ewing and Lonardi (1971) also noted the presence of Eocene sediments in this region of large canyons, as well as canyons on the southern Argentine margin, which may be particularly well developed because they are cut into thick, fine-grained Eocene sediments by persistent, strong currents. Cursory analysis of the ArgentineSPAN-(TM) seismic lines in the area suggest that these layered sediments also exist in somewhat shallower water south of the zone of canyons.

Hanna et al. (1976) and Ross (1976) described several new, non-reworked Eocene diatom species from Vema cores collected in this area. Core VM12-46 (47.483° S, 59.35° W; water depth 1167 m), described by D. Ericson and available on GeoMapApp (http://www.geomapapp.org), contains a fine-grained Eocene sediment with abundant coccoliths, diatoms, silico-flagellates, radiolarian and sponge spicules as well as common benthic foraminifera.

Eocene sediments on the upper slope are overlain by a prominent but now buried sediment drift in deep water, which is likely of Oligocene to early late Miocene age (Fig. 4; the "giant drift" of Hernández-Molina et al., 2010 and Grützner et al., 2012). This drift is buried to the west by the flanks of younger and shallower deposits (termed "mounded drifts") of mid- to late Miocene age, which developed sequentially within the south-central portion of the Argentine margin. Sediments likely of Pliocene to the Holocene age overlay the mounded drifts, although they are often more localized. These younger sediments are generally interpreted as drifts, perhaps associated with the levees of channels, or deposits within channels, where the channels intersect flow along the margin. Drifts are also present farther north along the margin (e.g., Hernández-Molina et al., 2015) with drifts apparently associated with flows of Antarctic Intermediate Water (AAIW), Upper Circumpolar Deep Water (UCDW), North Atlantic Deep Water (NADW), Lower Circumpolar Deep Water (LCDW) and Antarctic Bottom Water (AABW).

Violante et al. (2010) and Grützner et al. (2011, 2012, 2016) suggested that increased sediment flux to the margin during the Miocene may in part be related to an uplift in the Andes that in turn is due to increased Miocene Pacific Ocean crustal spreading and subduction rates, which peaked at about 10 to 20 Ma (Pardo-Casas and Molnar, 1987; Martinod et al., 2010). However, the routes or processes by which

Andean sediments reach the margin and are redistributed within the margin are not well understood.

The shift in deposition from primarily shallow-water Eocene sediments to deep-water, drifted Oligocene sediments appears to mark the deepening of the Antarctic Circumpolar Current (ACC) in the Oligocene (Katz et al., 2011) and the first entry of northward-flowing deep waters into the Argentine Basin (Uenzelmann-Neben et al., 2016). The establishment of a shallow ACC in the Eocene played an important role in isolating Antarctica and allowing for the growth of continental ice sheets (Katz et al., 2011), and the thick, shallow-water (now the upper slope) Eocene sediments described along the southern Argentine margin may have accumulated in response to the formation of a shallow ACC and associated shallow northward flow along the Argentine margin. The ACC apparently strengthened and deepened into the Oligocene as the Tasman Gateway and then the Drake Passage deepened, leading to the development of the modern four-layer structure as well as deep northward flow in the Argentine Basin (Katz et al., 2011; Figs. 2 and 4).

The mid–late Miocene is a particularly important time in terms of climate history and global ocean circulation. During the early Miocene, the Antarctic Ice Sheet (AIS) appears to have fluctuated in size, with concomitant changes in sea level of about ±20 m (e.g., Foster et al., 2012). The mid-Miocene was characterized by the mid-Miocene Climatic Optimum (MCO), which extends from about 17 to 15 Ma. This was a time of reduced AIS volume (∼ 10–25 % of the modern AIS), high pCO_2 (up to ∼ 450 ppm) and global temperatures warmer than today. Following the MCO, more complex oceanic circulation patterns developed during the mid-Miocene Climatic Transition (MMCT) from about 14.2 to 13.8 Ma. Possible important events that occurred at that time include the emplacement of large volcanic complexes (such as the Columbia River Basalts, CRB), which would have affected pCO_2 (Armstrong McKay et al., 2014), the Andean uplift with an impact on atmospheric circulation and weathering patterns (Violante et al., 2010; Grützner et al., 2011 and 2012), and the closing of the Tethys seaway, which changed global ocean circulation patterns (Hamon et al., 2013). Climate deterioration continued into the late Miocene, leading to the initiation and growth of the West Antarctic Ice Sheet (Shevenell et al., 2004). Climatic deterioration has continued into the Pleistocene although the major current systems that were established between the end of the Miocene and the late Pliocene appear to have continued to the present day (Hernández-Molina et al., 2009; Preu et al., 2012, 2013). However, factors other than ocean currents have also been important to the development of the margin, including sea level change, climate variability and glaciation and uplift in the Andes (Violante et al., 2010; Grützner et al., 2011 and 2012). These kinds of factors can also control the timing, locations and rates of sediment input, which can also affect margin evolution.

4 Drilling to investigate the tectonic, paleoceanographic, sedimentation, and biosphere history of the APVCM – recommendations from the workshop

Workshop participants agreed that scientific ocean drilling off Argentina (both in deep and shallow water) will contribute to the understanding of the role that the southern region has played in climate evolution and associated processes and will provide opportunities for focused studies.

The APVCM provides outstanding targets for investigating sedimentation and paleoceanographic conditions from the Cretaceous to the Holocene. The unique setting in the target region is linked to the tectonic evolution of Antarctica, the Southern and South Atlantic oceans, and the Andes. Specific questions and hypotheses were discussed in groups regarding several main sub-topics.

4.1 Tectonic evolution

One sub-topic discussion group was focused on developing a strategy to identify targets that highlight the opening of the South Atlantic and allow for testing the various models for the breakup of Gondwana and emplacement of shear zones, for example as expressions of transcurrent boundaries. SDRs and associated magnetic/gravity anomalies are important volcanic and geophysical features that can constrain geotectonic models of the opening of the South Atlantic and the evolution of its margins. We need to better understand the structure, fragmentation and thermal evolution of SDRs, which can be identified in seismic lines. We need to collect in situ samples for age dating and we need to determine the likely depths of events related to SDR emplacement and evolution. We also need to better characterize the geochemical composition and mineralogy of the SDR layers to better perceive their emplacement and thermal evolution. Drilling and sampling the SDRs of the Argentina Basin (deep-water realm of the APVCM) will allow us to address the following scientific objectives related to challenges 8, 9 and 10 of the Earth connections theme in the IODP Science Plan for 2013–2023 (IODP-SP):

- What is the age and composition of the SDRs?
- What was the source of magma (asthenosphere vs. deep mantle plumes) for the initial melts emplaced during the early opening of the South Atlantic, and what does this tell us about models of continental rifting/fragmentation?
- What was the nature of magma and continental crust interactions during SDR emplacement, and what does this indicate about crustal anatexis, crustal lithology, and composition of gases delivered to the ocean and/or atmosphere during emplacement?

– How has the structural, tectonic and thermal evolution of the margin influenced the both large-scale and local sedimentation patterns on the margin over time?

4.2 Paleoceanography and stratigraphy

This sub-group engaged in a discussion of the opening of the South Atlantic and how the changing configuration of the ocean basins and distribution of landmasses affected the evolution of the ocean and climate. Since the age of the APVCM allows one (in theory) to tap into sediments back as far as the mid-Late Cretaceous, it may be possible to sample sediments that record the successive oceanic-anoxic events (OAEs) that occurred during the mid-Cretaceous "Super Greenhouse" (Aptian–Turonian), a time with characteristically high atmospheric CO_2 concentrations and very warm deep-ocean and polar surface temperatures. These kinds of records from this region (and time period) exist (e.g., DSDP (Deep Sea Drilling Project) sites 327, 511) but they are limited with enigmatic findings. The stratigraphic evolution of the Argentine Basin during the Eocene through to the present day, as demonstrated in seismic profiles, and its relationship to the global ocean conveyor belt circulation and paleoclimate at that time and forward into modern times, is far from understood. While many key circulation events are interpreted from layering patterns on seismic profiles, the origin of the seismic layering and the ages of significant seismic reflections are yet to be directly determined. This is an important step in order to fully exploit the seismic signature of margin evolution. However, it is likely that sediment records obtained from this margin (from both shallow and deep water) will provide important and possibly expanded and continuous sequences for detailed biostratigraphic and magnetostratigraphic studies during important time periods. Analysis of these records can help to illuminate questions relevant to challenges 1 and 4 of IODP-SP's climate and ocean change theme such as

– When did marine sedimentation begin, how rapidly did the South Atlantic deepen and when did northern-sourced water impact this region?

– How are Cretaceous OAEs expressed in this area and does this expression change as the South Atlantic widened and deepened during the Late Cretaceous? What is the importance of circulation changes vs. productivity in the formation of OAEs?

– What was the nature of the deep-water mass in the South Atlantic during the Late Cretaceous "Super Greenhouse"? At what point is there evidence for a significant contribution from southern-sourced (Antarctic) deep water?

– Can depth transects of sites representing different times in the evolution of the South Atlantic circulation be found at different latitudes along the margin to determine the spatial and temporal evolution of circulation along the margin?

– Can scientific drilling help to further decipher the peculiar and significant impact of the Miocene on the atmospheric evolution of our planet? How was the Neogene shaped globally through processes taking place on or recorded in sediments of the APVCM?

4.3 Sedimentology

This sub-group considered the sediment record from a somewhat different perspective than the "Paleoceanography and sedimentology" topic, and questions were raised related to links between climate, sediment accumulation, atmospheric circulation and the Andean orogeny, which is the most prominent tectonic feature in the Southern Hemisphere (Ghiglione et al., 2016). One particular example is that records from the continental margin will extend and complement records of wind-blown sediments recovered from Argentine loess deposits and Patagonian lakes (Heil Jr. et al., 2010; Lisé-Pronovost et al., 2015). These kinds of topics pertain to IODP-SP's climate and ocean change theme challenges 1 and 3:

– Does a signal of Andean orogeny exist in the sedimentary record of the Argentine margin? If so, what does it look like and how should it be interpreted?

– Can we identify connections between paleo-climate and sedimentation patterns and rates in the region?

– Did processes in this region have an impact on global sedimentation rates and patterns?

– Can we identify and track material in a "source-to-sink" framework from the Andes to the Argentine margin as well as to the various basins?

– How did Andean tectonics affect the global ocean and atmospheric circulation (wind) patterns and conditions?

– Has Andean dust/loess affected primary bioproductivity during the Neogene, and might that signal also be reflected in CO_2 uptake/release signatures imprinted in the sediment deposits?

– What can we learn about how Andean volcanism evolved and how those volcanic process and the record of uplift and erosion help us understand the subduction processes here?

– What can the sediment recorded in margin sediments tell us about temporal variability of the sources of material to the margin and in the nature of along-slope and across-slope transport processes?

4.4 Biosphere and geochemistry

This sub-group was focused on discussing the variable presence, quality and quantity of organic matter along the APVCM, because reactions related to organic matter decomposition provide the energy needed by subsurface biosphere communities. In many areas microbial life and the cycling of elements is studied in steady-state environments while seismic profiles from the Argentine margin demonstrate a dynamic sedimentary environment. The APVCM is thereby considered and treated as a temporal and spatial non-steady-state depositional system, which is highly impacted by complex and dynamic sediment reworking processes (Hensen et al., 2003; Riedinger et al., 2014; Razik, 2014). Gravity-driven sediment deposition, sea level variations, strong currents and complex paleo-productivities across the short-to-long-term timescales are all contributing factors to generating complex geochemical cycling and biosphere activity. Buried organic-rich layers can be re-activated under certain temperature and pressure changes, thus providing food for subsurface microbial communities. Organic substrates can diffuse into adjacent, often organic-lean, sediment layers, and this new energy source can cause strong alteration of the sedimentary record long after deposition. Since little data exist for a non-steady-state sediment depositional system along and across a passive margin, the APVCM represents a perfect playground to examine the diversity and activity of subsurface microbial communities and their responses to dynamic changes in their sedimentary environment. Geomicrobiological and bio-geochemical (in conjunction with detailed physical-property) studies in such deposits could be pursued with a modest addition of the appropriate shipboard personnel and relates to challenges 5 and 7 of IODP-SP's biosphere frontiers theme:

- How does the diversity and activity of microbial life vary with depth, geochemistry, and sediment composition and age across the APVCM?
- Furthermore, does microbial activity change with non-steady-state sedimentation?
- How do the amounts and fluxes of carbon change in time and space across the APVCM in relation to variations in primary external parameters? Are carbon and nutrients preferentially stored in sediment during times of rapid sediment accumulation and returned to the ocean during times of slow sedimentation? How does that affect the CO_2 input/release from the sediments?

5 Augmenting data and data management methods

Development of APVCM-specific drilling proposals to address the objectives cited above will require the acquisition of additional data sets. Specifically, the following was suggested during the workshop:

Priority no. 1: obtain additional seismic data sets, including cross-lines to complement existing seismic data, for possible target sites. Such new seismic lines should be acquired using methods that resolve deeper sedimentary structures in addition to the upper sedimentary sequences. These data can be used to develop several drilling transects at different latitudes to target the collection of important Paleogene and Neogene sequences as well as to support drilling to deeper targets such as SDRs and Mesozoic sediments.

Action no. 1: augment existing high-quality seismic data (e.g., Grützner et al., 2012), for example through GEOMAR's three-dimensional (3-D) P-Cable (Planke et al., 2009; Planke and Berndt, 2002) and/or using other seismic systems, such as provided through the U.S. National Science Foundation (NSF) or other research grants.

Action no. 2: evaluate existing sediment samples and collect new gravity and piston cores near potential drill sites to document the age, nature and character of the near-surface material to support the potential transect-oriented IODP proposals.

Priority no. 2: coordinate with Pampa Azul, a strategic project of scientific research along the Argentine margin supported by the Argentine state (http://en.mincyt.gob.ar/accion/pampa-azul-9465). As stated on the Pampa Azul web site, the main objective of Pampa Azul is to help deepen scientific knowledge as the basis of conservation policies and management of natural resources, promote technological innovations applicable to the sustainable exploitation of natural resources and the development of industries related to the sea, strengthen the maritime awareness of Argentine society and support with scientific information and presence the country's sovereignty in the South Atlantic area. The Pampa Azul initiative was a one of the workshop sponsors and several of the attendees were associated with Pampa Azul. We encourage linkages between any scientific drilling campaign on the APVCM and Pampa Azul investigators. Argentina provides an excellent example for developing a vibrant, highly ambitious ocean research program (Pampa Azul). Coordinating with Pampa Azul through this IODP-sponsored workshop provided an important mechanism to begin important collaborations between the Argentine ocean research community and IODP investigators.

Priority no. 3: encourage the development of continent–ocean transect drilling proposals for joint evaluation by IODP and ICDP (International Continental Scientific Drilling Program). Important and complementary records come from both continental and marine settings, and a full understanding of margin evolution and requires working in both settings.

6 Outcomes of the workshop

The main outcome of this workshop is the formation of several working groups addressing the various scientific top-

ics briefly outlined in this report, and committed to preparing several pre-/full proposals to IODP that are appropriate for the R/V *JOIDES* resolution. As of January, 2017 two preliminary proposals are active in the IODP system and full proposals for these proposals have been invited; see https://www.iodp.org/proposals/active-proposals for full details. The 903-Pre "Argentine margin seaward dipping reflectors" considers the early opening of the South Atlantic and especially the sampling of the SDRs that formed in a non-hotspot setting and the overlying Cretaceous and Cenozoic sediments. Secondary objectives include the evolution of atmospheric circulation and the diversity and activity of microbial life under non-steady-state conditions. 911-Pre "Argentine margin paleoceanographic transects" develops a "transect" approach to better understand the evolution of Southern Ocean water structure over a broad vertical and temporal range. Secondary objectives include how the passive margin architecture responds to Cenozoic climate and tectonics and the microbial variability through time under different climate, deep-water circulation and sediment-flux regimes. Developing these and other pre-/full proposals for the time window when the R/V *JOIDES* resolution is likely to operate in the South Atlantic will probably require the collection of additional data and coordination amongst the international partners.

7 Relationship to IODP Science Plan for 2013–2023 and beyond

The scientific objectives for potential IODP drilling proposals are central aspects of the International Ocean Discovery Program as formulated in the Science Plan for 2013–2023 *Illuminating Earth's Past, Present, and Future*. Knowledge acquired as a result of this drilling project will significantly advance the IODP theme "climate and ocean change: reading the past, informing the future", specifically challenges 1 "how does Earth's climate system respond to elevated levels of atmospheric CO_2?", 3 "what controls regional patterns of precipitation, such as those associated with monsoons or El Niño?" and 4 "how resilient is the ocean to chemical perturbations?", as well as the "Earth connections: deep processes and their impact on Earth's surface environment" theme, specifically challenges 8 "what are the composition, structure, and dynamics of Earth's upper mantle?", 9 "how are seafloor spreading and mantle melting linked to ocean crustal architecture?", and 10 "what are the mechanisms, magnitude, and history of chemical exchanges between the oceanic crust and seawater?" Throughout the workshop we have been learning how to integrate objectives related to biosphere frontiers with those of other themes. This has been very successful and drilling resulting from this workshop will significantly advance the IODP theme "biosphere frontiers: deep life, biodiversity, and environmental forcing of ecosystems", specifically challenges 5 "what are the origin, composition and global significance of subseafloor communities" and 7 "how sensitive are ecosystems and biodiversity to environmental change?"

8 Societal relevance and responsibility

The interconnection of this IODP project with Pampa Azul and corresponding initiatives (for example with the German DFG-BMBF) provides opportunities for early-career scientists among the various countries. ICDP at the German Research Centre for Geosciences (GFZ) in Potsdam actively fosters and sponsors such efforts and incentives via financial and logistical support. We also encourage syndicated, perhaps educational television, documentaries about scientific drilling on the Argentine margin as projects develop. This type of activity can help to inform the general public, whose tax dollars finance these studies, and raise favorable awareness for these types of international collaborations at a time of significant geo-political and economic challenges. This is just one aspect of interacting with the public at all levels in order to generate a deeper understanding and appreciation for the importance of scientific drilling both on land and in the ocean.

9 Conclusions

The evolution of the Argentine Continental Margin has been affected by climate, current, sea level and tectonic processes, as well as by sediment input patterns and depositional history along this roughly 5000 km long coast line. All of these characteristics, coupled with the fact that this is a critically important, yet under-sampled, portion of the World Ocean, makes the Argentine Continental Margin an important region for IODP scientific drilling. Workshop participants agreed that scientific ocean drilling off Argentina will contribute to the understanding of the role that the southern region has played in climate evolution and associated processes and will provide opportunities for focused studies. The APVCM provides outstanding targets for investigating sedimentation patterns, climatic, paleo-circulation and paleoceanographic conditions, biosphere and geochemistry from the Cretaceous to the Holocene. The evolution of this important setting is also linked to the evolution of the World Ocean as well as to the tectonic evolution of Antarctica, the Southern and South Atlantic oceans, and the Andes.

Author contributions. Report authors consist of the workshop steering committee.

Competing interests. Authors Roberto A. Violante, Thomas Gorgas, Ernesto Schwarz, Jens Grützner, Gabriele Uenzelmann-Neben and F. Javier Hernández-Molina are proponents of IODP scientific drilling proposals 903-Pre and/or 911-Pre.

Table 1. IODP workshop: developing scientific drilling proposals for the Argentina Passive Volcanic Continental Margin (APVCM) – basin evolution, deep biosphere, hydrates, sediment dynamics and ocean evolution.

Workshop participants, Buenos Aires, 8–11 September 2015		
Name	Institution	E-mail
Ariztegui, Daniel	University of Geneva, Switzerland	daniel.ariztegui@unige.ch
Beilinson, Elisa	CIG – UNLP, Argentina	beilinson@cig.museo.unlp.edu.ar
Berndt, Christian	Christian-Albrechts-University, Germany	cberndt@geomar.de
Bolatti, Nestor	YPF – Offshore, Argentina	nestor.bolatti@ypf.com
Bozzano, Graziella	Servicio de Hidrografía Naval, Argentina	grazi.hidro.gov.ar@gmail.com
Briggs, Brandon	University of Alaska - Anchorage, USA	bbriggs@uaa.alaska.edu
Cuitiño, José	CENPAT – CONICET, Argentina	jcuitino@cenpat-conicet.gob.ar
Dickens, Gerald	Rice University, USA	jerry@rice.edu
Esteban, Federico	IGeBA – UBA, Argentina	federico.esteban@gmail.com
Flood, Roger	Stony Brook University, USA	roger.flood@stonybrook.edu
Garcia Chapori, Natalia	SACMa – IDEAN – UBA, Argentina	nataliag@gl.fcen.uba.ar
Gerster, Ricardo	YPF – Offshore, Argentina	ricardo.gerster@ypf.com
Ghidella, Marta	Instituto Antartico Argentino, Argentina	mghidella@gmail.com
Gomez, Fernando	CICTERRA Córdoba, CONICET, Argentina	fernandogomez411@gmail.com
Gorgas, Thomas	GFZ, Potsdam, Germany	tgorgas@gfz-potsdam.de
Gruetzner, Jens	Alfred-Wegener-Institut, Germany	jens.gruetzner@awi.de
Heil, Chip	University of Rhode Island, USA	chiph@uri.edu
Hernández-Molina, F. Javier	Royal Holloway University, London, UK	javier.hernandez-molina@rhul.ac.uk
Iglesia Llanos, Paula	IGeBA – UBA, Argentina	mpiglesia@gl.fcen.uba.ar
Isola, José	IGeBA – UBA, Argentina	jose.isola91@gmail.com
Jimenez, Mariano	Urien & Assoc., Argentina	mariano_registrado@hotmail.com
Kress, Pedro R.	YPF – Offshore, Argentina	pkress@ypf.com
Kulhanek, Denise	IODP-JRSO-TAMU JRSO, USA	kulhanek@iodp.tamu.edu
Leon Zayas, Rosa	University of Delaware, USA	rleonzay@udel.edu
Malumian, Norberto	CONICET, Argentina	n.malumian@yahoo.com
Medina Ketze, Joao Marcelor	Instituto do Petróleo e Recursos Naturais, PUCRS, Brazil	jketzer@pucrs.br
Orgeira, Maria Julia	CONICET – UBA, Argentina	orgeira@gl.fcen.uba.ar
Paterlini, C. Marcelo	COPLA – Servicio de Hidrografía Naval, Argentina	cmpaterlini@yahoo.com.ar
Perez Panera, Juan P.	Y-Tec, Argentina	perezpanera@gmail.com
Ramos, Victor	UBA – CONICET, Argentina	andes@gl.fcen.uba.ar
Rapalini, Augusto	IGeBA – UBA – CONICET, Argentina	rapalini@gl.fcen.uba.ar
Reuber, Kyle	University of Houston & ION – GeoVentures, USA	kyle.reuber@iongeo.com
Riedinger, Natascha	Oklahoma State University, USA	natascha.riedinger@okstate.edu
Schwarz, Ernesto	CIG – UNLP – CONICET, Argentina	eschwarz@cig.museo.unlp.edu.ar
Selva, Carlos	Y-Tec, Argentina	carlos.selva@ypf.com
Slowey, Niall	Dept of Oceanography, TAMU, USA	slowey@geos.tamu.edu
Soto, Matías	ANCAP Uruguay	msoto@fcien.edu.uy
St-Onge, Guillaume	Université du Québec à Rimouski, Canada	guillaume_st-onge@uqar.ca
Tassone, Alejandro	IGeBA – UBA – CONICET. Pampa Azul, Argentina	atassone@gl.fcen.uba.ar
Troisi, Ariel	Servicio de Hidrografía Naval, Argentina	atroisi@hidro.gov.ar
Uenzelmann-Neben, Gabriele	Alfred-Wegener-Institut, Germany	gabriele.uenzelmann-neben@awi.de
Urien, Carlos Maria	Urien & Assoc., Argentina	uriencm@fibertel.com.ar
Violante, Roberto A.	Servicio de Hidrografía Naval. Pampa Azul, Argentina	rober.a.violante@gmail.com
Wehrmann, Laura	Stony Brook University, USA	laura.wehrmann@stonybrook.edu
Wright, Jim	Rutgers University, USA	jdwright@rci.rutgers.edu

Acknowledgements. We thank NSF-USSSP, ECORD/ICDP, COPLA, Ministry of Foreign Office, Ministry of Science (MINCYT), Pampa Azul, YPF, Y-Tec, IGeBA, CIG-CONICET-UNLP, the German IODP Koordinationsbüro, the Pontifical Catholic University of Rio Grande do Sul, Brazil, and ANCAP for generously providing logistical and financial support for the APVCM workshop and event attendees. COPLA Coordinator Frida Armas Pfirter and Minister Osvaldo Másrico deserve special thanks for their hospitality and for doing a superb job hosting this event (which received rave reviews from the attendees) in concert with a competent technical service team at the venue. Supporting Institutions in Argentina were the Argentina Hydrographic Survey and the Instituto de Geologia de Costas y del Cuaternario-University of Mar del Plata. Research was conducted in the framework of the "Drifters" Research Group of the Royal Holloway University of London. We appreciate the constructive feedback from various reviewers of the original workshop proposal, in particular Ann Holbourn (Kiel University), and also the reviewers of this workshop report. We especially acknowledge Manika Prasad, Christian Berndt and, in particular, Denise Kulhanek (IODP-JRSO-TAMU) and Jim Wright (Rutgers), who led efforts to submit the first two APVCM pre-proposals (903-Pre and 911-Pre). Most importantly, thanks go to all workshop attendees and participating scientists for their enthusiastic and ongoing contributions before, during and after the event, thereby helping to develop pre-proposals as concrete outcomes from this workshop. All investigators, workshop attendees and updates can be found on the ICDP project website at http://apvcm.icdp-online.org. Additional details can also be found at http://usoceandiscovery.org/workshops/. Contribution no. 1434 of the School of Marine and Atmospheric Sciences, Stony Brook University.

Edited by: J. Behrmann
Reviewed by: two anonymous referees

References

Armstrong McKay, D. I., Tyrrell, T., Wilson, P. A., and Foster, G. L.: Estimating the impact of the cryptic degassing of Large Igneous Provinces: A mid-Miocene case-study. Earth and Sciences Letters, 403, 254–262, doi:10.1016/j.epsl.2014.06.040, 2014.

Bender, V. B., Hanebuth, T. J. J., and Chiessi, C. M.: Holocene shifts of the Subtropical Shelf Front off southeastern South America controlled by high and low latitude atmospheric forcings, Paleoceanography, 28, 481–490, doi:10.1002/palo.20044, 2013.

Bozzano, G., Violante, R. A., and Cerredo, M. E.: Middle slope contourite deposits and associated sedimentary facies off NE Argentina, Geo-Mar. Lett., 31, 495–507, doi:10.1007/s00367-011-0239-x, 2011.

Broecker, W.: The great ocean conveyor, Oceanography, 4, 79–89, doi:10.5670/oceanog.1991.07, 1991.

Chiessi, C. M., Ulrich, S., Mulitza, S., Pätzold, J., and Wefer, G.: Signature of the Brazil-Malvinas Confluence (Argentine Basin) in the isotopic composition of planktonic foraminifera from surface sediments, Mar. Micropaleontol., 64, 52–66, doi:10.1016/j.marmicro.2007.02.002, 2007.

Ewing, M. and Lonardi, A. G.: Sediment transport and deposition in the Argentine Basin. 5. Sedimentary structures of the Argentine margin, basin and related provinces, Phys. Chem. Earth, 8, 125–156, doi:10.1016/0079-1946(71)90017-6, 1971.

Foster, G. L., Lear, C. H., and Rae, J. W. B.: The evolution of pCO_2, ice volume and climate during the middle Miocene, Earth Planet Sc. Lett., 341–344, 243–254, doi:10.1016/j.epsl.2012.06.007, 2012.

Friedrich, O., Norris, R. D., and Erbacher, J.: Evolution of middle to Late Cretaceous oceans – A 55 m.y. record of Earth's temperature and carbon cycle, Geology, 40, 107–110, doi:10.1130/G32701.1, 2012.

García Chapori, N., Laprida, C., Watanabe, S., Totah, V., and Violante, R. A.: Mid-Late Pleistocene benthic foraminifera from Southwestern South Atlantic: driven by primary productivity or watermass properties?, Micropaleontology, 60, 195–210, 2014.

García Chapori, N., Chiessi, C. M., Bickert, T., and Laprida, C.: Sea-surface temperature reconstruction of the Quaternary western South Atlantic: New planktonic foraminiferal correlation function, Palaeogeogr. Palaeocl., 425, 67–75, doi:10.1016/j.palaeo.2015.02.027, 2015.

Ghiglione, M. C., Sue, C., Ramos, M., Tobal, J. E., and Gallardo, R. E.: The Relation Between Neogene Denudation of the Southernmost Andes and Sedimentation in the Offshore Argentine and Malvinas Basins During the Opening of the Drake Passage. *Chapter 5* in: Geodynamic Evolution of the Southernmost Andes, edited by: Ghiglione, M. C., 206 pp., ISBN: 978-3-319-39727-6, 2016.

Gladczenko, T. P., Hinz, K., Eldholm, O., Meyer, H., Neben, S., and Skogseid, J.: South Atlantic volcanic margins, J. Geol Soc. London, 154, 465–470, doi:10.1144/gsjgs.154.3.0465, 1997.

Govin, A., Holzwarth, U., Heslop, D., Ford Keeling, L., Zabel, M., Mulitza, S., Collins, J. A., and Chiessi, C. M.: Distribution of major elements in Atlantic surface sediments (36N°–49°S): Imprints of terrigenous input and continental weathering, Geochem. Geophy. Geosy., 13, Q01013, doi:10.1029/2011GC003785, 2012.

Granot, R. and Dyment, J.: The Cretaceous opening of the South Atlantic Ocean, EPSL, 414, 156–163, doi:10.1016/j.epsl.2015.01.015, 2015.

Grützner, J., Uenzelmann-Neben, G., and Franke, D.: Variations in bottom water activity at the southern Argentine margin: indications from a seismic analysis of a continental slope terrace, Geo-Mar. Lett, 31, 405–417, doi:10.1007/s00367-011-0252-0, 2011.

Grützner, J., Uenzelmann-Neben, G., and Franke, D.: Variations in sediment transport at the central Argentine continental margin during the Cenozoic, Geochem. Geophy. Geosy., 13, Q10003, doi:10.1029/2012GC004266, 2012.

Grützner, J., Uenzelmann-Neben, G., and Franke, D.: Evolution of the northern Argentine margin during the Cenozoic controlled by bottom current dynamics and gravitational processes, Geochem. Geophy. Geosy., 17, 3131–3149, doi:10.1002/2015GC006232, 2016.

Hamon, N., Sepulchre, P., Lefebvre, V., and Ramstein, G.: The role of eastern Tethys seaway closure in the Middle Miocene Climatic Transition (ca. 14 Ma), Clim. Past, 9, 2687–2702, doi:10.5194/cp-9-2687-2013, 2013.

Hanna, G. D., Hendey, I. N., and Brigger, A. L.: Some Eocene diatoms from South Atlantic cores, Part I. California Academy of Sciences, Occ. Papers, 123, 1–19, 1976.

Heil Jr., C. W., King, J. W., Zarate, M., and Schultz, P. H.: Climatic interpretation of 1.9 Ma environmental magnetic record of loess deposition and soil formation in the central eastern Pampas of Buenos Aires, Argentina, Quaternary Sci. Rev., 29, 2705–2718, doi:10.1016/j.quascirev.2010.06.024, 2010.

Heine, C., Zoethout, J., and Müller, R. D.: Kinematics of the South Atlantic rift, Solid Earth, 4, 215–253, doi:10.5194/se-4-215-2013, 2013.

Hensen, C., Zabel, M., Pfeifer, K., Schwenk, T., Kasten, S., Riedinger, N., Schulz, H. D., and Boetius, A.: Control of sulfate pore-water profiles by sedimentary events and the significance of anaerobic oxidation of methane for burial of sulfur in marine sediments, Geochim. Cosmochim. Ac., 67, 2631–2647, doi:10.1016/S0016-7037(03)00199-6, 2003.

Hernández-Molina, F. J., Paterlini, M., Violante, R., Marshall, P., de Isasi, M., Somoza, L., and Rebesco, M.: Contourite depositional system on the Argentine Slope: An exceptional record of the influence of Antarctic water masses, Geology, 37, 507–510, doi:10.1130/G25578A.1, 2009.

Hernández-Molina, F. J., Paterlini, M., Somoza, L., Violante, R., Arecco, M. A., de Isasi, M., Rebesco, M., Uenzelmann-Neben, G., Neben, S., and Marshall, P.: Giant mounded drifts in the Argentine Continental Margin: Origins and global implications for the history of thermohaline circulation. Mar. Petrol. Geol., 27, 1508–1530, doi:10.1016/j.marpetgeo.2010.04.003, 2010.

Hernández-Molina, F. J., Soto, M., Piola, A. R., Tomasini, J., Preu, B., Thompson, P., Badalini, G., Creaser, A., Violante, R., Morales, E., and de Santa Ana, H.: A contourite depositional system along the Uruguyan continental margin: Sedimentary, oceanographic and paleocenographic implications, Mar. Geol., 378, 333–349, doi:10.1016/j.margeo.2015.10.008, 2015.

Hinz, K., Neben, S., Schreckenberger, B., Roeser, H. A., Block, M., Gonçalves de Souza, K., and Meyer, H.: The Argentine continental margin north of 48° S: Sedimentary successions, volcanic activity during breakup Mar. Petrol. Geol., 16, 1–25, doi:10.1016/S0264-8172(98)00060-9, 1999.

Katz, M. E., Cramer, B. S., Toggweiler, J. R., Esmay, G., Liu, C., Miller, K. G., Rosenthal, Y., Wade, B. S., and Wright, J. D.: Impact of Antarctic Circumpolar Current development on Late Paleogene ocean structure, Science, 332, 1076–1079, doi:10.1126/science.1202122, 2011.

Krastel, S., Wefer, G., Hanebuth, T. J. J., Antobreh, A. A., Freudenthal, T., Preu, B., Schwenk, T., Strasser, M., Violante, R., and Winkelmann, D.: Sediment dynamics and geohazards off Uruguay and the de la Plata region (northern Argentina and Uruguay), Geo-Mar. Lett., 31, 271–283, doi:10.1007/s00367-011-0232-4, 2011.

Lastras, G., Acosta, J., Muñoz, A., and Canals, M.: Submarine canyon formation and evolution in the Argentine Continental Margin between 44°30'S and 48°S, Geomorphology, 128, 116–136, doi:10.1016/j.geomorph.2010.12.027, 2011.

Lisé-Pronovost, A., St-Onge, G., Gogorza, C., Haberzettl, T., Jouve, G., Francus, P., Ohlendorf, C., Gebhardt, C., and Zolitschka, B., and PASADO Science Team: Rock-magnetic proxies of wind intensity and dust since 51,200 cal BP from lacustrine sediments of Laguna Potrok Aike, southeastern Patagonia, EPSL, 411, 72–86, doi:10.1016/j.epsl.2014.11.007, 2015.

Loegering, M. J., Anka, Z., Autin, J., di Primio, R., Marchal, D., Rodriguez, J. F., Franke, D., and Vallejo, E.: Tectonic evolution of the Colorado Basin, offshore Argentina, inferred from seismo-stratigraphy and depositional rates analysis, Tectonophysics, 604, 245–263, doi:10.1016/j.tecto.2013.02.008, 2013.

Lonardi, A. G. and Ewing, M.: Sediment transport and distribution in the Argentine Basin. 4. Bathymetry of the continental margin, Argentine Basin and other related provinces. Canyons and sources of sediments, Phys. Chem. Earth, 8, 79–121, doi:10.1016/0079-1946(71)90016-4, 1971.

Martinod, J., Husson, L., Roperch, P., Guillaume, B., and Espurt, N.: Horizontal subduction zones, convergence velocity and the building of the Andes, Earth Planet Sc. Lett., 299, 299–309, doi:10.1016/j.epsl.2010.09.010, 2010.

Moulin, M., Aslanian, D., and Unternehr, P.: A new starting point for the South and Equatorial Atlantic Ocean, Earth-Sci. Rev., 98, 1–37, doi:10.1016/j.earscirev.2009.08.001, 2010.

Muñoz, A., Cristobo, J., Rios, P., Druet, M., Polonio, V., Uchipi, E., Acosta, J., and Atlantis Group: Sediment drifts and cold-water coral reefs in the Patagonian upper and middle continental slope, Mar. Petrol. Geol., 36, 70–82, doi:10.1016/j.marpetgeo.2012.05.008, 2012.

Pardo-Casas, F. and Molnar, P.: Relative motion of the Nazca (Farallon) and South-American plates since late Cretaceous time, Tectonics, 6, 233–248, doi:10.1029/TC006i003p00233, 1987.

Planke, S. and Berndt, C.: "Anordning for seismikkmåling", Patent 20021140, 2002.

Planke, S., Erikson, F. N., Berndt, C., Mienert, J., and Masson, D.: P-Cable High-Resolution Seismic, Oceanography, 22, 85–85, doi:10.5670/oceanog.2009.09, 2009.

Preu, B., Schwenk, T., Hernández-Molina, F. J., Violante, R., Paterlini, M., Krastel, S., Tomasini, J., and Spiess, V.: Sedimentary growth pattern on the northern Argentine slope: the impact of North Atlantic Deep Water on southern hemisphere slope architecture, Mar. Geol., 329–331, 113–125, doi:10.1016/j.margeo.2012.09.009, 2012.

Preu, B., Hernández-Molina, F. J., Violante, R., Piola, A. R., Paterlini, C. M., Schwenk, T., Voigt, I., Krastel, S., and Spiess, V.: Morphosedimentary and hydrographic features of the northern Argentine margin: the interplay between erosive, depositional and gravitational processes and its conceptual implications, Deep-Sea Res. Pt. I, 75, 157–174, doi:10.1016/j.dsr.2012.12.013, 2013.

Razik, S.: How magnetics and granulometry of continental margin sediments reflect terrestrial and marine environment of South America and West Africa. Dissertation for the doctoral degree in natural sciences (Dr. rer. nat.) at the Faculty of Geosciences of the Bremen University, 147 pp., 2014.

Razik, S., Chiessi, C. M., Romero, O. E., and von Dobeneck, T.: Interaction of the South American Monsoon System and the Southern Westerly Wind Belt during the last 14 kyr, Palaeogeogr. Palaeocl., 374, 28–40, doi:10.1016/j.palaeo.2012.12.022, 2013.

Riedinger, N., Formolo, M. J., Lyons, T. W., Henkel, S., Beck, A., and Kasten, S.: An inorganic geochemical argument for coupled anerobic oxidation of methane and iron reduction in marine sediments, Geobiology, 12, 172–181, doi:10.1111/gbi.12077, 2014.

Ross, R.: Some Eocene diatoms from South Atlantic cores, Part II., California Academy of Sciences, Occ. Papers, 123, 21–27, 1976.

Ryan, W. B. F., Carbotte, S. M., Coplan, J. O., O'Hara, S., Melkonian, A., Arko, R., Weissel, R. A., Ferrini, V., Goodwillie, A., Nitsche, F., Bonczkowski, J., and Zemsky, R.: Global Multi-

Resolution Topography synthesis, Geochem. Geophy. Geosy., 10, Q03014, doi:10.1029/2008GC002332, 2009.

Shevenell, A. E.: Middle Miocene Southern Ocean cooling and Antarctic cryosphere expansion, Science, 305, 1766–1770, doi:10.1126/science.1100061, 2004.

Torsvik, T. H., Rousse, S., Labails, C., and Smethurst, M. A.: A new scheme for opening of the South Atlantic Ocean and the dissection of an Aptian salt basin, Geophys. J. Int., 177, 1315–1333, doi:10.1111/j.1365-246X.2009.04137.x, 2009.

Uenzelmann-Neben, G., Weber, T., Grützner, J., and Thomas, M.: Transition from the Cretaceous ocean to Cenozoic circulation in the western South Atlantic – A twofold reconstruction, Tectonophysics, doi:10.1016/j.tecto.2016.05.036, in press, 2016.

Violante, R. A., Paterlini, C. M., Costa, I. P., Hernández-Molina, F. J., Segovia, L. M., Cavallotto, J. L., Marcolini, S., Bozzano, G., Laprida, C., Garcia-Chapori, N., Bickert, T., and Spiess, V.: Sismostratigrafia y Evolucion Geomorfologica del Talud Continental Adyacente al Litoral del Este Bonarense, Argentina, Latin American Journal of Sedimentology and Basin Analysis, 17, 33–62, http://ref.scielo.org/qnx2ts, 2010.

Voigt, I., Henrich, R., Preu, B. M., Piola, A. R., Hanebuth, T. J. J., Schwenk, T., and Chiessi, C. M.: A submarine canyon as a climate archive – interaction of the Antarctic Intermediate Water with the Mar del Plata Canyon (Southwest Atlantic), Mar. Geol., 341, 46–57, doi:10.1016/j.margeo.2013.05.002, 2013.

Take part in a MagellanPlus Workshop in 2017

The MagellanPlus Workshop Series Programme is designed to support scientists in developing new and innovative science proposals for submission to IODP and ICDP.

Granted 2017 MagellanPlus Workshops will cover topics such as Tyrrhenian Magmatism and Mantle Exhumation (5–7 June, Bologna, Italy), Santorini-Kolumbo Marine Volcanic System (Athens, Greece, 21–23 November) and Carbon Cycling at the Ultraslow Arctic Spreading Ridge System (*dates and location to be determined*). The Australasian Regional Workshop for building new IODP Proposals will be organised in Sydney, Australia (*13–16 June*). A workshop granted in 2017 "Structure and Evolution of Magmatic and Hydrothermal Volcanic Systems in offshore collapse/resurgent calderas – Development of an IODP Drilling Proposal at Campi Flegrei linking to active ICDP Drilling Initiatives" was already held from 25–28 February 2017.

Scientists who are interested to take part in a 2017 MagellanPlus workshop will find detailed information on the MagellanPlus website: http://www.ecord.org/science/magellan-plus/

IODP and ICDP at EGU 2017

A joint ECORD/IODP-ICDP exhibition booth had been organised at the EGU General Assembly 2017 in Vienna, Austria. The exhibition booth served as a focal point to catch up with the latest news and achievements from both IODP and ICDP programmes. Scientists and visitors also had the opportunity to get involved in both programmes by meeting ECORD and ICDP representatives and leading scientists and learn more about logging and petrophysical activities achieved during recent ICDP projects and IODP expeditions.

Two joint IODP-ICDP science sessions ("ICDP-IODP Townhall Meeting" and "Achievements and Perspectives in scientific ocean and continental drilling") were also well attended.

Call for IODP-ICDP Sessions at AGU fall meetings

Following discussions with the AGU Fall Meeting Program Chair, Denis-Didier Rousseau, a three-year plan (2017–2019) for IODP-ICDP sessions at the AGU has been defined, culminating with the celebration of the AGU Centennial in 2019. We have highlighted three overarching, societally relevant themes that are well aligned with both IODP and ICDP science plan themes. They fit with the AGU "SWIRLS" which help to find interdisciplinary solutions through the sharing of research, discoveries and approaches across disciplines. These themes (and examples of topics; identified priorities are underlined) are the following:

1. Georesources, Storage, and Sustainability (fits with AGU SWIRLS: "natural resources" and "Science and Society")
   - Unconventional Energy: Supercritical and magma geothermics, EGS, methane and gas hydrates, hydrogen resources and storage
   - Deep Carbon fluxes and storage
   - Water resources: Groundwater vs. Seawater

2. Climate, Environment and Ecosystem (fits with AGU SWIRLS: "Climate" and "Earth Processes")
   - Life in extreme environments: the hidden biosphere
   - Links between geological and biological systems at depth
   - Analogs and models of recent climate changes in geological archives
   - Impact of climate and ocean changes on ecosystems
   - Impact of Earth processes on Earth's environment

3. Geological Hazards (fits with AGU SWIRL: "Extreme events and Hazards")
   - Monitoring and mitigating man-made geohazards? (e.g., induced seismicity, landslides)
   - Hazards in the geological record: from improving risk assessment and prediction of catastrophic events towards mitigation
   - Underlying mechanisms of geological hazards: faulting, earthquakes, volcanoes, impacts

We seek potential conveners (who must be AGU members) to submit AGU session proposals on these three overarching themes. Please keep us informed so that actions and proposal submissions can be coordinated. The deadline for proposal submission for AGU 2017 has already expired, but the call is still open for the AGU 2018 and AGU 2019 fall meetings.

Jamie Austin (IODP Forum; jamie@ig.utexas.edu), Gilbert Camoin (ECORD; camoin@cerege.fr), Uli Harms (ICDP; ulrich@gfz-potsdam.de), Denis-Didier Rousseau (AGU; fallmeetingchair@agu.org)

Schedules

IODP – Expedition schedule http://www.iodp.org/expeditions/

USIO operations	Platform	Dates	Port of origin
1 367 South China Sea A	JOIDES Resolution	7 Feb–9 Apr 2017	Hong Kong / Hong Kong
2 368 South China Sea B	JOIDES Resolution	9 Apr–11 Jun 2017	Hong Kong / Shanghai
3 371 Tasman Subduction	JOIDES Resolution	27 Jul–26 Sep 2017	Townsville / Hobart
4 369 Australia Cretaceous Climate and Tectonics	JOIDES Resolution	26 Sep–27 Nov 2017	Hobart / Fremantle

ICDP – Project schedule http://www.icdp-online.org/projects/

ICDP project	Drilling dates	Location
1 Songliao Basin	Apr 2014–Jul 2017	Songliao Basin, China
2 Oman	Dec 2016–Apr 2017	Oman
3 Koyna	Dec 2016–May 2017	Koyna, India
4 DSEIS	Apr–Oct 2017	Orkney, South Africa
5 Sustain	Jul–Sep 2017	Surtsey Volcano, Iceland

Locations

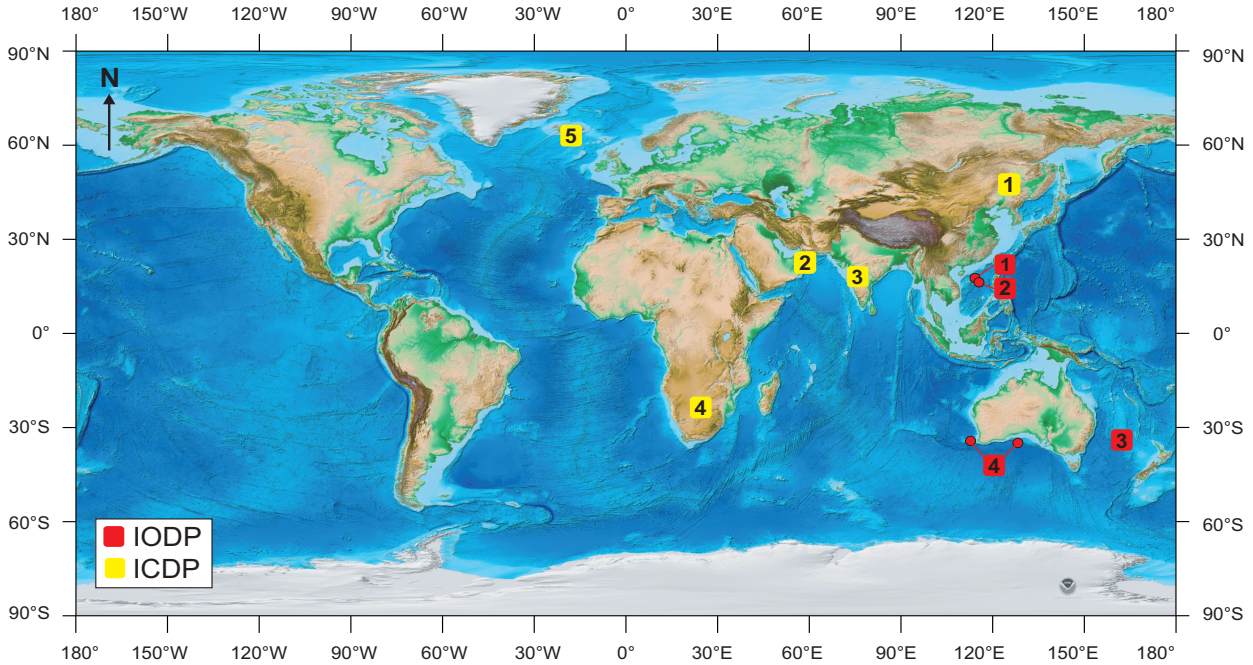

Topographic/bathymetric world map courtesy of NOAA (Amante, C. and B.W. Eakins, 2009. ETOPO1 1 Arc-Minute Global Relief Model: Procedures, Data Sources and Analysis. NOAA Technical Memorandum NESDIS NGDC-24. National Geophysical Data Center, NOAA. doi:10.7289/V5C8276M).